



Anti-SARS-CoV-2 vaccine strategies: immunogenicity evaluation of two vaccine candidates

Axelle Amen

► To cite this version:

Axelle Amen. Anti-SARS-CoV-2 vaccine strategies: immunogenicity evaluation of two vaccine candidates. Pharmaceutical sciences. 2022. dumas-03542629

HAL Id: dumas-03542629

<https://dumas.ccsd.cnrs.fr/dumas-03542629>

Submitted on 25 Jan 2022

HAL is a multi-disciplinary open access archive for the deposit and dissemination of scientific research documents, whether they are published or not. The documents may come from teaching and research institutions in France or abroad, or from public or private research centers.

L'archive ouverte pluridisciplinaire **HAL**, est destinée au dépôt et à la diffusion de documents scientifiques de niveau recherche, publiés ou non, émanant des établissements d'enseignement et de recherche français ou étrangers, des laboratoires publics ou privés.



AVERTISSEMENT

Ce document est le fruit d'un long travail approuvé par le jury de soutenance.

La propriété intellectuelle du document reste entièrement celle du ou des auteurs. Les utilisateurs doivent respecter le droit d'auteur selon la législation en vigueur, et sont soumis aux règles habituelles du bon usage, comme pour les publications sur papier : respect des travaux originaux, citation, interdiction du pillage intellectuel, etc.

Il est mis à disposition de toute personne intéressée par l'intermédiaire de [l'archive ouverte DUMAS](#) (Dépôt Universitaire de Mémoires Après Soutenance).

Si vous désirez contacter son ou ses auteurs, nous vous invitons à consulter la page de DUMAS présentant le document. Si l'auteur l'a autorisé, son adresse mail apparaîtra lorsque vous cliquerez sur le bouton « Détails » (à droite du nom).

Dans le cas contraire, vous pouvez consulter en ligne les annuaires de l'ordre des médecins, des pharmaciens et des sages-femmes.

Contact à la Bibliothèque universitaire de Médecine Pharmacie de Grenoble :

bump-theses@univ-grenoble-alpes.fr

Année : 2022

**STRATÉGIES VACCINALES ANTI-SARS-COV-2 : ÉVALUATION DE
L'IMMUNOGÉNICITÉ DE DEUX CANDIDATS VACCINAUX**

MÉMOIRE DU DIPLÔME D'ÉTUDES SPÉCIALISÉES
INNOVATION PHARMACEUTIQUE ET RECHERCHE
TENANT LIEU DE

THÈSE
POUR LE DIPLÔME D'ÉTAT DE DOCTEUR EN PHARMACIE

Par Mme Axelle AMEN

[Données à caractère personnel]

MÉMOIRE SOUTENU PUBLIQUEMENT À LA FACULTÉ DE PHARMACIE DE
GRENOBLE

Le 14/01/22

DEVANT LE JURY COMPOSÉ DE :

Président du jury :

Mme le Pr Raphaële GERMI (PharmD, PhD)

Membres :

M. le Pr Pascal POIGNARD (MD, PhD) (directeur de thèse)

Mme le Pr Florence MORFIN-SHERPA (PharmD, PhD)

M. le Pr Jean-Yves CESBRON (MD, PhD)

M. le Dr Xavier FONROSE (PharmD, PhD)

M. le Dr Pascal FENDER (PhD)

L'UFR de Pharmacie de Grenoble n'entend donner aucune approbation ni improbation aux opinions émises dans les mémoires ; ces opinions sont considérées comme propres à leurs auteurs.

ENSEIGNANTS - CHERCHEURS Année 2021 / 2022

Doyen de la Faculté - Pr. Michel SEVE
 Vice-Doyen Pédagogie - Mr Pierre CAVAILLES
 Vice-Doyen Recherche – Pr. Walid RACHIDI

STATUT	NOM	PRENOM	LABORATOIRE	HDR
MCF	ALDEBERT	DELPHINE	TIMC-IMAG UMR 5525 CNRS, ThREx	Oui
PU-PH	ALLENET	BENOIT	TIMC-IMAG UMR 5525 CNRS, ThEMAS	Oui
PU	BAKRI	ABDELAZIZ	TIMC-IMAG UMR 5525 CNRS	Oui
CDD	BARDET	JEAN-DIDIER	TIMC-IMAG UMR 5525 CNRS, ThEMAS	
MCF	BATANDIER	CECILE	LBFA – INSERM U1055	
PU-PH	BEDOUCH	PIERRICK	TIMC-IMAG UMR 5525 CNRS, ThEMAS	Oui
MCF	BELAIDI-CORSAT	ELISE	HP2, Inserm U1042	Oui
MAST	BELLET	BEATRICE	-	
MCF	BOUCHERLE	BENJAMIN	DPM - UMR 5063 CNRS	
PU	BOUMENDJEL	AHCENE	LRB /INSERM U 1039	Oui
MCF	BOURGOIN	SANDRINE	TIMC	
MCF	BRETON	JEAN	LCIB – UMR E3 CEA	Oui
MCF	BRIANCON-MARJOLLET	ANNE	HP2 – INSERM U1042	Oui
PU	BURMEISTER	WILHEM	UVHCI- UMI 3265 EMBL CNRS	Oui
MCU-PH	BUSSER	BENOIT	Institute for Advanced Biosciences, UGA / Inserm U 1209 / CNRS 5309	Oui
Professeur Emérite	CALOP	JEAN		Oui
MCF	CAVAILLES	PIERRE	IAB	
MCU-PH	CHANOINE	SEBASTIEN	CR UGA - INSERM U1209 - CNRS 5309	
AHU	CHEVALIER	SIMON	TIMC IMAG	
MCF	CHOISNARD	LUC	DPM – UMR 5063 CNRS	
MCU-PH	CHOVELON	BENOIT	DPM – UMR 5063 CNRS	
MAST	COMBE	JEROME	-	
PU-PH	CORNET	MURIEL	TIMC-IMAG UMR 5525 CNRS, ThREx	Oui
Professeur Emérite	DANEL	VINCENT	-	Oui
Professeur Emérite	DECOUT	JEAN-LUC	DPM – UMR 5063 CNRS	Oui
MCF Emérite	DELETRAZ-DELPORTE	MARTINE	LPSS – EAM 4129 LYON	équiv.
MCF	DEMEILLERS	CHRISTINE	TIMC-IMAG UMR 5525 CNRS	Oui
PU-PH	DROUET	CHRISTIAN	GREPI EA7408	Oui
PU	DROUET	EMMANUEL	IBS – UMR 5075 CEA CNRS HIV & virus persistants Institut de Biologie Structurale	Oui
MCF	DURMORT	CLAIRE	IBS – UMR 5075 CEA CNRS	Oui
PU-PH	FAURE	PATRICE	DPM – UMR5063	Oui
MCF	FAURE-JOYEUX	MARIE	HP2 – INSERM U1042	Oui

Mise à jour le 06/09/2021 Sana HACHANI

STATUT	NOM	PRENOM	LABORATOIRE	HDR
PRCE	FITE	ANDREE	-	
MCU-PH	GARNAUD	CECILE	TIMC-IMAG UMR 5525 CNRS, TheReX	
PRAG	GAUCHARD	PIERRE-ALEXIS	-	
MCU-PH	GERMI	RAPHAELE	IBS – UMR 5075 CEA CNRS HIV & virus persistants Institut de Biologie Structurale	Oui
MCF	GEZE	ANNABELLE	DPM – UMR 5063 CNRS	Oui
MCF Emérite	GILLY	CATHERINE	DPM – UMR 5063 CNRS	équiv.
PU	GODIN-RIBUOT	DIANE	HP2 – INSERM U1042	Oui
MCF	GONINDARD	CHRISTELLE	LECA – UMR CNRS 5553	
Professeure Emérite	GRILLOT	RENEE	-	Oui
MCF	GUIEU	VALERIE	DPM – UMR 5063 CNRS	
CDD	HENNEBIQUE	AURELIE	TIMC-IMAG UMR 5525 CNRS, TheREx	
MCF	HININGER-FAVIER	ISABELLE	LBFA – INSERM U1055	
MCF	KHALEF	NAWEL	TIMC-IMAG UMR 5525 CNRS	
MCF	KOTZKI	SYLVAIN	HP2 – UMR S1042	
MCF	KRIVOBOK	SERGE	DPM – UMR 5063 CNRS	Oui
AHU	LEENHARDT	JULIEN	INSERM – U1039	
PU	LENORMAND	JEAN-LUC	TIMC-IMAG UMR 5525 CNRS, TheREx	Oui
PU	MARTIN	DONALD	TIMC-IMAG UMR 5525 CNRS	Oui
PRCE	MATTHYS	LAURENCE	-	
AHU	MINOVES	MELANIE	HP2 – INSERM U1042	
PU	MOINARD	CHRISTOPHE	LBFA - INSERM U1055	Oui
PU-PH	MOSSUZ	PASCAL	IAB – INSERM U1209	Oui
MCF	MOUHAMADOU	BELLO	LECA – UMR 5553 CNRS	Oui
MCF	NICOLLE	EDWIGE	DPM – UMR 5063 CNRS	
MCF	OUKACINE	FARID	DPM – UMR 5063 CNRS	Oui
MCF	PERES	BASILE	DPM – UMR 5063 CNRS	Oui
MCF	PEUCHMAUR	MARINE	DPM – UMR 5063 CNRS	Oui
PU	PEYRIN	ERIC	DPM – UMR 5063 CNRS	Oui
AHU	PLUCHART	HELENE	TIMC-IMAG – UMR 5525 CNRS, ThEMAS	
PU	RACHIDI	WALID	BGE/BIOMICS/ CEA	Oui
PU	RAVELET	CORINNE	DPM – UMR 5063 CNRS	Oui
PU	RIBUOT	CHRISTOPHE	HP2 – INSERM U1042	Oui
Professeure Emérite	ROUSSEL	ANNE-MARIE	-	Oui
PU-PH	SEVE	MICHEL	TIMC	Oui
MCF	SOUARD	FLORENCE	DPM – UMR 5063 CNRS	Oui

Mise à jour le 06/09/2021 Sana HACHANI

STATUT	NOM	PRENOM	LABORATOIRE	HDR
MCF	SPANO	MONIQUE	IBS – UMR 5075 CEA CNRS	
MCF	TARBOURIECH	NICOLAS	IBS – UMR 5075 CEA CNRS	
CDD	TRUFFOT	AURELIE		
MCF	VANHAVERBEKE	CECILE	DPM – UMR 5063 CNRS	
MCF	WARTHÉR	DAVID	DPM	
Professeur Emérite	WOUESSIDDJEWE	DENIS	-	Oui

AHU : Assistant Hospitalo-Universitaire

ATER : Attachés Temporaires d'Enseignement et de Recherches

BCI : Biologie du Cancer et de l'Infection

CHU : Centre Hospitalier Universitaire

CIB : Centre d'Innovation en Biologie

CRI : Centre de Recherche INSERM

CNRS : Centre National de Recherche Scientifique

DCE : Doctorants Contractuels Enseignement

DPM : Département de Pharmacochimie Moléculaire

HP2 : Hypoxie Physiopathologie Respiratoire et Cardiovasculaire

IAB : Institute for Advanced Biosciences

IBS : Institut de Biologie Structurale

LAPM : Laboratoire Adaptation et Pathogénèse des Microorganismes

LBFA : Laboratoire Bioénergétique Fondamentale et Appliquée

LCBM : Laboratoire Chimie et Biologie des Métaux

LCIB : Laboratoire de Chimie Inorganique et Biologie

LECA : Laboratoire d'Ecologie Alpine

LPSS : Laboratoire Parcours Santé Systémique

LR : Laboratoire des Radio pharmaceutiques

MAST : Maître de Conférences Associé à Temps Partiel

MCF : Maître de Conférences des Universités

MCU-PH : Maître de Conférences des Universités et Praticiens Hospitaliers

PAST : Professeur Associé à Temps Partiel

PRAG : Professeur Agrégé

PRCE : Professeur certifié affecté dans l'enseignement

PU : Professeur des Universités

PU-PH : Professeur des Universités et Praticiens Hospitaliers

SyMMES : Systèmes Moléculaires et nanoMatériaux pour l'Energie et la Santé

TIMC-IMAG : Laboratoire Technique de l'Imagerie, de la Modélisation

UMR: Unité Mixte de Recherche

UVHCI: Unit of Virus Host Cell Interactions

Remerciements

Aux membres de mon jury

A la Pr Raphèle Germi. Je te remercie d'avoir accepté de présider mon jury de thèse et de juger ce travail. Je tiens également à te remercier pour la très grande disponibilité dont tu as toujours fait preuve à mon égard, et pour avoir accepté de partager avec bonne humeur ton bureau avec moi. C'est toujours un plaisir de te voir au CHU.

A la Pr Florence Morfin-Sherpa, au Pr Jean-Yves Cesbron, au Dr Xavier Fonrose et au Dr Pascal Fender, pour avoir accepté de faire partie de mon jury de thèse et d'apporter une lecture critique sur ce travail grâce à leurs expertises respectives.

A mon directeur de thèse(s)

A Pascal. Merci de m'avoir accueillie dans cette formidable équipe il y a maintenant 5 ans, pour m'avoir proposé des sujets passionnants, qui m'ont fait grandement évoluer scientifiquement. Merci de m'avoir renouvelé ta confiance pour mener à bien ce projet en parallèle de ma thèse de sciences, où j'ai encore eu la chance de profiter de tes avis scientifiques toujours pertinents. Je te souhaite beaucoup de projets riches en anticorps neutralisants de toutes sortes, grâce au pipeline que tu auras eu la ténacité de faire installer à Grenoble.

Surtout, merci pour tous les conseils de randonnées, de restaurants de montagne, de podcasts qui auront égayé les pauses déjeuners !

Au service de virologie du CHU de Grenoble :

Au service de virologie du CHU de Grenoble : Au Pr Morand, Pr Larrat, Dr Faure, Dr Signori-Schmuck et tout.e.s les technicien.n.e.s pour leur accueil bienveillant durant toutes ces années.

A mes collègues de l'Institut de Biologie Structurale :

Special thanks to Sebastian, for your incredible patience, dedication, and passion for teaching (a sometimes very loudly and unstoppable passion!), I owe you a lot. Thanks for having made baby Axelle grow in the lab! If I glow a little bit today, it certainly because of you! I wish you a bright scientific future, full of galectins of all kinds.

A mes compères de paillasse, sans qui ma thèse aurait été nettement moins drôle :

A Romi, ma binôme de karaoké de laboratoire (team furby joyeux !!) Je te souhaite un futur à la hauteur de ton talent et de ton ambition ! (Quand tu en auras assez de sauver le monde du HIV, on construira enfin notre bar- salon de poterie féministe, pendant que Jean- Mi se moquera de nous.) Tu me manques.

A Jean-Mi(croondes), pour avoir toléré mes blagues douteuses sur ton prénom. Merci pour les fous rires interminables, les pauses double café vanille et les repas à base de « pizzas qui seraient meilleures chauffées ». Que la force des purificateurs de protéines t'accompagne pour ta dernière ligne droite.

A Benjamin, le roi des répertoires d'anticorps simulés et des lignes de codes mystérieuses, pour ta bonne humeur permanente.

A Marlyse, pour tous tes conseils techniques toujours à propos, mais surtout pour les innombrables recommandations de bons restaurants grenoblois!

A Isabelle, ingénierie sur-efficace, sur-dynamique et sur-motivée ! Merci pour tous tes conseils, dans la vie pro comme dans la vie perso !

A Laurence, marraine la bonne fée du laboratoire, toujours prête à rendre service, lancer une miniprep ... ou proposer des petits chocolats pour égayer les après-midis !

A Audrey le rhino et Alessandra le chamois, super lab-managers, vous m'avez toutes les deux tant appris. Merci pour votre gentillesse et votre soutien pendant les coups de moins bien de cette longue épopée.

A Héloïse, stagiaire passionnée et passionnante, qui aura égayé l'été 2020 placé sous le signe des ELISA.

Aux collaborateurs que j'ai eu la chance de rencontrer pendant ce projet : Miss Guidenn et le trio Fender : Chris, Salomé, et Solène ! Cela a été un plaisir de travailler avec vous, et j'espère avoir l'occasion de renouveler cette expérience. Mention spéciale à Pascal Fender, pour ta gentillesse, ta bonne humeur et ta réactivité !

Au Pr Winfried Weissenhorn, pour la confiance qu'il m'a accordé pour la réalisation des manipes d'évaluation de l'immunogénicité.

A mes enseignants

Au Pr Emmanuel Drouet, qui, sans le savoir, a orienté durablement mon parcours dès la première année grâce à son formidable enseignement de microbiologie destiné aux futurs pharmaciens.

Au Pr Jean-Luc Lenormand, professeur modèle pour son implication auprès des étudiants, et avec qui j'ai eu la chance d'enseigner en T.P. Votre pédagogie est une grande source d'inspiration.

A la Dr Delphine Aldebert, pour son accueil lors de mon stage volontaire de recherche de 3^{ème} année, qui a su me transmettre sa passion de la recherche.

Au Pr Cracowski, pour m'avoir le premier suggéré l'idée d'une revue anti-SARS-CoV-2.

A mes ami.e.s

L'Amie de toujours, la siamoise, la sœur, la jumelle : Laura - Petzélé. Merci d'avoir toujours été là, pour traverser joyeusement l'enfance, l'adolescence et l'âge adulte, mais surtout la crise de la trentaine à venir ! Tous ces moments ont été remplis de rires et de merveilleux souvenirs : les galas de natation synchronisées, nos premières vacances de grandes à l'UCPA, les voyages en Allemagne, au Chili, au Canada, à Montpellier et à Valence.... Je nous souhaite encore de belles micro-aventures toutes les deux, dans la Drôme, certes, mais pas que !

A Marianne Cumou, l'amatrice des bons mots qui « comptent +1000 », pour avoir partagé le collège, le lycée, puis la fac de pharma et les sorties GUCEM avec moi !

Aux amis que j'ai eu la chance de rencontrer sur les bancs de la fac (pour les plus assidus...) : A Auré, je nous souhaite de pouvoir encore refaire le monde des milliers de fois un verre de rouge à la main ! Et à Laura, ma couturière personnelle de chaussons tous doux !

A Lolo et Lélé, le duo gagnant, hâte de vous retrouver autour de ravioles des Grands Goulets, ou d'une leçon de twerk ! Merci pour tous ces week-ends placés sous le signe des fous rires !

A Camille, amie dans l'adversité du concours !

A Bérengère, pour nos dimanches-films de préparation de l'internat et pour nos nouveaux mardis -poterie !

An Alex und Klara. Danke für diese unzerstörbare Freundschaft, die die Jahre und die Entfernung überbrückt, ohne zu erlahmen. Ihr seid inspirierende Frauen und ich bin stolz, euch als Freundinnen zu haben.

A Emy, doctorante des quatre coins d'Europe, pour nos annuelles retrouvailles d' été au casse-croute à Dédé.

Aux amis que je n'attendais pas, Anthony, Alex et Maurane, pour nos discussions philosophiques et la passion du DEBAT !!

Aux belles rencontres du GUCEM, et surtout les copines de canyoning-resto, Andréa et Noémie, mais aussi William, le fameux scout belge organisateur !

A mes amis co-internes

A la petite team IPR grenobloise, mais surtout à Caro, pour m'avoir montré le chemin avec brio (quelle idée...), et à Antho, pour prendre fièrement la relève !

A Capucine, toujours prête à me moufler dans les grandes voies ! Merci de toujours me suivre dans mes plans plus ou moins foireux (au hasard les sorties spéléo...) Aux copines sportives, toujours prêtes à se joindre à nous : Anaëlle et Claire M !

A Tristan et Maud, et les voyages de darons dans leur Scénic. Vivement notre prochaine sortie gastronomique au Burger King !

Aux dinosaures, fine fleur de la biologie médicale : Simon, VTH, Claire, Théo, Léa, Aurélie, Fanny, VJP... Merci d'avoir égayé mon internat qui sans vous n'aurait pas été le même : les week-ends ski, les soirées, les concours de déguisement, les repas ratatouille/ frites de l'internat, les pauses soleil au R3...

A ma famille

A mes parents, pour leur soutien inconditionnel pendant ces longues années d'études. Merci d'avoir toujours cru en moi, et souvent à ma place... Mention spéciale pour l'aide logistique des années concours, des ravitaillements aux lessives tardives ! Mais surtout, merci de m'avoir transmis votre passion de la montagne, me permettant de me connecter avec ce qui compte vraiment, la nature, pendant les week-ends bien mérités. Je nous souhaite encore plein de belles randonnées et de via ferratas !

A mon frère, le seul, l'unique ! Merci d'avoir toujours été là (même à distance), de m'avoir supportée et de m'avoir fait rire. Je tiens à toi comme Mortie à King Julian.

A mes grands-parents (présents et partis), voici la première Docteure de la famille !

A ma belle-famille. Merci pour les séances piscine en pleine canicule, les paniers de courgettes qui font déborder le frigo, les boutures et les mille autres attentions ! A Coco la belle-sœur, pour les hamburgers du samedi soir et ta patience pendant nos parties d'overcooked !

A Quentin, pour le bonheur de vivre avec toi au quotidien. Merci pour ton infinie gentillesse, qui sublime ma vie depuis des années. Je t'aime.

Table des matières

Remerciements	7
Table des illustrations.....	16
Annexe	16
Liste des abréviations	17
Avant-propos	21
CHAPITRE 1 - TRAVAIL BIBLIOGRAPHIQUE : STRATÉGIES VACCINALES ANTI SARS CoV 2	23
1. Bref résumé de l'article en français	25
1.1 Les vaccins à virus entiers	26
1.2 Vaccins basés sur le spicule :	27
1.2.1 Les vaccins basés sur l'utilisation de spicule recombinant	27
1.2.2 Les vaccins géniques	27
1.3 Discussion et conclusion	29
2. Article original (rédigé en anglais) : COVID-19 vaccines : current platforms and future challenges	33
2.1 Introduction	33
2.2 Whole-virus based vaccines	36
2.2.1 Live attenuated viral vaccines	36
2.2.2 Inactivated vaccine	37
2.3 Spike-based vaccines	38
2.3.1 Recombinant spike glyprotein-based vaccines	40
2.3.1.1 Sub-unit vaccines	40
2.3.1.2 Nanoparticle vaccines and VLPs.....	41
2.3.2 Gene-based vaccines.....	42
2.3.2.1 Viral-vectored genetic vaccines.....	42
2.3.2.2 Nucleid acid-based vaccines	44
mRNA vaccines.....	44
DNA vaccines.....	45
2.4 Discussion.....	46
3. Bibliography	50
CHAPITRE 2 -TRAVAIL EXPERIMENTAL : ÉVALUATION DE L'IMMUNOGÉNICITÉ DE DEUX CANDIDATS VACCINAUX	55

1.Méthodologie	57
1.1 Méthodologie du test ELISA.....	57
1.2 Méthodologie du test de neutralisation.....	58
2. Induction de puissantes réponses anticorps neutralisantes anti-SARS-CoV-2 par immunisation, via l'utilisation d'une plateforme de multimérisation versatile inspirée des adénovirus.	63
2.1 Bref résumé de l'article en français :.....	63
2.2 Article original (rédigé en anglais) : Elicitation of potent SARS CoV 2 neutralising antibody responses through immunization with a versatile adenovirus-inspired multimerization platform.....	67
3. Une stratégie d'immunisation par pseudoparticules virales décorées de glycoprotéine S du SARS-CoV-2 protège les macaques de l'infection	103
3.1 Bref résumé de l'article en français	103
3.2 Article original (rédigé en anglais) : Immunization with synthetic SARS CoV 2 glycoprotein virus-like-particles protects macaques from infection	107
DISCUSSION	157
CONCLUSION	167
ANNEXE	173
SERMENT DE GALIEN	177
RESUME.....	183
ABSTRACT	185

Table des illustrations

Figure 1 : Comparative theoretical advantages of the different vaccine platforms that can be used in terms of cellular and humoral immune responses.

Figure 2 : Antigen choice for vaccine design.

Figure 3 : Principe de l'ELISA direct.

Figure 4 : Principe du test de neutralisation.

Figure 5 : Etapes de développement d'un vaccin.

Annexe

Tableau 1 : Tableau récapitulatif, simplifié et résumé des caractéristiques des deux études.

Liste des abréviations

ADCC: Antibody-Dependent Cell-mediated Cytotoxicity

ADCP: Antibody-Dependent Cellular Phagocytosis

ADE: Antibody Dependent Enhancement

ADN: Acide DésoxyriboNucléique

ARN: Acide Ribonucléique

ARNm: Acide Ribonucléique messager

Ac: Anticorps

AcN: Anticorps Neutralisant

BCR: B Cell Receptor

CD8: Cluster de Différenciation 8

HRP: Horseradish peroxidase

ELISA: Enzyme Linked Immunosorbent Assay

IC50: Concentration Inhibitrice médiane

Ig: Immunoglobuline

ND50: Dilution Neutralisante médiane.

OMS: Organisation Mondiale de la Santé

RBD: Receptor Binding Domain

RLU: Unité Relative de Lumière

TTIV: Thrombocytopénie immunitaire Thrombopénique Induite par le Vaccin

VOC: Variant Of Concern

WHO: World Health Organisation

Avant-propos

Le travail de recherche présenté dans ce document s'intéresse aux diverses stratégies vaccinales anti-SARS-CoV-2 et à des travaux développés à l'Institut de Biologie Structurale de Grenoble. Il est basé sur des articles rédigés en langue anglaise.

La première partie de cette thèse est un travail de recherche bibliographique ayant permis l'écriture d'une revue de la littérature des vaccins anti-SARS-CoV-2. Cette revue introductory permet de comprendre le contexte des travaux de recherche présentés dans la seconde partie. Elle aborde les problématiques rencontrées lors du choix de l'antigène pour le design vaccinal et présente les différentes stratégies utilisées lors du développement des vaccins anti-SARS-CoV-2.

La seconde partie de cette thèse est expérimentale. Elle présente les résultats obtenus pour deux projets d'évaluation pré-clinique de candidats vaccinaux anti-SARS-CoV-2, développés à l'IBS par les équipes du Pr Weissenhorn et du Dr Fender. L'évaluation de l'immunogénicité de ces candidats a été effectuée en collaboration avec l'équipe du Pr Poignard, équipe dans laquelle je réalise également ma thèse de sciences. J'ai réalisé la titration des réponses anticorps spécifiques du SARS-CoV-2, par la technique de l'ELISA (Enzyme Linked Immunosorbent Assay). J'ai également réalisé les analyses statistiques correspondantes pour le projet du Dr Fender. Les deux articles issus de ces projets sont à l'heure de ma soutenance en cours de révision, ils seront amenés à évoluer en fonction des remarques finales des reviewers.

Conçu comme une aide à la lecture, un tableau récapitulatif simplifié des deux études est mis à disposition à la fin de ce manuscrit, en annexe.

CHAPITRE 1

TRAVAIL BIBLIOGRAPHIQUE STRATÉGIES VACCINALES ANTI-SARS-CoV-2

1. Bref résumé de l'article en français

Le 11 mars 2020, devant la rapide propagation, le nombre et la fatalité des cas de COVID-19, l'Organisation Mondiale de la Santé (OMS) a catégorisé l'épidémie de SARS-CoV-2 comme une pandémie. Depuis, la pandémie a continué à faire des ravages autour du monde, causant au moins 5,3 millions de morts (chiffres de décembre 2021). Grâce à des avancées scientifiques majeures, des vaccins anti-COVID-19 ont rapidement été disponibles dans certains pays, permettant de ralentir la propagation de nouveaux cas. Cependant, l'apparition de variants du SARS-CoV-2, résistants à l'immunité post-infection et à l'immunité vaccinale, menace les progrès réalisés jusque-là. Nous exposerons les différentes stratégies vaccinales déployées pour développer une immunité protectrice contre le COVID-19, et de potentielles nouvelles pistes de développement. Ce résumé introductif est une version volontairement simplifiée et succincte de l'article de revue en anglais correspondant.

Pour comprendre les stratégies de mise au point de vaccins mentionnées plus bas, il est important de connaître quelques caractéristiques du SARS-CoV-2. La surface du SARS-CoV-2, un virus à ARN enveloppé, est décorée de spicules homotrimériques glycosylés de la glycoprotéine S (spike). Cette protéine est responsable de l'attachement du virus au récepteur ACE-2 retrouvé à la surface de certaines cellules du corps humain, notamment au niveau de l'épithélium pulmonaire. La fixation du spicule au récepteur ACE-2 permet l'entrée du virus dans les cellules cibles, puis sa multiplication. Il a par ailleurs été démontré que les patients infectés par le SARS-CoV-2 développent des anticorps anti-spicule et que certains de ces anticorps (Ac) ont des fonctions neutralisantes, c'est-à-dire sont capables de bloquer l'entrée du virus dans la cellule. Les taux élevés d'Ac neutralisants (AcN) sont associés à une meilleure protection contre le développement de formes sévères ou contre les réinfections, que ce soit dans les modèles animaux ou chez les patients infectés. Les AcN étant par ailleurs considérés comme un des mécanismes d'action principaux des vaccins anti-viraux, l'induction d'une réponse AcN est rapidement devenue un des objectifs majeurs de la vaccination anti-COVID-19, et le spike l'antigène de choix dans la mise au point des vaccins.

Brièvement, deux stratégies de développement d'un vaccin peuvent être distinguées et seront décrites ci-dessous. La méthode la plus ancienne consiste en l'utilisation du pathogène entier,

sous forme inactivée ou atténuée. A l'inverse, la méthode la plus moderne repose sur la mise au point rationnelle du vaccin, en sélectionnant avec précision l'antigène à utiliser et la technique de vectorisation adaptée.

1.1 Les vaccins à virus entiers

On distingue dans cette catégorie les virus vivants atténués et les virus inactivés. Ces vaccins contenant le virus entier, ils induisent des réponses humorales dirigées contre le spicule, dont des Ac neutralisants, mais aussi contre d'autres protéines virales, ainsi que des réponses cellulaires T cytotoxiques, ceci essentiellement pour les vaccins atténués.

Les vaccins à virus atténué utilisent des virus toujours capables de réPLICATION, mais qui ont perdu leur pathogénicité par accumulation de mutations, dont certaines vont toucher des gènes responsables de virulence. L'accumulation de mutations se fait de façon classique au fil de nombreux passages sur des lignées cellulaires souvent d'origine animale, qui aboutiront à une adaptation progressive du virus, et éventuellement à une perte du pouvoir pathogène. Ce processus est long, aléatoire, et ne permet pas d'exclure ensuite une réversion à l'état virulent. Il tend donc à être remplacé par des techniques de génie génétique visant à modifier ou à éliminer directement les gènes de virulence. Le seul candidat vaccin anti-COVID-19 à virus vivant atténué en phase 3, Codagenix, utilise enfin une technique d'inactivation novatrice basée sur la dé-optimisation de codons.

Dans le cas de vaccins à virus inactivés, les virus sont cultivés en laboratoire, puis récoltés et inactivés par des techniques physico-chimiques (utilisation de solvants, radiations, chaleur...), les privant définitivement de leur capacité de réPLICATION. L'immunogénicité de virus non réPLICATIFS est amoindrie, ils doivent être administrés avec des adjuvants pour obtenir une réponse immunitaire correcte. L'inactivation peut également modifier la conformation des glycoprotéines de surface, impactant la réponse humorale dirigée contre ces dernières. Trois vaccins inactivés sont largement utilisés aujourd'hui, essentiellement mis au point en Chine et en Inde : le Coronavac, le BBV152 et le BBIBP. Si cette technique est efficace et sûre, elle nécessite d'importantes capacités de culture cellulaire, processus long et peu adapté à une modification rapide du vaccin en cas d'émergence de nouveaux variants.

1.2 Vaccins basés sur le spicule :

Les vaccins basés sur l'utilisation du spicule peuvent soit utiliser cet antigène sous forme de protéine recombinante directement injectée au patient, soit être basés sur le matériel génétique codant pour le spicule, alors produit par les cellules du patient. Ces techniques nécessitent un important travail de caractérisation puis d'optimisation de l'antigène, comme expliqué plus en détail dans la revue.

1.2.1 Les vaccins basés sur l'utilisation de spicule recombinant

Deux méthodes d'utilisation du spicule recombinant comme antigène se distinguent. La première est l'injection de la protéine, accompagnée d'adjuvant : ce sont les vaccins sous-unitaires. Relativement peu immunogène, ce type de vaccin doit généralement être administré à des doses assez importantes et de façon répétée. De nombreux vaccins sous-unitaires anti-COVID ont été développés. Parmi eux, le vaccin Finlay FR-2 est basé sur un RBD recombinant couplé à la toxine tétanique.

L'autre option est la vectorisation du spicule recombinant par formulation de cette protéine avec des nanoparticules. Ces particules de relativement grande taille (1-1000 nm) peuvent à la fois être phagocytées par les cellules dendritiques et entrer dans les ganglions lymphatiques, assurant une forte réponse immunitaire. Présentés de façon répétée (multimérique) à la surface de la nanoparticule, les antigènes peuvent être reconnus par plusieurs BCR à la surface des lymphocytes B, entraînant une meilleure activation cellulaire et déclenchant ainsi la réponse immunitaire. C'est le cas du vaccin de Novavax, pour lequel des spicules sont assemblées de façon multimériques, formant une nanoparticule. Certains vaccins utilisent la capacité d'auto-assemblage de protéines virales pour former une pseudo-particule virale (VLP pour virus like particle en anglais) servant de nanoparticules. Le seul vaccin anti-COVID-19 utilisant cette stratégie et en phase 3 d'essais cliniques est le vaccin de Medicago.

1.2.2 Les vaccins géniques

L'injection du matériel génétique encodant l'antigène d'intérêt pour son expression dans les cellules du patient lui permet d'adopter une glycosylation et une conformation proche de la forme native de l'antigène tel qu'il est à la surface du virus, ce qui favorise une réponse Ac de bonne qualité. Avec les vaccins géniques, les peptides dérivés de la synthèse de l'antigène sont également présentés au système immunitaire via les protéines du Complexe Majeur

d’Histocompatibilité de classe I, pouvant induire une réponse cellulaire T CD8. Par ailleurs, la synthèse de la séquence codante pour l’antigène d’intérêt dans un vecteur vaccinal de type génique est un processus très rapide et versatile, rendant cette plateforme adaptée à un contexte pandémique. Il existe deux types de vaccins géniques : les vaccins géniques à vecteurs viraux, et les vaccins à acide nucléique, avec parmi eux les vaccins à ARN et les vaccins à ADN.

Les vaccins à vecteurs viraux sont très immunogéniques, bien tolérés et facilement stockables. La stratégie la plus fréquemment utilisée consiste à se servir d’un virus à la réPLICATION défective comme vecteur, souvent un Adénovirus modifié. Un inconvénient à l’utilisation d’un virus dont la prévalence est élevée dans la population générale est l’existence d’une pré-immunité contre le vecteur, pouvant diminuer l’immunogénérité du vaccin. Parmi les vaccins anti-COVID-19 les plus avancés, Astra Zeneca a contourné ce problème en utilisant un adénovirus de chimpanzé comme vecteur pour son vaccin ChAdOx1. ChAdOx1 est un vaccin non réPLICATIF codant pour la version non stabilisée du spicule.

Les vaccins à ARNm comportent la séquence codant pour l’antigène, avec généralement des modifications des nucléotides utilisés pour éviter une reconnaissance par le système immunitaire inné (vaccin à ARNm modifié). L’ARNm est formulé avec différentes compositions possibles de lipides ou de polymères, afin à la fois d’être protégés de la dégradation et d’augmenter l’absorption par les cellules présentatrices de l’antigène. Deux vaccins ARNm ont été parmi ceux autorisés les plus rapidement après le début de la pandémie, mis au point par Pfizer-BioNTech et Moderna.

A la différence des vaccins à ARNm, le matériel génétique injecté dans les vaccins à ADN est transcrit dans le noyau de la cellule. Afin que le plasmide encodant l’antigène atteigne le noyau, des routes d’administration particulières doivent être utilisées, rendant pour l’instant l’utilisation de ce genre de vaccin à grande échelle plus difficile. Pour exemple, le vaccin anti-COVID d’Inovio, un des vaccins les plus avancés en essais cliniques, s’administre en transcutané à l’aide d’un dispositif breveté. Un des avantages principaux des vaccins à ADN est leur grande stabilité.

1.3 Discussion et conclusion

Nous avons vu que de plusieurs vaccins anti-COVID-19 ont démontré lors des essais de phase 3 une très bonne efficacité contre l'apparition de symptômes et les formes sévères de la maladie, et sont maintenant sur le marché. Les deux vaccins les plus efficaces sont ceux à ARNm, mis au point par Pfizer et Moderna. La capacité de ces vaccins à protéger contre la COVID-19 a été confirmée dans les conditions réelles d'utilisation à grande échelle. Au-delà de la capacité des vaccins à éviter la maladie, de nombreuses études suggèrent qu'ils diminueraient la charge virale et la durée d'excrétion en cas d'infection, ayant donc un impact également sur la transmission, en tous cas pour la souche originelle de SARS-CoV-2.

Les vaccins anti-COVID sur le marché sont donc efficaces mais également bien tolérés, mis à part quelques rares réactions d'anaphylaxie, possibles lors de l'administration de tout vaccin. L'effet indésirable le plus grave, la thrombocytopénie immunitaire thrombopénique induite par le vaccin (TTIV), a été observé en phase 4 lors de l'administration des vaccins d'Astra-Zeneca et de Johnson & Johnson. Un autre effet indésirable récemment rapporté est la myocardite inflammatoire au décours d'une vaccination par vaccin à ARNm, ces deux effets indésirables restant extrêmement rares.

Malgré leur haute efficacité et leur bon profil de tolérance, deux facteurs font planer une menace sur le succès des vaccins anti-COVID-19. Le premier est l'affaiblissement progressif de la réponse immunitaire quelques mois après la vaccination. Le second est l'apparition de variants préoccupants du SARS-CoV-2, possédant une transmission augmentée, et une capacité potentielle à échapper à la réponse immunitaire induite par la vaccination ou développée par des individus convalescents, notamment du fait de mutations et changements consécutifs sur le spicule ou plus spécifiquement le RBD. Ces deux facteurs, baisse de l'immunité et apparition de variants, justifient le recours à l'administration d'une troisième dose, potentiellement avec un vaccin différent des deux premières injections, afin d'induire une réponse Ac plus élevée et plus prolongée. La diminution de l'efficacité mentionnée précédemment est principalement évaluée par une diminution des titres d'AcN. Il faut cependant garder à l'esprit que certaines plateformes vaccinales sont capables d'induire des réponses cellulaires T CD8+, aidant également à la protection anti-COVID-19, et qui pourraient persister plus longtemps.

La probabilité de l'émergence des variants étant corrélée à la circulation du virus dans la population globale, la meilleure façon de l'empêcher est le maintien des mesures de précaution, associé à des campagnes de vaccination massives avant même que de nouveaux variants émergent. En complément de ces mesures, il est possible d'imaginer la mise sur le marché rapide de vaccins adaptés aux variants. Par exemple, Moderna a très rapidement lancé un nouveau vaccin adapté au variant B.1.351, en modifiant la séquence codante pour le spicule, qui est actuellement testé en essais cliniques.

Afin d'éviter l'apparition d'une pandémie de cette ampleur dans le futur, des investissements massifs devront être fait dans les infrastructures de surveillance en augmentant les capacités de séquençage pour la détection de la (ré)émergence de pathogènes à potentiel pandémique. Par ailleurs, suivant l'observation que les virus au sein d'une même famille partagent les mêmes caractéristiques, les étudier de façon détaillée permettra à l'humanité d'être mieux préparée en cas d'émergence d'un pathogène au sein de cette famille. Cette stratégie a été théorisée par B. Graham et K. Corbett sous le nom d'« approche par prototype de pathogène ».

Deux mille vingt-deux sera probablement l'année de l'émergence de vaccins anti-COVID-19 de seconde génération, pouvant remplacer les premiers vaccins développés, grâce à des avancées notables, notamment en termes de stockage, de facilité de production, de coûts... Ces vaccins de seconde génération pourront ainsi venir en renfort des capacités de production globale, permettant à la population mondiale de rêver à une couverture vaccinale complète et un retour à l'état prépandémique.

2. Article original (rédigé en anglais) : COVID-19 vaccines : current platforms and future challenges

2.1 Introduction

On the 11th of March 2020, the WHO declared a state of pandemic due to SARS-CoV-2, the causative agent of COVID-19. Ever since, the pandemic has continued unabated throughout the world, causing as of December 2022, more than 5,3 million deaths (1). Thanks to recent scientific advances and the combined efforts of the scientific community, a number of vaccines have been rapidly developed across the world. Their use, although impaired by unequal distribution across the planet, started to put a dent in the course of the pandemic, but the appearance of new coronavirus variants, potentially resistant to vaccine-induced immunity, may jeopardize the progresses made so far. In this review we will expose the different vaccines strategies that have been developed to date to elicit protective immunity against COVID-19 and discuss potential new avenues.

Vaccines are “a simple, safe and effective way of protecting people against harmful diseases before they come in contact with them” as defined by the WHO. To be effective on a broad scale, immune responses need to be induced in a large fraction of the vaccinees and offer long term protection, ideally during years or even a lifetime. Similarly, vaccines against COVID-19 aim to prevent disease, in particular severe cases. They can also have further goals and consequences: to prevent infection, transmission, and long COVID. All these goals have been to various extents fulfilled by current vaccines, although some aspects of vaccination outcomes are still being studied.

A good understanding of the virus lifecycle and physiopathology, based notably on previous research work on other pathogenic human coronaviruses such as MERS-CoV (2) and SARS-CoV (3), has helped the rapid design of COVID vaccines. As for the other coronaviruses, SARS-CoV-2 has various structural proteins: the nucleocapsid (N), membrane (M), envelope (E) and spike (S). The viral spike is made of a trimer of the S glycoprotein, which belongs to type 1 fusion proteins and is composed of two domains: S1 and S2 (4). The S1 domain binds to the ACE-2 receptor on target cells through its Receptor Binding Domain (RBD) (5), leading to conformational changes from pre-fusion to post-fusion form, leading to viral entry. Cells expressing the ACE-2 receptor are very abundant in the trachea and lung epithelium (among

other localizations), explaining much of the virus tropism and physiopathology. Two entry pathways have been described for SARS-CoV-2, either through direct fusion at the cell membrane or following endocytic uptake. In both cases, fusion requires cleavage of the S2 domain through either the cell surface protease TMPRSS2 or cathepsins located in endocytic vesicles. Infection of target cells is largely dependent on the expression of such factors.

The viral spike is of particular importance for vaccine design as, being exposed on the viral surface and used for entry, it is the target of neutralizing antibodies. One of the main mechanism of action of neutralizing antibodies (nAbs) is the blocking of viral entry blocking by inhibition of the interaction between viral surface proteins and cell receptors (ACE-2 receptor in the case of SARS-CoV-2) (6). Neutralization is considered as one of the main mechanism of anti-viral vaccine-induced protection and as such, vaccines aiming to induce nAbs and therefore using the spike protein as an antigen have been sought early on to fight COVID-19 (7) (8). In addition, beside their neutralizing capacity, nAbs can potentially trigger Fc-mediated functions such as complement activation, antibody dependent phagocytosis (ADCP), and antibody dependent cell-mediated cytotoxicity (ADCC). All these effector functions may also potentially play a role in antibody (Ab)-mediated protection against disease (9).

SARS-CoV-2 research has from early on focused on confirming the existence and activity of anti-spike nAbs, leading to the rapid isolation of potent nAbs and their development for COVID-19 prevention and treatment. Rapidly, studies further confirmed the importance of nAbs in protection against SARS-CoV-2 infection and COVID-19. Most of infected people were shown to develop anti-spike humoral immunity with various levels of detectable nAbs (10) (11), and a correlation was shown between the presence of nAbs and protection against reinfection (12). Furthermore, it was demonstrated in various animal models that passive transfer of immune serum or later on of monoclonal nAbs could protect against reinfection and disease (13) (14) (15). This was also further evidenced by protection of individuals through administration of monoclonal nAbs (16) (17). Of note, the importance of effector functions such as ADCC and ADCP in protection are less clear. There was an early fear that a SARS-CoV-2 vaccine could lead to Antibody Dependent Enhancement (ADE) of disease through Fc binding (18), from observations made in vitro and in vivo with MERS-CoV (19) and SARS-CoV (20). Fortunately, to date, observations from vaccination campaign in real-world settings did not report any ADE-related effects. Although early emphasis has been on nAbs, T cells are certainly an important component of vaccine induced immunity, in particular to prevent severe

forms of the infection, likely conferring an advantage to vaccine platforms able to elicit both strong B and T cell responses (21) .

Roughly, two broad approaches can be used to design a vaccine: approaches largely based on empirical know-how and classical/historical platforms: using the pathogen as a whole, but deprived of its virulence capacity, in two possible forms, either live attenuated or inactivated. Immunisation with the modified pathogen induces an immune response mimicking to different extent the one developed through natural infection. Towards the end of the 20th century and beginning of the 21st century, new approaches based on rational vaccine antigen design were developed, involving in particular the selection of precise antigens, and new vectorisation methods. Such approaches require an understanding of correlates of protection and in the case of COVID-19, have been essentially focused on using the spike as an antigen, as explained above.

A very large number of vaccines and vaccine candidates have thus been developed since the beginning of the pandemic (an exhaustive list can be followed through WHO vaccine landscape tracker (22)), exceeding all the expectations from scientists predicting that a licensed vaccine would not be available before 2022 (23). Many have failed, a large number are still in development, and a number have now been authorized for emergency used, or fully approved. This review proposes an overview of current SARS-CoV-2 vaccines strategies with emphasis on phase 3 studied and authorized vaccines as of November 2021.

Sars-Cov-2 vaccines

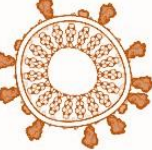
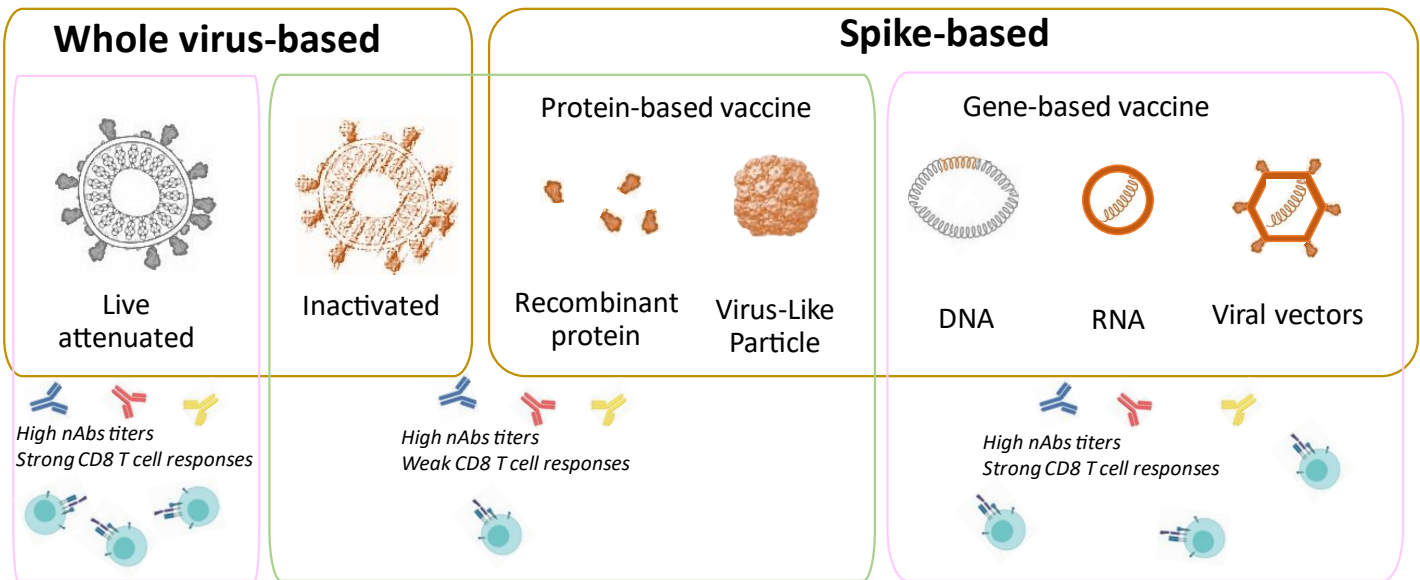



Figure 1: Comparative theoretical advantages of the different vaccine platforms that can be used in terms of cellular and humoral immune responses. Adapted from Pr Crackowski.

2.2 Whole-virus based vaccines

Whole-virus based vaccines use viruses deprived from their virulence capacities, either through attenuation or inactivation. They also aim to elicit spike specific neutralizing antibodies, as explained previously, but in addition they eventually may elicit other Abs (against internal proteins) of less clear interest, along with T cell responses. Regarding cytotoxic CD8 T cell responses, they are essentially induced by attenuated vaccines, and not so much by the inactivated ones.

2.2.1 Live attenuated viral vaccines

In this approach, the virus remains able to replicate, but due to an attenuation process, leads to the elicitation of protective immune responses in absence of disease. A balance therefore has to be achieved: the virus must be attenuated enough to avoid pathogenicity but remain able to replicate enough to induce protective immune responses. Different attenuation methods have been used in the past: classically the virus is passaged a numerous amount of times on various cell types, often from animal origin, or in animal models, in order to lose its

in vivo pathogenicity/virulence, through progressive accumulation of mutations. This approach is time consuming and empirical, which makes it less suitable for emerging pathogens in a pandemic as for SARS-CoV-2. In addition, a risk of reversion may remain, as well as the possibility to be pathogenic when administered to immunocompromised patients. Modern alternatives have enabled an accelerated attenuation process and have also been optimized to abrogate the risk of virulence reversion. They are largely based on a precise understanding of viral genes important for virulence and the construction via biotechnology of a virus with deletions or modifications of these genes. No COVID-19 vaccine using such method has advanced to date to clinical trials. Alternatively, a more recent and innovative approach for attenuation, based on codon deoptimization, has been developed by Codagenix which vaccine candidate is now advancing to phase 2-3 (24). Interestingly, this vaccine candidate is administered through a nasal spray in order to induce mucosal immunity.

2.2.2 Inactivated vaccine

Inactivated viruses have been used since the early days of vaccinology to produce many different anti-viral vaccines, as the common measles, mumps and rubella vaccines. Consequently, virus inactivation methods have been used by many to produce a COVID-19 vaccine. Inactivated virus vaccines are made from viruses cultivated in large scales and then inactivated through chemical (beta propiolactone, formalin...) or physical processes (heat, gamma irradiation...). Such process fully blocks the ability of the virus to replicate, nevertheless allowing through immunization the elicitation of a protective immune response. Inactivated virus-based vaccines consequently have a better safety profile than those using attenuated viruses. However, the lack of replication tends to strongly decrease the immunogenic potential compared to attenuated virus vaccines, thus inactivated virus vaccines require the use of adjuvants and multiple dose administration. The inactivation process may also be detrimental to surface glycoproteins, decreasing their quantity or modifying their conformation, which may negatively impact antigenicity and immunogenicity and thus the quality of the elicited nAb response. In addition, cellular cytotoxic responses are inconsistently induced by inactivated virus vaccines in contrast to the attenuated ones. Overall, inactivated virus vaccines thus tend to induce strong Ab responses but rather poor cellular immunity (CD8).

The most advanced vaccines in this category are from Sinovac Biotech with its Coronavac vaccine (25), Bharat Biotech with its BBV152 vaccine and Sinopharm with its BBIBP. Those

have now been largely approved and are being used across the world. Of note, different adjuvancement techniques have been chosen for these vaccines. For example, BBV152 is formulated with a toll like receptor (TLR) 7/8 agonist molecule, adsorbed to alum (Algel), when BBIBP and CoronaVac are more classically formulated with alum. Interestingly, the French vaccine maker Valneva also designed a vaccine based on chemically inactivated coronaviruses, that recently advanced to phase 3.

2.3 Spike-based vaccines

Rational vaccine design based on immunization with a single antigen first requires the identification of correlates of protection. As explained above, nAbs targeting the S proteins of SARS-CoV-2 have been shown to protect in animal models and in humans, as well as correlate with protection in convalescent individuals, leading to the development of a great number of spike-based vaccines, essentially aiming at eliciting nAb responses.

Spike-based vaccines can be of 2 natures: protein-based vaccines using recombinant spike or sub-domains, or genomic vaccines carrying the gene encoding for the spike, as detailed below. Proper antigen design is a crucial step for these approaches. As mentioned above, the S glycoprotein assembles in a trimer and vaccines based on the whole viral spike have all been designed using a trimeric conformation. Such strategy largely came from studies in the HIV vaccine field, that demonstrated a better antigenicity of the gp120 protein in its trimeric form as compared to the monomer (26). However, the S trimer in its prefusion conformation is in a metastable state, making it difficult to produce and leading to heterogenous batches (27). Thus, techniques have been developed to block the SARS-CoV-2 spike in a pre-fusion metastable state, making it a suitable antigen to induce nAbs. One of this technique consists in proline substitution, extensively studied on other class I viral fusion glycoproteins (28) from HIV, RSV (29), Flu (Hemagglutinin), Ebola, PiV5, Nipah and Hendra viruses (30). Because of their chemical properties, prolines both disfavour helix formation and confer local rigidity to a polypeptide chain. Proline substitutions had notably also been applied to other coronaviruses, such as SARS-CoV and MERS-CoV (2), and the same strategy was thus applied for the design of the SARS-CoV-2 spike to be used in vaccines. This led to the design of a SARS-CoV-2 prefusion spike stabilized by two substitutions (K986P and V987P), called S-2P. All spike-based vaccines in phase 3 clinical trials and beyond are based on the S-2P conformation, with the exception of the Astra Zeneca, CansinoBio5 and Gamaleya vaccines which are based on the

S wild type sequence. The use of this wild-type conformation has been proposed as a hypothesis for the somehow lower efficacy of the Astra-Zeneca vaccine (30). Following the S-2P design, a new construction was described with four more prolines substitutions, and shown to be even more stable (31). Further-generation of SARS-CoV-2 vaccines may contain hexa-pro-spikes or newly designed stabilized antigens potentially even more promising (32) (i.e : S2G-delta-HR2, a spike deprived from its heptad repeat 2 domain, responsible for spike metastability).

An alternative to the use of the whole S protein for nAbs induction is to use the RBD, which is the principal target of nAbs following infection (33). However, it has been shown that there are neutralizing epitopes outside the RBD (34) and using the whole S could be advantageous as it may elicit broader nAb responses. In addition, for platforms able to induce CD8 T cells, choosing to use of the whole spike protein instead of the RBD may allow for the elicitation of T cells against a greater diversity of epitopes, thus potentializing cellular responses.

Finally, although the majority of vaccines in this category have been based on spike only, a few have chosen to incorporate other proteins. We can cite as examples the use of a synthetic poxvirus platform to design a multi-antigenic SARS CoV 2 vaccine candidate co-expressing the spike and nucleocapsid antigens (35), and the Immunity Bio vaccine, an adenovirus-based viral vectored vaccine carrying two genes, one coding for the spike protein and the other for the nucleocapsid. Using several proteins instead of the spike only as antigens (multi-antigenic vaccines) notably increases the number of T cells epitopes targeted and may potentially offer a better protection.

Choice of immunogen

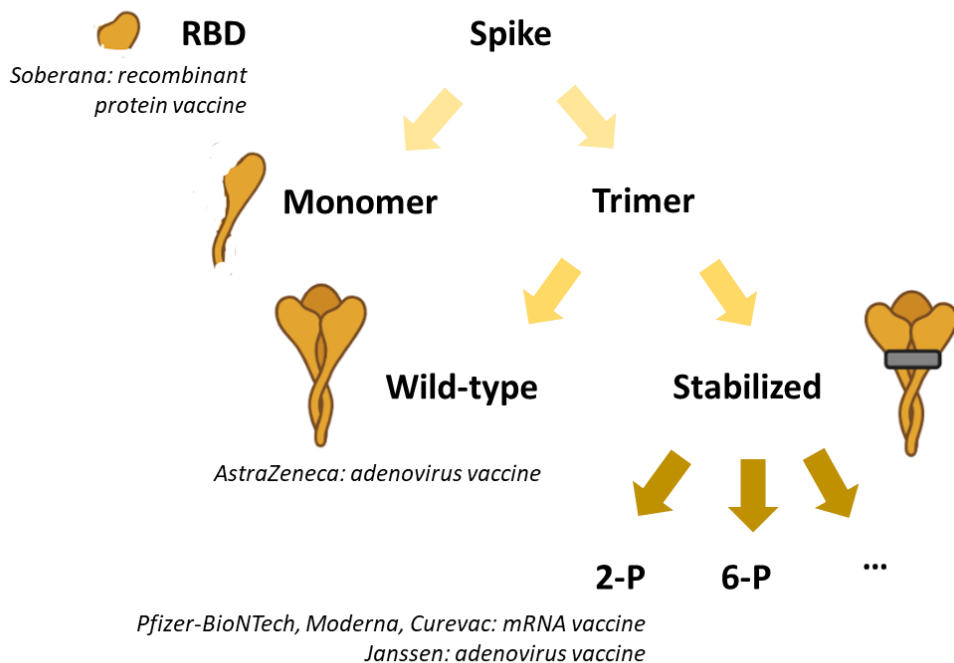


Figure 2: Antigen choice. Different antigenic forms of the S glycoprotein can be chosen when designing a SARS-CoV-2 vaccine, each having different advantages in term of immunogenicity and stability. Research teams have used either the S proteins as a whole or only the RBD. The spike can be produced either in a monomeric or a trimeric form. Trimeric spikes can be either in a wild type or in a stabilized conformation. Most of the vaccine candidates to date have been designed with the 2-P stabilized version of the spike, but new constructions will may be used in the future.

2.3.1 Recombinant spike glycoprotein-based vaccines

In this approach, protein antigens are directly used for immunization, in order to stimulate the immune system. Antigens can be either formulated as such, accompanied by adjuvants (protein sub-unit vaccines), or formulated with nanoparticles/VLPs.

2.3.1.1 Sub-unit vaccines

In such vaccines, proteins are nowadays produced through recombinant technology. The recombinant protein is expressed and purified, to be finally formulated with adjuvants. Indeed, because protein sub-unit vaccines are poorly immunogenic per se, they have to be administered

repeatedly, at relatively high dosage, and accompanied by adjuvants (36). Protein sub-unit vaccine design has benefited from significant advances made in the field of adjuvantation over the last decades. If before the 1990s, the only additive available was aluminium, new products have since entered the market: emulsions (i.e MF59 and AS0), toll-like receptor agonists (GpG) or combinations of immunopotentiators (QS-21 and MPL) (37). As elderly people immunity is waning with age, adjuvantation is also a powerful tool to increase vaccine immunogenicity in this population, which is also the most at risk to declare severe COVID-19.

In the COVID -19 field, 14 (as of December 2021) protein sub-unit vaccines have reached the stage of phase 3 clinical trial. Among them, the Anhui Biopharmaceutical and Finlay FR-2 vaccine are based on RBD protein, conjugated to tetanus toxoid and adjuvanted with aluminium for the latter.

2.3.1.2 Nanoparticle vaccines and VLPs

In this approach, protein antigens are formulated with nanoparticles (particles with size 1-1000 nm) to increase stability following injection and to enhance immunogenicity (38). Their relatively big size allows for both dendritic cells uptake and entry into the lymph node, stimulating both humoral and cellular immune responses. Broadly speaking, nanoparticles complexes can be formulated via in two different ways, either by adsorption at the surface or by encapsulation, each presenting different advantages. Encapsulation protects the antigen from proteases while nanoparticle surface decoration allows for the display of a high density of repetitive epitopes to be presented. This high epitope density or multimerization (39) tends to induce stronger B cell immune responses, notably via BCR cross-linking (40), favoring B cell activation. Nanoparticle-based vaccines are diverse and versatile: indeed, different antigens can be grafted onto the surface of a diversity of type of nanoparticles to create different vaccine candidates. For example, the Kwong team designed candidates based on nanoparticles from *Aquiflex aeolius* lumazine synthase and *Helicobacter pylori* ferritin grafted with various trimeric antigens (either from syncytial virus fusion F glycoprotein, parainfluenza virus type 3 F glycoprotein, or SARS-CoV-2 glycoprotein), allowing for a rapid turnaround design adapted to pandemic circumstances (41).

In the COVID-19 vaccines field, Novavax with its NVX-CoV2373 is the most advanced protein nanoparticle vaccine. NVX-CoV2373 is based on trimeric full-length protein S stabilized in a

pre-fusion conformation, produced in insect cells, that assemble in a multimeric pattern. Those nanoparticles are administered with the saponin-based M-Matrix adjuvant(42).

Among nanoparticle vaccines, virus-like particles (VLPs) are a particular sub-category. VLPs are “self-assembling systems that spontaneously form virus-shaped particles following expression of one or several viral proteins, often adopting a icosahedral or rod-like structure” (43). In the COVID-19 vaccine field, Medicago is the most advanced biotechnology firm in the VLP vaccine pipeline. Its candidate, CoVLP (for CoronaVirus Like Particle), is a VLP produced by the transient transfection of *Nicotiana benthamiana* plants, displaying stabilized pre-fusion spikes at its surface. CoVLP has recently advanced to phase 3 (44).

2.3.2 Gene-based vaccines

Gene-carrying vaccines are the most recent vaccine platforms developed. Two designs are available: viral-vectored vaccines and genomic vaccines (which comprise RNA and DNA vaccines), each of these platforms will be described below. They contrast with traditional vaccinology approaches where either the whole pathogen or protein subunits from it are directly administered. Instead, it is the genomic material coding for a protein (or proteins) chosen as immunogen which is injected to individuals for production in host cells. Once incorporated into host cells, the genomic material is processed via the cellular machinery to produce the desired antigen. This protein can be designed to get anchored on the cell surface or secreted, depending on the vaccine. Because protein expression takes place in host cells, proper folding, protein glycosylation and other posttranslational modifications are respected, thus mimicking the native conformation at viral surface as produced during natural infection. In addition, such pathway insures efficient presentation through CMH class I proteins and thus elicitation of strong T cell responses.

2.3.2.1 Viral-vectored genetic vaccines

Viral vectored vaccines are a great option, thanks to their usually high immunogenicity combined to good safety performances and easy storage conditions. As mentioned above, the goal of the viral vector is to carry the genomic information encoding for the antigen of choice. Consequently, viral vectors must be genetically stable, able to tolerate insertions in their genome, and non-pathogenic. Naturally poorly pathogenic or attenuated viruses can be used:

adenovirus, measles, modified vaccinia Ankara, vesicular stomatitis viruses have all been proposed as viral vectors. Adenoviruses are the most used vectors for SARS-CoV-2 vaccines. They are non-enveloped double stranded DNA (sDNA) viruses with big genomic content packaging capacity that make them popular (45). Even if viral vector vaccines have been used for many veterinary diseases, before COVID-19 pandemic only one vaccine had been approved to prevent a human disease: Ebola (using an Ad26-MVA based prime boost vaccine) (46).

Four different types of viral vectors vaccines exist (45): replication defective; replication competent, single cycle defective and finally multisegmented viral vectors (those last two being very rarely used). Use of replication defective vectors is the most popular strategy, notably because of its good safety profile: replication has been made impossible by deleting part of the viral genome. An example of this strategy is the Ad26.COV2.S vaccine developed by Johnson and Johnson, benefiting from the firm experience with its commercialized Ad26.ZEBOV/MVA-BN-Filo Ebola vaccine. Indeed, this non-replicating vaccine uses Ad26 as a vector to express the stabilized pre-fusion spike (47) (48).

In contrast, replicative vectors can perform several cycles. Because of this replication process, high immunogenicity profiles can be achieved. As a poorly pathogenic virus is used, the host immune system is able to control the infection by itself and clear the virus after a few cycles. Obviously, those vaccines are not usable in immunocompromised patients. Mucosal administration routes can be chosen for such replicative vectors, aiming to trigger immunity in a similar way as following natural infection. The most advanced replicative COVID-19 vaccine candidate, delns1-2019-ncov-rbd-opt1 (developed by Wantaiii) is precisely intranasal. The goal is to induce strong intra-nasal humoral response, to efficiently block infection and transmission.

A potential issue with strategies using common viruses as vectors is that a non-negligible fraction of the population can have a pre-existing anti-vector immunity, developed through natural infection, which may impair immunogenicity (49). An alternative to circumvent this problem is to use viruses infecting animals but not humans. This is the strategy used by AstraZeneca with the ChAdOx1 vaccine which uses a chimpanzee adenovirus as a vector (50). ChAdOx1 is a non-replicative vaccine encoding for the wild type version of the spike. Because pre-immunization can also be vaccine-induced and observed in a homologous prime-boost setting, some vaccines use heterologous prime-boost regimens with one type of virus for priming and another one for boosting. This strategy has been used by the Gamaleya Institute to

create an Ebola vaccine, based on a prime with Ad5 vector and a boost with a VSV vector (51) (52). Logically, they used their experience to develop the Gam-COVID-Vac vaccine (also known as Sputnik V vaccine). Gam-COVID-Vac is based on a heterologous prime-boost regimen: prime uses the Ad26, followed by injection 21 days later of a boost based on Ad5.

2.3.2.2 Nucleid acid-based vaccines

mRNA vaccines

While it is possible to inject naked RNA, most mRNAs vaccines are formulated with different lipid compositions, polymers or liposomes, preventing its degradation, and increasing its uptake by antigen presenting cells (53) (54). Moreover, to induce optimal immunogenicity and avoid recognition by innate immunity sensors (TLRs) and degradation, the antigen mRNA coding sequence has to be designed properly (55). Modifications enhancing stability such as addition of a 5' cap, modification of the poly A tail can be added. Notably in “modified” RNA vaccines, the use of naturally occurring modified nucleosides such as methylpseudouridines ensure that the mRNA does not activate innate immunity through TLR recognition, leading to proper translation and antigen expression. Both authorized COVID-19 mRNA vaccines, from Pfizer and Moderna, use modified nucleosides. However, mRNA vaccine with non-modified nucleosides but optimized non-coding regions such as the one from CureVac (CVnCoV) are also starting to prove highly immunogenic in recent studies (56).

Among mRNA vaccines, two designs can be distinguished: either “regular” mRNA vaccines, or self-amplifying mRNA vaccines. In the case of self-amplifying mRNA vaccine vaccines, an additional gene coding for a replicase is added to the sequence of interest. Replicases are enzymes that replicate the RNA before translation. The expected advantage of this supplementary step is to increase the quantity of genetic material available for ribosome transduction, and consequently the amount of protein produced (57). Theoretically, a far lower quantity of mRNA is required for inducing an equivalent immunogenicity, therefore reducing costs. “Regular” mRNA vaccines were the first vaccines approved in the COVID-19 vaccine landscape.

Indeed, Pfizer-BioNTech was the first firm to get an FDA authorization for a mRNA COVID-19 vaccine. The manufacturing of mRNA vaccines is a very flexible process and allowed Pfizer-

BioNTech to develop both soluble trimerized RBD and membrane bound full length prefusion stabilized spike protein vaccine candidates, respectively BNT162b1 (58) (59) and BNT162b2. The final choice driving the decision to select BNT162b2 coding for a membrane anchored spike protein was its milder systemic reactogenicity profile, together with a similar Ab responses compared to BNT162b1 (60) (61) (62). A week later, Moderna mRNA 1273 vaccine also got approved by the FDA. It is a lipid nanoparticle encapsulated mRNA vaccine that encodes for the prefusion stabilized spike protein. When administered to non-human primates (NHP), mRNA 1273 induced Ab production at levels superior to those observed in convalescent people and a rapid clearance of the viral replication in both upper and lower airways.

DNA vaccines (63)

The transcription of DNA vaccine takes place in the nucleus instead of the cytosol for RNA vaccines. Once inside the host cell nucleus, the DNA template is used to create many mRNAs, thus leading to the production of more antigens per cells compared to regular mRNA vaccines (64). (In this sense, DNA vaccine are somehow similar to self-amplifying mRNA vaccines). For plasmid to reach the nucleus, specific administration routes or devices had to be explored. The most documented option is the intramuscular administration with an electroporation device. This delivery strategy has been chosen by Inovio, with its INO-4800 vaccine administered by Cellectra, Innovio's patented electroporation device. A second route is the transdermal administration, that engages antigen presentation via dendritic cells. The third potential route is the most invasive and consists of intravenous injection of the vaccine, so that plasmidic DNA can reach secondary lymphoid organs. Because they for the most need special devices or special skills, administration methods required for DNA administration are still a major obstacle to the development of large-scale vaccination programs. However, DNA vaccines have two interesting advantages when compared to mRNA ones in mass-vaccination onsets. First, production of large quantities of plasmidic DNA in E.Coli strains allows a rapid scale-up in production capacities. Another major advantage is the thermostability of plasmidic DNA, stable as long as one year at room temperature, particularly convenient in countries with a poor cold-chain. One of the most advanced DNA vaccine in this pipeline, INO-4800 from Inovio, encoding for the whole spike protein, demonstrated it was well tolerated and induced high levels of Ab responses, and is currently studied in phase 3 clinical trials.

2.4 Discussion

As seen in this review, many different vaccines have emerged following the COVID-19 pandemic. Although some candidates did give some disappointing results and were abandoned, a number of approaches led to the development of safe and effective vaccines in a record time. Several vaccines have thus been authorized by the regulatory and health agencies of countries around the world, billions of people have now been vaccinated and studied in phase 4, generating a massive amount of data and publications. Overall, among authorized vaccines, the two most efficient appear to be the mRNA vaccines designed by Pfizer/BioNTech and Moderna, which both showed about 95% efficacy in phase 3 studies, with close to 100% efficacy against severe disease (61) (65). Nicely, real world effectiveness was further confirmed at similar levels (66). The adenovirus-based vaccines also showed strong efficacy, although overall lower than the RNA vaccines. In phase 3 studies the Gamaleya Sputnik vaccine showed 91% efficacy (51), compared to 76% and 72% for the AstraZeneca and J&J vaccines, respectively (67) (68). Of note, these numbers may vary, notably between populations, risk of being infected, and time since vaccination, which can all impact effectiveness. Concerning the inactivated vaccines, they also offer strong protection, the Sinopharm and CoronaVac ones having an efficacy of 79% and 51%, respectively (69) (70). Doses of these 2 vaccines have been delivered to more than 3 billion people world-wide, representing an important fraction of the global vaccination effort. Finally, the Novavax protein-based vaccine was recently shown to perform strongly, with 90% efficacy against symptomatic infection and 100% against moderate and severe disease in a Phase 3 trial (71).

Beyond the effectiveness of vaccines in reducing the onset of symptoms, several studies suggest that vaccines are also efficient at decreasing viral load and/or length of virus excretion in people infected despite vaccination, having therefore a potential impact on transmission (72) (73). Their potential effect on preventing long COVID is however still under investigation.

Overall, all vaccines authorized to date have been remarkably well tolerated, with a good safety track record. For the most, side effects have been mild and of short duration, serious safety problems being extremely rare. Apart from very rare anaphylaxis issues, the most serious undesirable effect has been observed following Astra-Zeneca (74) (75) and Johnson & Johnson vaccination, in the phase 4 follow up. This side effect termed vaccine induced prothrombotic immune thrombocytopenia (VITPI) is a condition of blood clots associated with low platelet

counts, that occurs following receipt of the vaccine. The likely mechanism is antibodies that induce massive platelet activation, reducing platelet count and causing thrombosis although the full mechanism remains to be elucidated. This effect led to suspension of the deployment of those vaccines to various extents, depending on the country, with mostly limitations based on young age. However, some countries have simply banned the use of the Astra-Zeneca and Janssen vaccines, such as Denmark on the 14th of April. If the causes of VIPIT remain to be elucidated, they are probably related to the use of the adenovirus viral vector and not the spike antigen, as these undesirable effects have not been observed with the other vaccine platforms. Another milder side effect has been observed following mRNA vaccination: myocarditis with for the most only mild and short-lived forms and rapidly get cured with proper anti-inflammatory treatment. Moreover, the study from Hippisley – Cox and al (76) showed that the risk of myocarditis following a mRNA vaccine was only significantly increased for people younger than 40. For older people, the risk was higher to suffer from a myocarditis caused by SARS-CoV-2 infection.

COVID-19 vaccines have therefore demonstrated a high effectiveness and a strong safety profile. However, two factors may jeopardize this remarkable success. First, it was rapidly realized that vaccine-elicited immunity had a tendency to wane over time, for all vaccines but more so for the inactivated ones (77). Concerning the mRNA vaccines, the Pfizer vaccine-induced immunity also appears to diminish somehow faster than following vaccination with the Moderna jab. The decline in nAbs titers with time was soon confirmed to be associated with a decrease in protection against infection, and to a lower extend against severe disease, suggesting a need for booster shots, that have been shown to greatly increase Ab levels (78).

As an additional concern and challenge to the control of the pandemic, new variants of SARS-CoV-2 rapidly emerged and started spreading around the globe. The variants of concern can present increased transmissibility, modified virulence and the potential ability to escape immunity from vaccinated and convalescent individuals. Indeed, changes are found in the RBD and outside in the S protein at sites targeted by neutralizing antibodies. Several variants of concern have now been characterized, none of them to date strongly evading vaccine immunity (79). However, such possibility is an additional argument to the need for a booster shot, as previously demonstrated in animal models, where administration of a third dose in an homologous prime-boosts schema restored nAbs levels against variants (80). Emergence of variants of concern also led to the design of vaccines adapted to new circulating strains, such as with mRNA vaccines which sequences can be rapidly modified and accommodate new

mutations. For example, Moderna rapidly launched a clinical trial (NCT04785144) with a new vaccine version adapted to B.1.351 variant.

As an additional approach to reinforce immunity through vaccination, “mix and matches” approaches (aka heterologous prime-boost(s) administration) are being studied (81) to find combinations that may lead to greater and more prolong Ab responses.

Of note, the decrease in vaccine efficacy discussed above likely depends essentially on decreasing serum neutralizing capacities against variants. However, as mentioned in introduction, some vaccine platforms, such as mRNA and viral vectors, can also induce strong CD8 T cell responses. Quite schematically, if the humoral response is held responsible for early protective immunity, the T cell response is held responsible for preventing severe disease. According to research made by the team of A Sette (83), T epitopes recognition from the B.1.1.7, B.1.351, P1 and B.1.429 variants is not significantly modified as compared to ancestral virus recognition, whether in convalescents or in people vaccinated with the Moderna or Pfizer jabs. This emphasizes the importance of induction of a potent T cell response to provide a robust immune response that could help resist most variants.

As the probability to see variants emergence is correlated with the active increased circulation of the virus in the global population, the best chance to tackle variants is to maintain mitigation measures, while vaccinating widely before variants could even emerge. To increase the number of vaccinees, experts underline the necessity to enlarge vaccinate children and increase vaccine access in low-income countries (82).

In any case, to prevent a pandemic of this magnitude from reappearing, major investments will have to be done in surveillance infrastructures (86) and in the research field, such as large scale sequencing to allow for a rapid detection of newly or re-emerging pathogens when still on a local scale (87). Indeed, over the past two decades, humanity has faced a viral threat almost every year with SARS, West Nile virus, pandemic influenza virus, Ebola virus, MERS CoV and Zika virus. This observation led to the creation of the Coalition for Epidemic Preparedness Innovations, aiming to promote vaccine development against infectious diseases with a pandemic potential. Notably, a coronavirus-related disease was already in the list of diseases that could threaten global world health in 2018 (88). Following the observation that viruses among the same family do often share relevant characteristics (structure of their surface protein, cellular tropism...), Dr Corbett and her team have proposed a “prototype pathogen approach”

to guide vaccine design. In this approach, research teams extensively study characteristics of viruses among a family, to be quickly prepared when a related pathogen emerge.

In the case of SARS-CoV-2, this could help the design of a “universal coronavirus vaccine” (89): a vaccine with a versatile design that could be applied to SARS-CoV 1 and 2, MERS-CoV as well as potential future emerging coronaviruses. In addition to financing vaccine design pipelines, investments will also have to be done in the monoclonal antibodies field. Indeed; as they can be developed in less than 4 months and administered as immunotherapies to symptomatic people, they can allow to fill the time gap between emergence of a pandemic pathogen and vaccine release (90).

In this regard, beyond scientific progress in the vaccine field, the extremely short development time needed to create COVID-19 vaccines has also been made possible by both accelerated regulatory procedures and improvement in communication techniques, allowing development of what Dr Rappuoli calls “internet-based-vaccines” (84). Indeed, the internet now allows instant data sharing on a global scale, which in the context of ground-breaking discoveries in molecular biology that allow gene cell-free synthesis from a known nucleotide sequence, with no need for laboratory culture of virus or proteins production, could lead to a vaccine revolution with almost immediate production of new adapted vaccines in automated facilities across the world (85).

To conclude this review on an optimistic point, 2022 may see the development of “second-generation vaccines”, ripping off the first-generation vaccines with improved capacities (including storage performances, production yields, costs...) and an ability to tackle variants. Second generation vaccines could allow worldwide population to dream of a full vaccine coverage by the end of 2022 and a return to a pre-pandemic life.

3. Bibliography

1. COVID-19 Map - Johns Hopkins Coronavirus Resource Center [Internet]. [cited 2021 Dec 15]. Available from: <https://coronavirus.jhu.edu/map.html>
2. Pallesen J, Wang N, Corbett KS, Wrapp D, Kirchdoerfer RN, Turner HL, et al. Immunogenicity and structures of a rationally designed prefusion MERS-CoV spike antigen. *Proc Natl Acad Sci U S A.* 2017;114(35):E7348–57.
3. Kirchdoerfer RN, Cottrell CA, Wang N, Pallesen J, Yassine HM, Turner HL, et al. Pre-fusion structure of a human coronavirus spike protein. *Nature.* 2016;531(7592):118–21.
4. Walls AC, Park YJ, Tortorici MA, Wall A, McGuire AT, Veesler D. Structure, Function, and Antigenicity of the SARS-CoV-2 Spike Glycoprotein. *Cell* [Internet]. 2020;181(2):281–292.e6. Available from: <https://doi.org/10.1016/j.cell.2020.02.058>
5. Wang Q, Zhang Y, Wu L, Niu S, Song C, Zhang Z, et al. Structural and Functional Basis of SARS-CoV-2 Entry by Using Human ACE2. *Cell.* 2020;181(4):894–904.e9.
6. Burton DR, Walker LM. Rational Vaccine Design in the Time of COVID-19. *Cell Host Microbe* [Internet]. 2020;27(5):695–8. Available from: <https://doi.org/10.1016/j.chom.2020.04.022>
7. Thomas F, Rogers1 2*, Fangzhu Zhao1, 3 4*, Deli Huang1* NB, Alison Burns1, 3 4, Wan-ting He1, 3 4, Oliver Limbo3 5, et al. Isolation of potent SARS CoV 2 neutralizing antibodies and protection from disease in a small animal model. 2020;963(August):956–63.
8. Wan J, Xing S, Ding L, Wang Y, Gu C, Wu Y, et al. Human-IgG-Neutralizing Monoclonal Antibodies Block the SARS-CoV-2 Infection. *Cell Rep* [Internet]. 2020;32(3):107918. Available from: <https://doi.org/10.1016/j.celrep.2020.107918>
9. Forthal DN. Functions of antibodies. *Antibodies Infect Dis.* 2015;25–48.
10. Sherina N, Piralla A, Du L, Wan H, Kumagai-Braesch M, Andréll J, et al. Persistence of SARS-CoV-2 specific B- and T-cell responses in convalescent COVID-19 patients 6–8 months after the infection. *Med* [Internet]. 2021; Available from: <https://doi.org/10.1016/j.medj.2021.02.001>
11. He Z, Ren L, Yang J, Guo L, Feng L, Ma C, et al. Seroprevalence and humoral immune durability of anti-SARS-CoV-2 antibodies in Wuhan , China : a longitudinal ,. *Lancet* [Internet]. 2021;397(10279):1075–84. Available from: [http://dx.doi.org/10.1016/S0140-6736\(21\)00238-5](http://dx.doi.org/10.1016/S0140-6736(21)00238-5)
12. Hansen CH, Michlmayr D, Gubbels SM, Mølbak K, Ethelberg S. Assessment of protection against reinfection with SARS-CoV-2 among 4 million PCR-tested individuals in Denmark in 2020 : a population-level observational study. 2021;6736(21):1–9.
13. Chandrashekhar A, Liu J, Martino AJ, McMahan K, Mercad NB, Peter L, et al. SARS-CoV-2 infection protects against rechallenge in rhesus macaques. *Science (80-).* 2020;369(6505):812–7.
14. Bao L, Deng W, Gao H, Xiao C, Liu J, Xue J, et al. Reinflection could not occur in SARS-CoV-2 infected rhesus macaques. *bioRxiv.* 2020;1–20.
15. McMahan K, Yu J, Mercado NB, Loos C, Tostanoski LH, Chandrashekhar A, et al. Correlates of protection against SARS-CoV-2 in rhesus macaques. *Nature* [Internet]. 2020;590(February). Available from: <http://dx.doi.org/10.1038/s41586-020-03041-6>
16. M. Dougan, A. Nirula, . Azizad. Bamlanivimab plus etesevimab in mild or moderate COVID 19. 2021;
17. Gupta A, Gonzalez-Rojas Y, Juarez E, Crespo Casal M, Moya J, Falci DR, et al. Early Treatment for Covid-19 with SARS-CoV-2 Neutralizing Antibody Sotrovimab. *N Engl J Med.* 2021;385(21):1941–50.
18. Arvin AM, Fink K, Schmid MA, Cathcart A, Spreafico R, Havenar-daughton C, et al. A perspective on potential antibody- dependent enhancement of SARS-CoV-2. *Nature* [Internet]. 2020;584(May):353–63. Available from: <http://dx.doi.org/10.1038/s41586-020-2538-8>
19. Wan Y, Shang J, Sun S, Tai W, Chen J, Geng Q, et al. Molecular Mechanism for Antibody-Dependent Enhancement of Coronavirus Entry. *J Virol.* 2019;94(5):1–15.
20. Liu L, Yuen K, Chen Z, Liu L, Wei Q, Lin Q, et al. Anti – spike IgG causes severe acute lung injury by skewing macrophage responses during acute SARS-CoV infection Find the latest version : Anti – spike IgG causes severe acute lung injury by skewing macrophage responses during acute SARS-CoV infection. 2019;4(4).
21. Wyllie D, Jones HE, Mulchandani R. SARS-CoV-2 responsive T cell numbers and anti-Spike IgG levels are both associated with protection from COVID-19: A prospective cohort study in keyworkers. 2021;
22. COVID-19 vaccine tracker and landscape [Internet]. [cited 2021 Dec 14]. Available from: <https://www.who.int/publications/m/item/draft-landscape-of-covid-19-candidate-vaccines>
23. Chen JW, Chen JM. Potential of live pathogen vaccines for defeating the COVID-19 pandemic: History and mechanism. *J Med Virol.* 2020;92(9):1469–74.
24. Wang Y, Yang C, Song Y, Coleman JR, Stawowczyk M, Tafrova J, et al. Scalable live-attenuated SARS-CoV-2 vaccine candidate demonstrates preclinical safety and efficacy. *Proc Natl Acad Sci U S A.*

- 2021;118(29):1–7.
25. Gao Q, Bao L, Mao H, Wang L, Xu K, Yang M, et al. Rapid development of an inactivated vaccine for SARS-CoV-2. *bioRxiv*. 2020;81(July):77–81.
 26. Moore JP, Saytientau QJ, Wyatt R, Sodroski J. Probing the Structure of the Human Immunodeficiency Virus Surface Glycoprotein gpl20 with a Panel of Monoclonal Antibodies. 1994;68(1):469–84.
 27. Kirchdoerfer RN, Wang N, Pallesen J, Wrapp D, Turner HL, Cottrell CA, et al. Stabilized coronavirus spikes are resistant to conformational changes induced by receptor recognition or proteolysis. *Sci Rep* [Internet]. 2018;8(1):1–11. Available from: <http://dx.doi.org/10.1038/s41598-018-34171-7>
 28. Fauci AS. The story behind COVID-19 vaccines. *Science* (80-). 2021;372(6538):109–109.
 29. Ahmad K, Malik HS, Bloom K, Milks KJ, Straight a F, Carroll CW, et al. Structure of RSV Fusion Glycoprotein. *Science* (80-). 2013;340(May):1113–7.
 30. Sanders RW, Moore JP. Virus vaccines: proteins prefer prolines. *Cell Host Microbe* [Internet]. 2021;29(3):327–33. Available from: <http://www.ncbi.nlm.nih.gov/pubmed/33705704>
 31. Hsieh AC, Goldsmith JA, Schaub JM, Divenere AM, Kuo H, Javanmardi K, et al. Structure-based Design of Prefusion-stabilized SARS-CoV-2 Spikes. 2020;
 32. He L, Lin X, Wang Y, Abraham C, Sou C, Ngo T, et al. Single component self assembling protein nanoparticles presenting the receptor binding domain and stabilized spike as SARS-CoV-2 vaccine candidates. 2021;(March):1–18.
 33. Barnes CO, Jette CA, Abernathy ME, Dam K-MA, Esswein SR, Gristick HB, et al. SARS-CoV-2 neutralizing antibody structures inform therapeutic strategies. *Nature*. 2020 Dec;588(7839):682–7.
 34. Voss WN, Hou YJ, Johnson N V., Kim JE, Delidakis G, Horton AP, et al. Prevalent, protective, and convergent IgG recognition of SARS-CoV-2 non-RBD spike epitopes in COVID-19 convalescent plasma. *bioRxiv*. 2020;5268(May):1–11.
 35. Chiuppesi F, Salazar M d'Alincourt, Contreras H, Nguyen VH, Martinez J, Park Y, et al. Development of a multi-antigenic SARS-CoV-2 vaccine candidate using a synthetic poxvirus platform. *Nat Commun* [Internet]. 2020;11(1). Available from: <http://dx.doi.org/10.1038/s41467-020-19819-1>
 36. Scotti N, Rybicki EP. Virus-like particles produced in plants as potential vaccines. *Expert Rev Vaccines*. 2013;12(2):211–24.
 37. Del Giudice G, Rappuoli R, Didierlaurent AM. Correlates of adjuvanticity: A review on adjuvants in licensed vaccines. *Semin Immunol* [Internet]. 2018;39(May):14–21. Available from: <https://doi.org/10.1016/j.smim.2018.05.001>
 38. Zhao L, Seth A, Wibowo N, Zhao CX, Mitter N, Yu C, et al. Nanoparticle vaccines. *Vaccine* [Internet]. 2014;32(3):327–37. Available from: <http://dx.doi.org/10.1016/j.vaccine.2013.11.069>
 39. Graham BS, Gilman MSA, McLellan JS. Structure-based vaccine antigen design. *Annu Rev Med*. 2019;70:91–104.
 40. Pati R, Shevtsov M, Sonawane A. Nanoparticle vaccines against infectious diseases. *Front Immunol*. 2018;9(OCT).
 41. Zhang B, Chao CW, Tsybovsky Y, Abiona OM, Hutchinson GB, Moliva JI, et al. A platform incorporating trimeric antigens into self-assembling nanoparticles reveals SARS-CoV-2-spike nanoparticles to elicit substantially higher neutralizing responses than spike alone. *Sci Rep* [Internet]. 2020;10(1):1–13. Available from: <https://doi.org/10.1038/s41598-020-74949-2>
 42. Tian JH, Patel N, Haupt R, Zhou H, Weston S, Hammond H, et al. SARS-CoV-2 spike glycoprotein vaccine candidate NVX-CoV2373 immunogenicity in baboons and protection in mice. *Nat Commun*. 2021;12(1).
 43. Bachmann MF, Jennings GT. Vaccine delivery: A matter of size, geometry, kinetics and molecular patterns. *Nat Rev Immunol*. 2010;10(11):787–96.
 44. Ward BJ, Gobeil P, Séguin A, Atkins J, Boulay I, Charbonneau PY, et al. Phase 1 trial of a Candidate Recombinant Virus-Like Particle Vaccine for Covid-19 Disease Produced in Plants. *medRxiv*. 2020;(1):1–58.
 45. Lundstrom K. Viral Vectors for COVID-19 Vaccine Development. 2021;
 46. Pollard AJ, Launay O, Lelievre JD, Lacabaratz C, Grande S, Goldstein N, et al. Safety and immunogenicity of a two-dose heterologous Ad26.ZEBOV and MVA-BN-Filo Ebola vaccine regimen in adults in Europe (EBOVAC2): a randomised, observer-blind, participant-blind, placebo-controlled, phase 2 trial. *Lancet Infect Dis*. 2020;493–506.
 47. Madewell ZJ, Yang Y, Jr IML, Halloran ME, Dean NE. Safety and immunogenicity of the Ad26.COV2.S COVID-19 vaccine candidate: interim results 2 of a phase 1/2a, double-blind, randomized, placebo-controlled trial. *medRxiv*. 2020;1–13.
 48. Stephenson KE, Le Gars M, Sadoff J, de Groot AM, Heerwagh D, Truyers C, et al. Immunogenicity of the Ad26.COV2.S Vaccine for COVID-19. *Jama* [Internet]. 2021;02215:1–10. Available from: <http://www.ncbi.nlm.nih.gov/pubmed/33704352>

49. Dan H. Baroucha, b, *, Sandra V. Kikc, Gerrit J. Weverlingc, Rebecca Dilana, Sharon L. Kinga, Lori F. Maxfielda, Sarah Clarka, David Ng'ang'aa, Kara L. Brandariza, Peter Abbinka, Faruk Sinangild, Guy de Bruyne, Glenda E. Graye, Surita Rouxf, Linda-Gail Bek and JG. International Seroepidemiology of Adenovirus Serotypes 5, 26, 35, and 48 in Pediatric and Adult Populations. *Bone*. 2008;23(1):1–7.
50. Graham SP, McLean RK, Spencer AJ, Belij-Rammerstorfer S, Wright D, Ulaszewska M, et al. Evaluation of the immunogenicity of prime-boost vaccination with the replication-deficient viral vectored COVID-19 vaccine candidate ChAdOx1 nCoV-19. *bioRxiv*. 2020;1–11.
51. Logunov DY, Dolzhikova I V, Shchelyakov D V, Tukhvatulin AI, Zubkova O V, Dzharullaeva AS, et al. Safety and efficacy of an rAd26 and rAd5 vector-based heterologous prime-boost COVID-19 vaccine: an interim analysis of a randomised controlled phase 3 trial in Russia. *Lancet* [Internet]. 2021;6736(21):1–11. Available from: [http://dx.doi.org/10.1016/S0140-6736\(21\)00234-8](http://dx.doi.org/10.1016/S0140-6736(21)00234-8)
52. Dolzhikova I V., Zubkova O V., Tukhvatulin AI, Dzharullaeva AS, Tukhvatulina NM, Shchelyakov D V., et al. Safety and immunogenicity of GamEvac-Combi, a heterologous VSV- and Ad5-vectored Ebola vaccine: An open phase I/II trial in healthy adults in Russia. *Hum Vaccines Immunother* [Internet]. 2017;13(3):613–20. Available from: <http://dx.doi.org/10.1080/21645515.2016.1238535>
53. Bettini E, Locci M. SARS-CoV-2 mRNA Vaccines: Immunological Mechanism and Beyond. *Vaccines*. 2021;9(2):147.
54. Pardi N, Hogan MJ, Porter FW, Weissman D. mRNA vaccines—a new era in vaccinology. *Nat Rev Drug Discov* [Internet]. 2018;17(4):261–79. Available from: <http://dx.doi.org/10.1038/nrd.2017.243>
55. Sandbrink JB, Shattock RJ. RNA Vaccines: A Suitable Platform for Tackling Emerging Pandemics? *Front Immunol*. 2020;11(December):1–9.
56. Gebre MS, Rauch S, Roth N, Yu J, Chandrashekhar A, Mercado NB, et al. Optimization of Non-Coding Regions for a Non-Modified mRNA COVID-19 Vaccine. *Nature*. 2021;
57. Vogel AB, Lambert L, Kinnear E, Busse D, Erbar S, Reuter KC, et al. Self-Amplifying RNA Vaccines Give Equivalent Protection against Influenza to mRNA Vaccines but at Much Lower Doses. *Mol Ther* [Internet]. 2018;26(2):446–55. Available from: <https://doi.org/10.1016/j.ymthe.2017.11.017>
58. Sahin U, Muik A, Derhovanessian E, Vogler I, Kranz LM, Vormehr M, et al. COVID-19 vaccine BNT162b1 elicits human antibody and TH1 T cell responses. *Nature* [Internet]. 2020;586(7830):594–9. Available from: <http://dx.doi.org/10.1038/s41586-020-2814-7>
59. Mulligan MJ, Lyke KE, Kitchin N, Absalon J, Gurtman A, Lockhart S, et al. Phase I/II study of COVID-19 RNA vaccine BNT162b1 in adults. *Nature* [Internet]. 2020;586(7830):589–93. Available from: <http://dx.doi.org/10.1038/s41586-020-2639-4>
60. Walsh EE, French R, Falsey AR, Kitchin N, Absalon J, Gurtman A, et al. RNA-based COVID-19 vaccine BNT162b2 selected for a pivotal efficacy study. *medRxiv*. 2020;
61. Polack FP, Thomas SJ, Kitchin N, Absalon J, Gurtman A, Lockhart S, et al. Safety and Efficacy of the BNT162b2 mRNA Covid-19 Vaccine. *N Engl J Med*. 2020;383(27):2603–15.
62. Walsh EE, French RW, Falsey AR, Kitchin N, Absalon J, Gurtman A, et al. Safety and Immunogenicity of Two RNA-Based Covid-19 Vaccine Candidates. *N Engl J Med*. 2020;383(25):2439–50.
63. Smith T, Patel A, Ramos S, Elwood D, Zhu X, Yan J, et al. Rapid development of a synthetic DNA vaccine for COVID-19. 2020;1–26.
64. Fuller DH, Ph D, Berglund P, Ph D. Amplifying RNA Vaccine Development. 2020;2469–71.
65. Baden LR, El Sahly HM, Essink B, Kotloff K, Frey S, Novak R, et al. Efficacy and Safety of the mRNA-1273 SARS-CoV-2 Vaccine. *N Engl J Med*. 2021;384(5):403–16.
66. Dagan N, Barda N, Kepten E, Miron O, Perchik S, Katz MA, et al. BNT162b2 mRNA Covid-19 Vaccine in a Nationwide Mass Vaccination Setting. *N Engl J Med* [Internet]. 2021;1–12. Available from: <http://www.ncbi.nlm.nih.gov/pubmed/33626250>
67. Falsey AR, Sobieszczyc ME, Hirsch I, Sproule S, Robb ML, Corey L, et al. Phase 3 Safety and Efficacy of AZD1222 (ChAdOx1 nCoV-19) Covid-19 Vaccine. *N Engl J Med*. 2021;1–14.
68. Goepfert PA, Truyers C, Fennema H, Spiessens B, Offergeld K, Schepers G, et al. Safety and Efficacy of Single-Dose Ad26.COV2.S Vaccine against Covid-19. 2021;1–15.
69. Tanriover MD, Doğanay HL, Akova M, Güner HR, Azap A, Akhan S, et al. Efficacy and safety of an inactivated whole-virion SARS-CoV-2 vaccine (CoronaVac): interim results of a double-blind, randomised, placebo-controlled, phase 3 trial in Turkey. *Lancet*. 2021;398(10296):213–22.
70. Al Kaabi N, Zhang Y, Xia S, Yang Y, Al Qahtani MM, Abdulrazzaq N, et al. Effect of 2 Inactivated SARS-CoV-2 Vaccines on Symptomatic COVID-19 Infection in Adults: A Randomized Clinical Trial. *JAMA - J Am Med Assoc* [Internet]. 2021;326(1):35–45. Available from: <https://jamanetwork.com/>
71. Heath PT, Galiza EP, Baxter DN, Boffito M, Browne D, Burns F, et al. Safety and Efficacy of NVX-CoV2373 Covid-19 Vaccine. *n engl j med*. 2021;12.
72. Decreased SARS-CoV-2 viral load following vaccination. 2021;
73. Levine-tiefenbrun M, Yelin I, Katz R, Herzl E, Golan Z, Schreiber L, et al. Initial report of decreased

- SARS-CoV-2 viral load after inoculation with the BNT162b2 vaccine. *Nat Med* [Internet]. 2019; Available from: <http://dx.doi.org/10.1038/s41591-021-01316-7>
74. Greinacher A, Thiele T, Warkentin TE, Weisser K, Kyrle PA, Eichinger S. Thrombotic Thrombocytopenia after ChAdOx1 nCov-19 Vaccination. *N Engl J Med* [Internet]. 2021;1–10. Available from: <http://www.ncbi.nlm.nih.gov/pubmed/33835769>
75. Greinacher A, Thiele T, Warkentin TE, Weisser K. A Prothrombotic Thrombocytopenic Disorder Resembling Heparin-Induced Thrombocytopenia Following Coronavirus-19 Vaccination. :1–10.
76. Patone M, Mei XW, Handunnetthi L, Dixon S, Zaccardi F, Shankar-hari M, et al. Risks of myocarditis, pericarditis, and cardiac arrhythmias associated with COVID-19 vaccination or SARS-CoV-2 infection. 2021;
77. Wilder-Smith A, Mulholland K. Effectiveness of an Inactivated SARS-CoV-2 Vaccine. *N Engl J Med*. 2021;385(10):946–8.
78. SARS-CoV-2 Neutralization with BNT162b2 Vaccine Dose 3. 2021;
79. Bian L, Gao F, Zhang J, He Q, Mao Q, Xu M, et al. Effects of SARS-CoV-2 variants on vaccine efficacy and response strategies. *Expert Rev Vaccines* [Internet]. 2021;20(4):365–73. Available from: <https://doi.org/10.1080/14760584.2021.1903879>
80. Brinkkemper M, Brouwer PJM, Maisonnasse P, Grobben M, Caniels TG, Poniman M, et al. A third SARS-CoV-2 spike vaccination improves neutralization of variants-of-concern. *npj Vaccines*. 2021;6(1):1–6.
81. Deming ME, Lyke KE. A ‘mix and match’ approach to SARS-CoV-2 vaccination. *Nat Med* [Internet]. 2021;27(9):1510–1. Available from: <http://dx.doi.org/10.1038/s41591-021-01463-x>
82. Fontanet A, Autran B, Lina B, Kiely MP, Karim SSA, Sridhar D. SARS-CoV-2 variants and ending the COVID-19 pandemic. *Lancet*. 2021;397(10278):952–4.
83. Alison Tarke A, Sidney J, Methot N, Zhang Y, Dan JM, Goodwin B, et al. Negligible impact of SARS-CoV-2 variants on CD4 + and CD8 + T cell reactivity in COVID-19 exposed donors and vaccinees. *bioRxiv* [Internet]. 2021;2021.02.27.433180. Available from: <https://doi.org/10.1101/2021.02.27.433180>
84. Rappuoli R, Gregorio E De, Del G, Phogat S, Pecetta S. Vaccinology in the post – COVID-19 era. 2021;118(3):1–7.
85. Dormitzer PR, Suphaphiphat P, Gibson DG, Wentworth DE, Stockwell TB, Algire MA, et al. Synthetic generation of influenza vaccine viruses for rapid response to pandemics. *Sci Transl Med*. 2013;5(185):1–14.
86. Graham BS, Corbett KS. Prototype pathogen approach for pandemic preparedness: World on fire. *J Clin Invest*. 2020;130(7):3348–9.
87. Grange ZL, Goldstein T, Johnson CK, Anthony S, Gilardi K, Daszak P, et al. Ranking the risk of animal-to-human spillover for newly discovered viruses. *Proc Natl Acad Sci U S A* [Internet]. 2021;118(15):1–8. Available from: <http://www.ncbi.nlm.nih.gov/pubmed/33822740>
88. Si M, Al-shorbaji F, Millett P, Murgue B. The WHO R and D blueprint 2018 review of emerging infectious diseases requiring urgent research and development efforts. 2020;(January).
89. Dai L, Zheng T, Xu K, Han Y, Xu L, Huang E, et al. A Universal Design of Betacoronavirus Vaccines against COVID-19, MERS, and SARS. *Cell* [Internet]. 2020;182(3):722–733.e11. Available from: <http://dx.doi.org/10.1016/j.cell.2020.06.035>
90. Rogers TF, Zhao F, Huang D, Beutler N, Abbott RK, Ricketts J, et al. Rapid isolation of potent SARS-CoV-2 neutralizing antibodies and protection in a small animal model. 2020;

CHAPITRE 2

ÉVALUATION DE L'IMMUNOGÉNICITÉ DE DEUX CANDIDATS VACCINAUX

1.Méthodologie

Avant de nous intéresser aux résultats des deux études, un point de méthodologie s'impose pour mieux appréhender les techniques de l'ELISA (Enzyme Linked Immunosorbent Assay) et de la neutralisation, techniques réalisées dans le laboratoire du Pr P. Poignard. Ces deux tests sont complémentaires et très informatifs dans le contexte de l'évaluation d'un candidat vaccinal. L'ELISA permet notamment de déterminer la capacité des Ac contenus dans un sérum d'animal immunisé à reconnaître un antigène donné. Ce test permet donc de définir si des Ac spécifiques de l'antigène vaccinal ont été induits par la vaccination et de suivre l'évolution de leur titre.

Le test de neutralisation permet d'évaluer la fonctionnalité des Ac à travers la mesure de leur capacité neutralisante, la neutralisation étant définie comme la perte d'infectivité qui a lieu lorsque un Ac fixe un virion (1). La neutralisation est certainement un mécanisme prépondérant de la protection induite par les vaccins contre les infections virales et comme évoqué précédemment dans la revue, il semble exister une corrélation entre réponses neutralisantes et protection (2) (3). Il est important de souligner que les Ac possèdent d'autres activités fonctionnelles (4), non évaluées par le test de neutralisation, mais qui jouent un rôle dans la protection : induction de la cascade du complément, facilitation de l'opsonisation, cytotoxicité médiée par les Ac...

1.1 Méthodologie du test ELISA

Mon travail dans ce projet a consisté à mettre au point puis réaliser les expériences d'ELISA. La première étape consiste à déposer pour adsorption un antigène donné sur une plaque spécialement traitée pour fixer des protéines (*Maxisorp NUNC Immunoplate, #442404*). Dans le cas des études présentées, l'antigène peut être du spike, du RBD ou de l'ADDomer. L'adsorption est réalisée sur la nuit en incubant les plaques à 4°C. Le lendemain, les plaques sont lavées avec du PBS-Tween 0,05% à l'aide d'un laveur de plaques (*Thermoscientific plate washer #5165040*). Ensuite est réalisée une étape de blocage par dépôt d'une solution de PBS-BSA 3%. La BSA se fixe sur les espaces de la plaque non recouverts par l'antigène, empêchant ensuite la fixation aspécifique des Ac. Après une heure d'incubation à température ambiante pour le blocage et une étape de lavage, les sérum à tester sont déposés dans les puits. Ces sérum sont testés à différentes dilutions, effectuées en cascade, afin d'en déterminer le titre. Après une nouvelle incubation d'une heure suivie de cinq lavages, l'Ac secondaire, couplé à

l'enzyme HRP (horseradish peroxydase) est ajouté. Cet Ac provient d'une autre espèce que celle dont on veut doser les Ac, et dans notre cas va s'accrocher aux parties constantes des immunoglobulines murines ou simiennes à doser (*Goat anti-mouse IgG (H+L) secondary Ab conjugated to HRP (JIR #115-035-062)*) ou (*Goat anti-monkey H+L antibody conjugated to HRP (Invitrogen #PA1-84631)*). Après une heure, le substrat de l'enzyme HRP est ajouté (TMB) et une réaction colorimétrique rapide s'ensuit. Afin de bloquer la réaction, une solution acide de H₂S0₄ (1M) est ajoutée à 1 minute et 10 secondes. La densité optique est ensuite lue à 450 nm à l'aide du lecteur de plaque TECAN Spark 10M.

- ④ Ajout du substrat.
Mesure de la réaction colorimétrique.
- ③ Reconnaissance par l'anticorps secondaire
- ② Fixation des anticorps du sérum sur l'antigène
- ① Adsorption de l'antigène

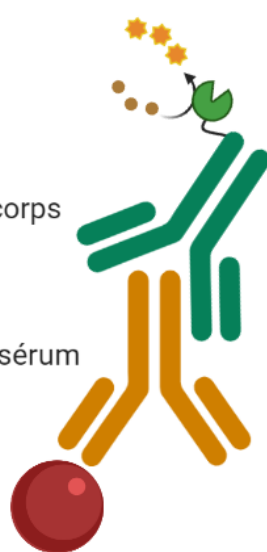


Figure 3 : Principe de l'ELISA direct

1.2 Méthodologie du test de neutralisation

Le test de neutralisation utilisé dans les études présentées dans ce manuscrit a été mis au point par la Dr M. Buisson, et a ensuite été réalisé par différents membres de l'équipe (I. Bally et Dr S. Dergan - Dylon).

Des pseudovirus SARS-CoV-2 ont été utilisés, afin de ne pas avoir à travailler avec des particules infectieuses, et permettre des manipulations en laboratoire de confinement P2. Les pseudovirus sont capables d'infecter des cellules cibles mais ne peuvent réaliser un second cycle d'infection, ne présentant donc pas de danger expérimental. Les pseudovirus sont créés par co-transfection de cellules HEK 293T par trois plasmides : un pour gag (pour assurer le bourgeonnement), un pour la luciférase qui servira de gène rapporteur, et un pour le spike du SARS-CoV-2 (délété de 18 acides aminés en position C-term). Trois jours après la transfection, les pseudovirus sont récoltés, centrifugés, filtrés à l'aide d'un filtre 0,45µm et concentrés 50

fois (*Amicon Ultra MWCO 100kDa*), aliquotés et stockés à -80°C. Avant usage, les pseudovirus sont titrés sur des cellules HeLa exprimant le récepteur ACE-2 à leur surface, pour connaître la concentration à laquelle on obtient une RLU de 150 000 Unité Relative de Lumière par puits de plaque 96 puits. Ce titre a été choisi car il permet une plage dynamique assurant une mesure adéquate du taux de neutralisation. Pour le test de neutralisation, les pseudovirus sont incubés en plaque 96 puits avec du sérum dilué en série (ou des anticorps monoclonaux) pendant une heure à 37°C. Des cellules HeLa-ACE-2 sont ensuite ajoutées pour une seconde incubation de deux jours à 37°C. Après 24h d'incubation, les cellules sont supplémentées en milieu de culture complet (*DMEM Gibco #11966-025 ; FBS VWR #97068-086*). Au bout des deux jours, le milieu de culture est aspiré et les cellules lysées (*Cell lysis buffer (Ozbioscience # LUC1000)*). La luciférase contenue dans les cellules infectées par les pseudovirus est ainsi accessible, et l'ajout de son substrat, la luciférine, induit une réaction colorimétrique. Ainsi, si les Ac ont un effet neutralisant, ils empêcheront l'entrée des pseudovirus porteurs du gène de la luciférase dans les cellules cibles HeLa-ACE2, ce qui se traduira par une diminution des RLU mesurées par rapport au virus seul, sans Ac. Les RLU sont également mesurées à l'aide du lecteur de plaque TECAN Spark 10M.

Afin de pouvoir comparer des sérum entre eux, sont calculées les concentrations inhibitrices médianes : l'IC50 et la ND50, qui correspondent toutes les deux à la dilution de sérum pour laquelle on obtient 50% du signal maximal, en ELISA et en neutralisation respectivement. Ces valeurs sont calculées à l'aide du logiciel Graph Pad.

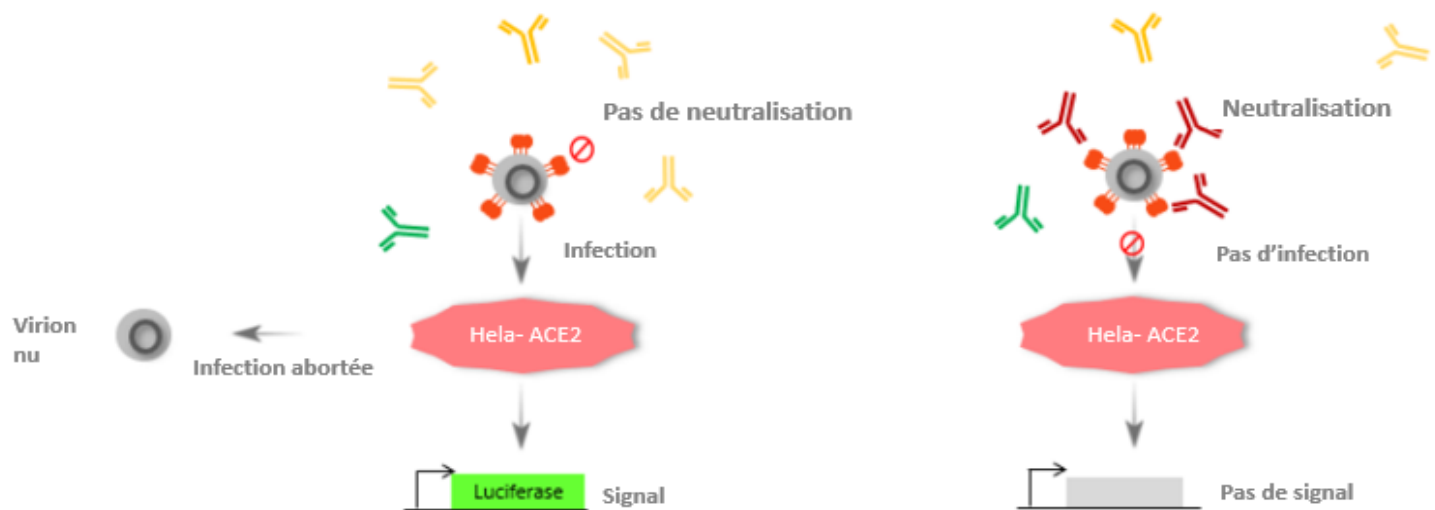


Figure 4 : Principe du test de neutralisation, adapté de R. Rouzeau (5)

1. Burton DR, Mascola JR. Antibody responses to envelope glycoproteins in HIV-1 infection. *Nat Immunol*. 2016;16(6):571–6.
2. Earle KA, Ambrosino DM, Fiore-Gartland A, Goldblatt D, Gilbert PB, Siber GR, et al. Evidence for antibody as a protective correlate for COVID-19 vaccines. *Vaccine* [Internet]. 2021;39(32):4423–8. Available from: <https://doi.org/10.1016/j.vaccine.2021.05.063>
3. Khoury DS, Cromer D, Reynaldi A, Schlub TE, Wheatley AK, Juno JA, et al. Neutralizing antibody levels are highly predictive of immune protection from symptomatic SARS-CoV-2 infection. *Nat Med* [Internet]. 2021;27(7):1205–11. Available from: <http://dx.doi.org/10.1038/s41591-021-01377-8>
4. Forthal DN. Functions of antibodies. *Antibodies Infect Dis*. 2015;25–48.
5. Rouzeau R. Broadly neutralizing antibodies against HIV : design of isolation strategies and application to two elite neutralizers To cite this version : HAL Id : tel-03375033 Anticorps Neutralisants à Large Spectre contre le VIH : mise au point de stratégies d ' iso. 2021;

2. Induction de puissantes réponses anticorps neutralisantes anti-SARS-CoV-2 par immunisation, via l'utilisation d'une plateforme de multimérisation versatile inspirée des adénovirus.

2.1 Bref résumé de l'article en français :

En réponse à la pandémie de SARS-CoV-2, l'équipe du Dr Fender a utilisé une construction protéique nommée «ADDomer » pour le design d'un candidat vaccinal de type pseudo-particule virale. Cette nanoparticule non infectieuse, formée par assemblage spontané de sous unités protéiques dérivées de l'adénovirus humain de type 3, avait déjà démontré sa capacité à accepter l'insertion dans des boucles exposées à la surface de courts épitopes linéaires issus de pathogènes. Une nouvelle génération d'ADDomer a été conçue pour permettre cette fois l'attachement irréversible d'antigènes complexes à la surface de la pseudo-particule virale en utilisant le système Spy Tag- Spy Catcher. Ce système est dérivé de *Streptococcus pyogenes*, et permet une fixation covalente et spontanée entre le résidu aspartate du peptide ST et la lysine du peptide SC. Brièvement, la séquence codant pour le Spy-Tag (ST) a été insérée au niveau des boucles flexibles de la nanoparticule, boucles exposées à la surface et donc à la reconnaissance du système immunitaire. Des expériences de SDS Page, de microscopie électronique et de spectrométrie de masse ont confirmé la capacité du ADDomer-ST à capter le Spy-Catcher (SC). A la suite, la séquence codant pour le SC a été ajouté à la séquence du RBD en position N-term. Le RBD-SC a été produit en cellule d'insecte, permettant sa glycosylation. La taille de la construction a été vérifiée par SDS-Page.

Dans un second temps, des expériences ont été réalisées afin de vérifier les capacités de reconnaissance du récepteur ACE-2 par le RBD fixé à l'ADDomer. Cette reconnaissance a d'abord été étudiée par résonnance plasmidique de surface (SPR), puis en testant l'attachement des ADDomer-RBD aux ACE-2 exprimés à la surface de cellules HeLa transfectées. Enfin, une dernière expérience de compétition entre des pseudovirus SARS-CoV-2 et des ADDomer-RBD ou des RBD-ST seuls a mis en évidence la capacité des deux constructions à se fixer aux cellules HeLa ACE-2, empêchant la fixation du pseudovirus à ses cellules cibles.

Une fois la bonne conformation de la construction ADDomer-RBD vérifiée, l'étape suivante consistait à apprécier l'immunogénicité de ce candidat vaccinal dans un modèle animal. Le

modèle murin a été choisi. L'expérience a consisté à immuniser quatre groupes de souris : le premier a reçu le RBD seul, un second groupe a été vacciné par un mélange de RBD soluble et d'ADDomer dépourvu de ST, ADDomer ne pouvant donc pas lier le RBD-SC. Les troisième et quatrième groupes ont reçu l'ADDomer-RBD. Cependant, à la différence du groupe 3, le groupe 4 a reçu également une injection d'ADDomer-ST deux semaines avant le début de la première injection. Le but de cette injection supplémentaire était d'imiter le phénomène de pré-immunisation, que l'on peut observer dans les stratégies vaccinales basées sur l'utilisation d'un virus peu pathogène comme vecteur, si ce virus infecte déjà l'homme naturellement (c'est le cas de l'adénovirus de type 3). La réponse immunitaire développée contre le virus va bloquer le vecteur et donc réduire l'immunogénicité de la plateforme vaccinale. Ce phénomène est décrit plus en détail dans la partie introductive de cette thèse.

Ainsi, à l'exception du groupe 4, tous les groupes de souris ont reçu deux injections de la même dose de leurs candidats vaccinaux respectifs, espacées de deux semaines.

La réponse immunitaire humorale induite par la vaccination a d'abord été évaluée par mesure dans le sérum des taux d'immunoglobulines G (IgG) anti -RBD. Les groupes ayant reçu les ADDomer-RBD sont ceux pour lesquels l'augmentation des titres d'Ac anti-RBD a été visible dès le 13^{ème} jour, après une seule immunisation avec l'ADDomer-RBD, contrairement aux groupes 1 et 2 pour lesquels l'augmentation a n'a été visible à partir de J27, soit deux semaines après la deuxième injection. Entre J27 et J41, les taux d'Ac sont restés semblables pour tous les groupes. Il est intéressant de noter que les taux d'Ac du groupe 4 étaient toujours les plus élevés, suggérant un effet « boost » de la pré-immunisation ADDomer.

Afin de tester la fonctionnalité des Ac induits, les capacités de neutralisation du sérum ont été testées contre des pseudovirus SARS-CoV-2. A J41, les groupes 3 et 4 avaient de forts titres de neutralisation, contrairement aux groupes 1 et 2. Pour les groupes 3 et 4, des titres sont d'ailleurs détectables dès J13.

Cette étude démontre donc la capacité de la plateforme vaccinale à induire des Ac anti-RBD, spécifiques de l'immunogène injecté, et fonctionnels. De plus, si certains vaccins basés sur l'utilisation d'adénovirus humain (type 3, type 5) comme vecteurs ont vu leurs performances diminuées à cause de la pré-immunité anti-adénovirale présente dans la population générale, ce n'est pas le cas de ce candidat qui montre même de plus hauts titres d'Ac en cas de pré-immunisation avec l'ADDomer.

Dans le contexte pandémique actuel, il est intéressant de souligner la versatilité de cette plateforme vaccinale, qui permet de greffer des antigènes complexes à la surface de nanoparticules. Cette caractéristique est intéressante au regard de l'émergence de nouveaux variants du SARS-CoV-2 : des expériences sont actuellement en cours pour évaluer un ADDomer décoré de RBD issus du variant Bêta, mais d'autres pourraient être envisagées avec le variant Omicron. De manière plus large, il est possible d'envisager la greffe d'autre antigènes issus de pathogènes pour lesquels aucun vaccin n'est actuellement disponible.

2.2 Article original (rédigé en anglais) :

Elicitation of potent SARS-CoV-2 neutralizing antibody responses through immunization with a versatile adenovirus-inspired multimerization platform

Chevillard C^{1*}; Amen A^{1,3*}; Besson S^{1*}; Hannani D²; Bally I¹; Dettling V¹, Gout E¹; Moreau CJ¹; Buisson M¹; Gallet S¹, Fenel D¹, Vassal-Stermann E¹; Schoehn G¹, Poignard P^{1,3,4#}; Dagher MC¹ & Fender P^{1#}.

Authors affiliations

¹ CNRS, Univ. Grenoble Alpes, CEA, UMR5075, Institut de Biologie Structurale, 38042 Grenoble, France

² Univ. Grenoble Alpes, CNRS, UMR 5525, VetAgro Sup, Grenoble INP, TIMC, 38000 Grenoble, France

³ CHU Grenoble Alpes, 38000 Grenoble, France

⁴ Department of Immunology and Microbiology, The Scripps Research Institute, La Jolla, CA 92037, USA

#Correspondence to: pascal.fender@ibs.fr; pascal.poignard@ibs.fr

*Contributed equally to this work

ABSTRACT

Virus like particles (VLPs) are highly suited platforms for protein-based vaccines. In the present work, we adapted a previously designed non-infectious adenovirus-inspired 60-mer dodecahedric VLP (ADDomer) to display a multimeric array of large antigens through a SpyTag/SpyCatcher system. To validate the platform as a potential COVID-19 vaccine approach, we decorated the newly designed VLP with the glycosylated receptor binding domain (RBD) of SARS-CoV-2. Cryo-Electron Microscopy structure revealed that up to 60 copies of this antigenic domain could be bound on a single ADDomer particle, with the symmetrical arrangements of a dodecahedron. Mouse immunization with the RBD decorated VLPs already showed a significant specific humoral response following prime vaccination, greatly reinforced by a single boost. Neutralization assays with SARS-CoV-2 spike pseudo-typed-virus demonstrated the elicitation of strong neutralization titers, superior to those of COVID-19 convalescent patients. Remarkably, the existence of pre-existing immunity against the adenoviral-derived particles enhanced the antibody response against SARS-CoV-2. This plug and play vaccine platform represents a promising new highly versatile tool to combat emergent pathogens.

INTRODUCTION

Although genomic vaccine have recently demonstrated their capacity to elicit protective immune responses¹, protein-based vaccines remain highly attractive due to their lower cost, ease of transport and storage, crucial to reach developing countries and remote locations, as well as better social acceptation, as recently highlighted by hesitancy regarding COVID-19 RNA vaccines. Protein immunogenicity is highly increased through presentation to the immune system in a multimeric manner and a number of vaccine platforms have been developed to this aim, with various advantages and limitations². We have previously reported that a non-infectious virus like particle (VLP) derived from human Adenovirus of type 3 and consisting of 60 identical penton base monomers could be exploited to display epitopes of interest on its surface^{3–5}. In this vaccine platform, named ADDomer, exposed loops of the penton base protein were engineered to allow insertion of foreign peptides such as a linear neutralizing epitope from Chikungunya virus. However, this design did not permit the insertion of structurally complex antigens. To overcome this limitation while keeping the immunogenicity advantage of ADDomer, we describe here a redesigned platform offering a highly versatile capacity to display large and structurally complex antigens with potential post-translational

modifications. In order to decorate the adenovirus-based VLPs with large antigens, the SpyTag/SpyCatcher system^{6–9} was combined to the ADDomer technology. In this system, derived from *Streptococcus pyogenes*, an Aspartate residue from the 13 amino-acid SpyTag peptide (ST) can spontaneously create a covalent bond with a Lysine residue encompassed in the complementary SpyCatcher module (SC). We thus genetically inserted the sequence coding for the ST peptide into the ‘variable loop’ of the ADDomer that was previously used for small antigen insertion, yielding a VLP with 60 potential attachment sites for complex antigens engineered with an SC anchor.

In order to assess the newly developed platform, we decided to first test it as a potential candidate vaccine to elicit neutralizing antibodies (Nabs) against the severe acute respiratory syndrome coronavirus 2 (SARS-CoV-2). SARS-CoV-2 is an enveloped positive strand RNA virus belonging to the beta-coronavirus genus from the coronaviridae family. It is the etiological agent of COVID-19 and at the origin of the pandemic that started in December 2019, leading to 5 324 969 deaths as of December 17, 2021 (<https://covid19.who.int/>), and vast socio-economic consequences¹⁰. Protection against SARS-CoV-2 infection and COVID-19 can be mediated by neutralizing Abs targeting the envelope trimeric glycoprotein spike (S) exposed at the surface of the virus^{11,12}. Accordingly, spike-based vaccine approaches eliciting SARS-CoV-2 NAb responses have been successful at preventing COVID-19^{13–15}. The ectodomain of the S protein is divided into the S1 and S2 domains. The Spike protein binds to the host Angiotensin-Converting Enzyme 2 (ACE2) which serves as an entry receptor, as previously reported with SARS-CoV, responsible of the 2002-2004 SRAS outbreak^{16–19}. A subdomain of S1, named receptor binding domain (RBD), is the contact interface between the virus and the ACE2 receptor. Numerous studies have shown that the RBD comprises multiple distinct antigenic sites and is a prime target for Nabs in COVID-19 convalescent patients^{20–23}. These Nabs²⁴ strongly inhibit cell infection by SARS-CoV-2 by competing with the RBD-ACE2 interaction. Moreover, anti-RBD Nabs have been shown to confer protection against SARS-CoV-2 challenge in animal models of COVID-19, as well as to prevent COVID-19 in human, thus confirming the interest of using RBD as a vaccine immunogen^{25,26,27}.

This prompted us to use the RBD as the antigen to be displayed on our newly-designed VLP platform in order to engineer a novel COVID-19 vaccine approach. Here, we report that the newly designed platform can successfully be decorated with SARS-CoV-2 RBD and is highly immunogenic in mice, eliciting high neutralizing Ab titers.

RESULTS

Internal insertion of ST in ADDomer results in efficient SC cross-linking

ADDomer is a non-infectious 30 nm nanoparticle, formed from 12 bricks of the homo-pentameric penton base from the human adenovirus type 3. The ST sequence was inserted in the ADDomer gene in a region coding for the exposed flexible loop called the variable loop (Figure 1a). Due to the spontaneous homo-oligomerization of twelve pentameric penton base, sixty copies of ST are exposed on the surface of the ADDomer-ST (ADD-ST) particle. To assess whether the newly inserted ST sequence was accessible and functional on ADD-ST, incubation with different ratio of SC was performed. After boiling of samples, SDS-PAGE profile clearly showed that the incremental SC/ADD-ST ratio is correlated with the apparition of a band of higher molecular weight and the decrease of the intensity of bands related to unlinked moieties. Importantly, there was no remaining signal for undecorated ADD-ST after SC addition at the highest ratio thus reflecting the full decoration of the nanoparticle (Figure 1b). This result suggests an efficient and concentration-dependent formation of the ADD-ST/SC complex. Mass spectroscopy analysis confirmed that the ADD-ST doublet shifted by 13,3kDa (Figure 1c), which corresponds to the molecular weight (MW) of SC. The two peaks observed in mass spectroscopy is due to a second initiation codon in ADD-ST (starting at Methionine 25) without affecting the particle stability²⁸ and SC can bind to each form indifferently as shown by a similar shift of their MW corresponding to the addition of SC. Negative staining electron microscopy imaging performed on ADD-ST alone and ADD-ST fully decorated by SC showed that the integrity of the particle was not affected by the presence of SC and the grainy appearance of ADD-ST/SC likely reflects the presence of SC at the particle surface (Figure 1d). Altogether, these data show that SC cross-linking to ADD-ST is operational and can result in saturated decoration of the nanoparticle.

Cryo-EM analysis enables to visualize SC decoration on ADD-ST

In order to visualize the SC arrangement around the ADDomer particle, a structural study by cryo-electron microscopy was used. Fully decorated ADD-ST/SC particles were imaged on a Glacios electron microscope (Figure 2a). Image analysis was performed and the obtained 3D structure was compared to the structure of an undecorated ADDomer particle (EMD-0198). An extra-density corresponding to SC bound to the ADDomer ‘variable loop’ was clearly visible in ADD-ST/SC both in the density slice of the 3D map (Figure 2b) and in the isosurface representation of the structure (Figure 2c, purple density and supplementary movie). The resolution of the ADDomer particle is around 2.8 Å, allowing to clearly see the aminopeptidic

chain. However, the ST/SC part is not rigidly attached to the ADDomer, which explain why the corresponding density is fuzzy, and the structure not better defined (Supplementary Fig.1). The ADDomers have 2, 3 and 5 axis of symmetry, (the latter two being shown in Figure 2c), which is a characteristic of a dodecahedron meaning that SC are distributed accordingly. Interestingly, along the 3-fold axis SC are ~ 4.7 nm apart which is close to the Receptor Binding Domain (RBD) in the trimeric spike protein of SARS-CoV-2 (~ 4.1 nm), suggesting that the decorated particles would closely mimic the natural trimeric arrangement of RBDs (Figure 2d). Both the multivalency of SC displayed by the particle and the arrangements they have around the different symmetry axis could be an asset for vaccination purpose if an antigen is fused to this module.

Secreted RBD fused to SC is glycosylated and can be displayed at different ratios on the ADD-ST particle

To take advantage of the spontaneous and covalent linking of SC to ADD-ST, we reasoned that SC could be used as a versatile carrier to easily and efficiently fuse antigens, like in this SARS-CoV-2 vaccine development (Figure 3a), and in broader perspectives to diverse soluble proteins of interest. In the present study, the SARS-CoV-2 RBD was fused to the N-terminus of the SC (RBD-SC) and a melittin signal peptide was added to allow protein post-translational modifications (PTM) such as glycosylations and secretion from insect cells. To assess whether the secreted and purified RBD-SC was glycosylated, it was treated with N-glycosidase (PNGaseF) and the result showed a shift in the migration of the related band in SDS-PAGE gel, indicating that RBD-SC was indeed glycosylated (Figure 3b). As previously performed with unfused SC (Figure 1b), incremental amounts of RBD-SC were added to ADD-ST in order to decorate the particle with different ratio of cargos (from 0,03 to 3 copies of SC per particle monomers). The SDS-PAGE gel profile (Figure 3c) showed the correlated apparition of a band at higher molecular weight with increased concentrations of RBD-SC. This result reflects the covalent linking of RBD-SC to the ADD-ST monomers whereas the band corresponding to non-decorated ADD-ST monomer progressively faded away, disappearing when the particle is fully decorated. This result showed that the ADDomer platform can be decorated with different numbers of antigen copies exposed on its surface. Altogether, these experiments demonstrated that SC fusion to large antigens (~40kDa for RBD-SC) with post-translational modifications enable their covalent linking to the ADDomer platform and that the ratio of decoration can be adjusted according to desired applications.

ADDomers decorated of glycosylated RBD bind to ACE2

RBD is the subdomain of the SARS-CoV-2 spike protein that binds to the human ACE2 receptor. To assess the function of RBDs linked to the ADDomer particles, three different approaches were used. First, binding experiments at the molecular scale were performed using surface plasmon resonance (SPR) on immobilized dimeric human ACE2 fused to Fc domain of human IgG²⁹. Sensorgrams of ADD-RBD binding to immobilized human ACE2 showed a clear concentration-dependent binding of the RBD-decorated particles on ACE2 and a stable interaction with no visible dissociation at the end of injections (Figure 4a). The extremely slow dissociation rate ($4.57 \cdot 10^{-4} \text{ s}^{-1}$) agreed with a sub-nanomolar ‘apparent’ K_D ($3.09 \times 10^{-10} \text{ M}$). This apparent K_D is the result of an avidity with the decorated particle effect since the K_D of RBD-SC alone is slightly higher ($1.53 \cdot 10^{-8} \text{ M}$; Supplementary Figure 2). In any case, this result showed that the RBD is functional and that our platform somehow mimics viruses that evolved to take advantage of multivalent interactions with cellular receptors. In a second experiment at the cell scale, the direct binding of ADD-RBD onto HeLa cells stably expressing ACE2 was visualized by immunofluorescence using anti-ADDomer antibodies. The green signal seen at the periphery of HeLa-ACE2 cells in presence of ADD-RBD contrasted with the absence of signal observed with the same cells but in presence of undecorated ADD-ST particles. This result demonstrated that RBD at the surface of the particles induced the interaction with ACE2 present at the surface of the HeLa-Ace2 cells (Figure 4b). Finally, a competition experiment between a pseudo-typed virus harboring the SARS-CoV-2 spike and either RBD-SC or ADD-RBD was performed. Negative control was made with undecorated ADD-ST alone. As expected, both RBD-SC alone and ADD-RBD were able to compete with the pseudo-typed virus with a slightly higher efficiency for the RBD-decorated particle (Fig. 4c). Altogether, these experiments showed that RBD-SC is properly folded and can bind the ACE2 receptor at the molecular and cellular scales when applied alone (RBD-SC) or linked to the ADDomer particles (ADD-RBD).

RBD-decorated ADDomer elicits rapid anti-CoV2 Ab responses in mice, enhanced by adenovirus pre-immunity

Multivalent exposition of RBD antigens at the surface of the particle is likely to result in a better activation of the humoral system than RBD alone. However, one cannot exclude that ADDomer itself could also play an indirect role in the anti-SARS-CoV-2 response, especially in a population with preexisting adenovirus immunity. To address these two points, four groups of ten mice were designed (Figure 5a). The two first control groups were injected with RBD-SC

alone in the group 1 or with the same amount of unlinked RBD-SC plus naked-ADDomer (*i.e.* not displaying the antigen) in the group 2. The two other groups (groups 3 and 4) were vaccinated with ADD-RBD (*i.e.* RBD displayed at the particle surface) but the group 4 was pre-immunized with naked-ADDomer two weeks before the injection of ADD-RBD, in order to investigate whether anti-HAdV-3 penton base antibodies, as may possibly be found in individuals previously infected with adenovirus type 3, may impact the immunogenicity of ADD-RBD (Figure 5b). The presence of anti-ADDomer (*i.e.* HAdV-3 penton base adenovirus) antibodies in group 4 was checked by ELISA one day before the first immunization with ADD-RBD. The results (Supplementary Figure 3) show that all group 4 mice did mount an antibody response against naked-ADDomer. Then, the immune response against the RBD was monitored by ELISA at day 13 (post-1st immunization), 27 and 41 (post-2nd immunization). The RBD-decorated particles induced a significant anti-SARS-CoV-2 response after the first immunization (day 13, figure 5c), whereas no response was detectable in controls of group 1 (RBD-SC alone) or group 2 (ADDomer with not displayed SC-RBD). Interestingly, anti HAdV-3 penton base pre-immunity significantly enhanced the anti-RBD response.

Immunization boost increases both the amplitude and the duration of the response induced by ADD-RBD particles, independently of the anti-vector immunity

Two weeks after the second immunization (day 27), the anti-RBD response was clearly boosted for groups 3 and 4 that were injected with ADD-RBD, whereas the control groups 1 and 2 showed more heterogeneous responses (Figure 6a). This observation confirms that our vaccine platform displaying multivalent RBD antigens yields a rapid and efficient humoral response. The ADDomer technology applied to RBD antigen also demonstrated a long lasting immunogenic effect with anti-SARS-CoV-2 RBD antibodies remaining at the highest level at day 41 (Figure 6b). The difference between mice pre-immunized by ADDomer (group 4) or not (group 3) was less pronounced than after the first immunization, both groups reaching high and comparable levels. Altogether, these results showed that the second immunization enabled a high and long-lasting Ab response against the SARS-CoV-2 RBD using the ADDomer platform and that anti-vector pre-immunity is beneficial in particular to the initial responses (Figure 6c).

RBD-decorated ADDomer immunization elicits strong neutralizing Ab responses

Since the RBD is critical for binding to the SARS-CoV-2 receptor ACE2, antibodies elicited through immunization with the RBD (RBD-SC or ADDomer-RBD) can hinder the interaction between the Spike proteins and ACE2, blocking viral entry. The ability to neutralize the virus depends on the affinity of the antibodies for the RBD domain, as well as on the epitope

recognized. To assess the potency and efficacy of the antibodies induced in the four immunized groups of mice, the neutralization potency of sera (day 41) from vaccinated mice was assessed using SARS-CoV-2 spike (Wuhan strain) pseudo-typed lentivirus and ACE2-expressing HeLa cells. Only a partial and heterogeneous neutralization was obtained from group 1 and 2 sera in which RBD-SC was not displayed on ADDomer, even after two immunizations (Figure 7a, upper panels). Of note, sera from mice immunized with RBD-decorated ADDomer (groups 3 and 4) showed a better neutralization titer after a single immunization than group 1 and 2 after 2 immunizations (Supplementary Figure 4). After the second immunization, strong virus neutralization was observed in all mice from group 3 and 4 (Figure 7a, lower panels). Neutralization titers (ND_{50}) clearly showed that mice vaccinated with RBD-decorated ADDomer had significantly higher neutralizing activity than mice immunized with the same amount of antigen when not displayed on the platform (Figure 7b). Moreover, in accordance with the ELISA results (Figure 5c), the anti-vector response (group 4) slightly increased the neutralization titer compared to the naïve group (group 3), which emphasizes that a pre-existing HAdV-3 penton base immunity appears beneficial for our novel vaccine platform (Figure 7b). The neutralizing Ab titers reached in group 3 and 4 were overall superior to those from a cohort of convalescent COVID-19 patients composed of 50% mild (oxygen below 2L/min) and 50% severe (ICU) cases, and measured at 6 months after hospitalization³⁰ (Figure 7b)

DISCUSSION

In this study, we designed a novel and highly versatile vaccine platform amenable to large antigens by adapting the SpyTag/SpyCatcher technology to ADDomer, an adenovirus-inspired VLP^{5,6}. This technology has already been described for designing VLP-derived vaccine, however in these approaches SC was the moiety grafted to the VLPs while the antigens were fused to the Spy Tag^{7,31}. In our novel vaccine technology, we used the opposite configuration with SpyTag insertion in an internal loop of ADDomer, which minimized the risk of steric hindrance and functional impact on the spontaneous oligomerization of ADDomers. Insertion of ST in a surface-exposed loop of ADDomer did not impair the spontaneous assembly of twelve pentameric bricks (Figure 1d), thus creating a universal generic platform for multivalent antigen display. Experiments of saturating cross-linking with SC alone suggested that a full decoration (*i.e.* 60 copies) of the particle can be achieved (Figure 1b). Despite the flexibility of the loop in which ST was inserted, cryo-EM reconstruction of the ADD-ST/SC complex clearly showed an extra density corresponding to the SC interacting with ST fused to the ADDomer.

The data thus strongly suggested that the ADDomer could be used to display a multimerized array of antigens, a property that is crucial for the elicitation of strong Ab responses^{32,33,34}. Interestingly, the characteristic 2, 3 and 5-fold symmetry axis of a dodecahedron are easily visible in the 3D structure (Figure 2c), this spatial configuration showing that the SCs are distributed at different distances from each other according to the symmetry axis. Such distribution of the antigen could potentially further favor the immunogenicity of the VLP by offering different patterns of presentation of the antigen at the particle surface.

The COVID pandemic led us to first evaluate our newly designed platform as an anti-SARS-CoV-2 vaccine to be displayed through fusion to the SC N-terminus. It is worth noting that in the 3-fold axis of ADDomer, the SC adopts a pseudo-trimeric arrangement, which on the RBD decorated VLP closely mimics the tridimensional configuration of this domain in the SARS-CoV-2 spike glycoprotein (Figure 2d). The distance between SC in such configuration is 4,7 nm, which is in the same range as that between RBDs in the trimeric Spike protein (4,1 nm). Expressing soluble RBD fused to SC in insect cells resulted in N-glycosylation as expected³⁵ and did not affect the structure of SC, which retained its ability to cross-link to the ADD-ST vaccine platform in a dose dependent manner (Figure 3c). The proper folding of the glycosylated RBD exposed at the surface of the particles and its ability to bind ACE2 were assessed in a functional viral entry assay *via* competition with SARS-CoV-2 Spike pseudotyped virions (Figure 4c). A surface plasmon resonance (SPR) experiment confirmed the high affinity interaction of ADD-RBD to ACE2, the highly stable interaction observed suggesting an avidity effect of the multivalent particle exposing multiple copies of RBD (Figure 4a). Moreover, this experiment also shows that expressing RBD in insect cell leads to a functional SARS-CoV2 glycoprotein domain. Several vaccines using the baculovirus expression system in insect cells have been approved, such as vaccines against papillomavirus or hepatitis B. The Novavax COVID-19 vaccine candidate, based on an insect cell-produced trimeric S protein, is also advancing towards approval trials³⁶.

The ability of the RBD-decorated ADDomer to elicit an anti-SARS-CoV-2 humoral response was then studied in mice. As expected, we confirmed that displaying the RBD in a multimerized manner led to a strong improvement in immunogenicity (groups 3 and 4 *versus* groups 1 and 2). Indeed, this was clearly apparent from the first injection where the groups with decorated particles showed a significant anti-RBD response at Day 13 as measured in ELISA (Figure 5c), whereas no response was observed for the other groups. This observation is in agreement with experiments reported with other vaccine platforms that showed that injection of RBD or S-trimer alone did not produce significant responses^{31,37}. In our experiment, we chose to inject

5 μ g of RBD but a dose-response study would be necessary to determine the optimal amount. As a comparison, similar experiments carried out with a similar 60-mer platform showed that 0.9 μ g instead of 5 μ g of RBD resulted in a similar immune response paving the way to dose-sparing³⁸. After the second immunization, although a response was observed in the non-decorated groups, the titers attained in the decorated groups were about 10 fold greater (Figure 6a). Notably, the anti-RBD response in the latter groups endured over time with similar titers at 2 and 4 weeks following the second immunization (Figure 6b). The anti-SARS-CoV-2 RBD sera were further assessed for their capacity to neutralize S-protein pseudotyped lentivirus particles (Figure 7). As seen for binding responses, a neutralizing activity was observed in the RBD-decorated groups after the first immunization. Overall, a good correlation between ELISA and neutralizing titers was observed. Strong neutralizing titers were attained in all mice immunized with ADD-RBD after the boost immunization, superior to those of convalescent COVID-19 patients (Figure 7b), showing the ability of our vaccine platform to elicit functional Ab responses with a potential protective activity. The low titers obtained in mice immunized with RBD and naked ADDomer (no decoration) again demonstrated that the high immunogenicity achieved with the decorated VLPs originated from the antigen multimeric display. The T-cell response which also plays a role in the protection against COVID-19 was not studied in our work. Overall, the data are in adequacy with results obtained with similar vaccine platforms using multimeric display of the SARS-CoV-2 RBD on scaffolds such as the 24mer-ferritin, the 60-mer dodecahedral thermophilic aldolase^{31,38,39,40,41}. In contrast to these latter vaccine platforms, our particles originate from a human virus, Adenovirus serotype 3 (HAd3), which is known to have a relatively high seroprevalence^{42,43}. However, if HAdV-3 is globally among the most common types implicated in HAdV infections a great variation is observed by geographic regions. Indeed, HAdV-3 accounts for 15 to 87% of adenoviral respiratory infections with a greater prevalence in Asia than in Western countries⁴⁴. Neutralizing antibodies against HAdV-3 are mainly directed against the hexon protein which is not present in ADDomer made only of penton bases.

A potentially detrimental impact of preexisting immunity on the immunogenicity of adenovirus-based viral vectors has been described^{45,46}, which thus led us to explore whether such effect may also be encountered with our adenovirus-derived VLP platform. Interestingly, in contrast to adenovirus-viral vectors, our adenovirus-inspired VLP platform appears to benefit from pre-immunity against the VLP. Indeed, mice with immunity to ADDomer at the time of the first immunization were found to respond with greater Ab titers against RBD than naive mice (group 4 *versus* group 3, Figure 5c). This beneficial effect may be in particular explained

by the formation of immune complexes leading to a better uptake by antigen presenting cells, *via* Fc receptors, resulting in an increase in immunogenicity⁴⁷. This property persisted after the second immunization although the differences between groups 3 and 4 were less marked, probably due to an anti-ADDomer response generated in group 3 during the first injection. Of note, the prevalence, in individuals who have been infected with HAdV-3, of antibodies directed against the penton base, which is the only component of ADDomer, is not precisely known. Our present work anticipates that our platform could be used whatever the HAdV-3 immunological status of the patients, and the potential presence of anti-penton antibodies.

In conclusion, we designed a new adenovirus-inspired VLP platform that achieves high immunogenicity against the displayed antigen. In contrast to current platforms using the ST/SC system, we opted to engineer the ST on the VLP side, within the exposed VL. Thanks to this design, it can be envisaged to add another ST in a second exposed loop such as the RGD (RGDL), to further increase stoichiometry (up to 120 attachment sites). Moreover, for mosaic vaccine approaches, the RGDL can be used to insert another orthogonal attachment site such as a snoop tag to display a second antigen. As an added value, the use of two different attachment tags/loops allows for differential antigenic stoichiometries and display patterns. Indeed, the RGDLs are more central on the pentameric building block of the ADDomer than the VLs, which are exposed on the periphery, resulting in a greater distance between the VLs than the RGDLs at the pentamer level. Displaying antigens through attachment to these two loops will therefore lead to various patterns of antigen display at the VLP scale as shown in supplementary Figure 5. This will offer a large range of combinations to vary the stoichiometry of decoration as well as the distance between the antigens to potentially optimize immunogenicity⁴⁸. The versatility of the vaccine platform can thus be exploited to generate mosaic particles displaying RBDs from different betacoronaviruses³⁷ or SARS-CoV-2 variants to broaden NAb responses and protect against current and future variants of concern. A recent work described that 60-mer mosaic nanoparticles with four to eight distinct RBDs from betacoronaviruses can be generated. Remarkably, the codisplay of the SARS-CoV-2 RBD along with other RBDs showed that the combination of antigens on the same particle did not affect the elicitation of neutralizing antibodies against a particular RBD³⁷. Moreover, neutralization of both ‘matched’ and ‘mismatched’ strains was observed after mosaic priming suggesting that such particles might protect against several betacoronaviruses at once after a single injection.

More generally, our new versatile platform constitutes a putative tool in the preparedness to fight emerging pathogens that will remain to be investigated in viral challenge trials.

MATERIAL AND METHODS

Baculovirus production

The baculovirus expression system was used for both the production of ADDomer-SpyTag (ADD-ST) and for the RBD fused to SpyCatcher (RBD-SC). Synthetic DNA (Genscript) was cloned in the pACEBac1 using the restriction sites BamHI and HindIII. For RBD-SC, the SARS-CoV-2 spike sequence (320-554) was cloned upstream of the Spy Catcher and a hexa His-Tag was added in C-terminus of SC. This fusion protein was secreted using the melittin signal peptide present in the vector. Recombinant baculoviruses were made by transposition with an in house bacmid expressing Yellow Fluorescent Protein, as previously described⁵. Baculovirus were amplified on Sf21 cells at low multiplicity of infection (MOI) and after two amplification cycles were used to infect insect cells for 64-72h at high MOI. For ADD-ST production, the infected cells were pelleted and recovered whereas for RBD-SC cells were discarded and the supernatant was saved.

Protein Purification

ADDomer and ADD-ST purification

The ADDomer and ADD-ST was purified according to classical protocol⁴⁹. Briefly, after lysis of the insect cell pellet by 3 cycles of freeze-thaw in the presence of Complete protease inhibitor cocktail (Roche), and removal of debris the lysate was loaded onto a 20-40% sucrose density gradient. The gradient was centrifuged for 18h at 4°C on a SW41 Rotor in a Beckman XPN-80 ultracentrifuge. The dense collected fractions at the bottom of the tubes were dialyzed against Hepes 10 mM pH 7.4, NaCl 150 mM and then loaded onto a Macroprep Q cartridge (Bio-rad). After elution by a 150 to 600 mM linear NaCl gradient in Hepes 10mM pH 7.4, ADDomer-containing fractions were checked by SDS-PAGE and concentrated on Amicon (MWCO: 100kDa) with buffer exchange to Hepes 10 mM pH 7.4, NaCl 150 mM.

Spy Catcher (SC) purification

After lysis of the insect cell pellet as described above in the presence of Complete EDTA-free protease inhibitor cocktail, the clarified lysate was diluted 5-time in wash buffer (Hepes 10mM pH7.4, NaCl 150mM, imidazole 10mM and loaded onto a His Gravitrapp column (Cytiva) by gravity, with two passages of the lysate onto the column. The column was washed with the same buffer, then eluted by 200 mM Imidazole. The fractions were analyzed by SDS-PAGE,

pooled and Imidazole was withdrawn by buffer exchange using Amicon ultrafiltration devices (MWCO: 4 kDa).

RBD-SC purification

The insect cell supernatant was centrifuged after thawing for 15 min at 7,500 g and loaded onto a Hepes 10 mM pH7.4 pre-equilibrated Heparin column (Cytiva) of 5 ml for 500 ml of supernatant. The column was washed with Hepes 10 mM pH 7.4 for 25 mL then eluted for 10 mL with 0 to 500 mM linear NaCl gradient in Hepes 10 mM pH 7.4. The eluate was supplemented with 30 mM Imidazole-HCl and incubated with Ni-NTA beads (Qiagen), 2 ml of beads for 500 ml culture, for at least 1h at 4°C under gentle agitation. The beads were then poured into an empty column and the protein was eluted by 2 column volumes of 250 mM Imidazole in Hepes 10 mM pH 7.4, NaCl 150 mM. It was then submitted to buffer exchange using Amicon device (MWCO 30 kDa).

RBD purification

The following reagent was produced under HHSN272201400008C and obtained through BEI Resources, NIAID, NIH: Vector pCAGGS containing the SARS-CoV2, Wuhan-Hu-1 Spike Glycoprotein Receptor Binding Domain (RBD), NR-52309. Vector NR-52309 from BEI Resources was used for mammalian expression of the RBD alone used for ELISA. EXPI293 cells grown in EXPI293 expression medium were transiently transfected with the vector according to the manufacturer's protocol (Thermo Fisher Scientific). Five days after transfection, the medium was recovered and filtered through a 0.45 mm filter. Two-step protein purification on Aktä Xpress, with a HisTrap HP column (GE Healthcare) and a Superdex 75 column (GE Healthcare) was performed using 20 mM Tris pH 7.5 and 150 mM NaCl buffer. For the HisTrap, a wash step in 75 mM imidazole was performed and RBD was eluted in buffer supplemented with 500 mM imidazole before loading onto the gel filtration column run in equilibration buffer.

N-glycosidase treatment

RBD-SC was incubated for 1H at 37°C with the N-glycosidase PGNase F (kindly provided by Dr Nicole Thielens) at 1/100 ratio then run on gel next to the same amount of untreated RBD-SC.

Complex formation

ADD-SpyTag + SpyCatcher (ADD-ST/SC) for Cryo-EM:

The purified ADD-ST was mixed with an excess of purified SpyCatcher (ratio 1:4). The protein mix was incubated overnight at 25°C under shaking in Thermomixer (300 rpm). A purification step on a sucrose gradient was performed to remove the SpyCatcher in excess and to recover only the fully-decorated ADD-ST/SC at the bottom of the gradient. Buffer exchange was done in 10 mM Hepes, 150 mM NaCl and the sample was concentrated to 1.5 mg/ml.

ADD-SpyTag + SpyCatcher-RBD (ADD-RBD) for characterization and mice immunization experiments

Covalent complex formation was obtained by incubation of purified ADD-ST with purified RBD protein fused to SC (RBD-SC). Incubation was performed at 25°C under agitation on a Thermomixer at 300 rpm. RBD-SC ratio per ADD-ST was varied according to the experiment as indicated in the text. For immunization experiments, a ratio of 40 copies of RBD-SC per ADD-ST was chosen to leave minimal free RBD-SC. This ratio was calculated on SDS-PAGE using ImageLab software (Bio-Rad). Integrity of the ADD-RBD was checked by negative staining electron microscopy.

In vivo experiments and vaccination

Vaccination experiments have been performed according to ethical guidelines, under a protocol approved by the Grenoble Ethical Committee for Animal Experimentation and the French Ministry of Higher Education and Researcher (reference number: APAFIS#27765-2020102114206782 v2). 5-week-old female Balb/c mice were purchased from Janvier (Le Genestet St. Isle, France). For all mice groups, vaccines were in PBS and adjuvanted with one volume of ADDavax (Invivogen). All the mice received 2 vaccine doses at 2 weeks of interval (Day 0 and Day 14) starting at 8-weeks of age. Each mice group received subcutaneously the corresponding vaccine as indicated within the paper in 100 µl final volume, in the right flank. Pre-immunized group received 2 weeks before the first dose of vaccine (day -15) the ADDomer vector alone (5 µg in 100 µl final volume, in the right flank). The day before each vaccination, and 2 and 4 weeks after the last vaccination, 100 µl of blood was withdrawn for serologic tests. For retro-orbital blood sampling, mice were anesthetized with 4% Isoflurane.

ELISA

The antigens (either RBD or ADDomer) were diluted at 1 μ g/ml in PBS and 50 μ l were coated overnight at 4°C, in a 96 well plate (Maxisorp NUNC Immunoplate, #442404). Plates were washed using a ThermoScientific Microplate washer (#5165040). After three washes with 100 μ l of PBS-Tween 0.05%, plates were blocked with PBS-BSA 3% for one hour. Mouse serum was serially diluted in PBS and incubated for one hour (50 μ l/well) at room temperature. After five washes with PBS-Tween 0.05%; a goat anti mouse IgG (H+L) secondary Ab linked to HRP (JIR 115-035-062) diluted at 1/2,500 in PBS-Tween 0.05% was added for one hour. After five washes, 50 μ l of TMB substrate was distributed per well. The enzymatic reaction was stopped after 70 sec by addition of 50 μ l of H₂S0₄ (1M), and plates were read at 450nm with a TECAN Spark 10M plate reader.

Electron microscopy

Negative staining

3.5 μ L of samples were adsorbed on the clean side of a carbon film previously evaporated on mica and then stained using 2% (w/v) Sodium Silico Tungstate pH 7.4 for 30 s. The sample/carbon ensemble was then transferred to a grid and air-dried. Images were acquired under low dose conditions (<30 e-/ \AA^2) on a F20 electron microscope operated at 120 kV using a CETA camera.

Cryo-EM

Quantifoil grids (300 mesh, R 1.2/1.3) were negatively glow-discharged at 30 mA for 45 s. 3.5 μ l of the sample were applied onto the grid, and excess solution was blotted away with a Vitrobot Mark IV (FEI) (blot time: 6 s, blot force: 0, 100% humidity, 20 °C), before plunge-freezing in liquid ethane. The grid was transferred onto a 200 kV Thermo Fisher Glacios microscope equipped with a K2 summit direct electron detector for data collection. Automated data collection was performed with SerialEM, acquiring one image per hole, in counting mode. Micrographs were recorded at a nominal \times 36,000 magnification giving a pixel size of 1.145 \AA (calibrated using a β -galactosidase sample) with a defocus ranging from -0.6 to -2.35 μ m. In total, 1038 movies with 40 frames per movie were collected with a total exposure of 40 e-/ \AA^2 .

Image processing and cryo-EM structure refinement

Movie drift correction was performed with Motioncor2⁵⁰ using frames from 2 to 40. CTF determination was performed with Relion 3.1.2 (Scheres 2012). 939 movies out of 1038 were kept at this stage. Particles selection have been done using the Laplacian filter with a diameter between 30 and 40 nm. A total of 77 323 particles have been automatically selected, boxed into 480x480 pixel² boxes and submitted to 2D classification. After extensive selection and generation of an initial model imposing I1 symmetry, 3D refinement followed by CTF Refine and post-processing generated a final reconstruction including 10163 particles with a resolution of 2.76 Å (Fourier Shell = 0.143) (applied B-factor -82)

Immunofluorescence Microscopy

HeLa-ACE2 cells (kindly provided by Dr David Nemazee) were seeded on polylysine coated glass coverslips the day before the experiment. Coverslips were incubated for 1H at 4°C with 0.75ug of either ADD-ST or ADD-RBD in 50µl of pre-chilled DMEM. Coverslips were washed three time in cold PBS then fixed for 10 minutes with -20°C methanol. Fixed cells were blocked for 1H in PBS supplemented by 3% Normal Goat Serum , then incubated for 1H with 1/1,000 rabbit HAd3 anti penton base serum. After three PBS washes cells were incubated with 1/250 antiRabbit Alexa488 Ab (ThermoFischer A32721), washed three time in PBS then nuclei were counterstained with Hoechst 33258 for 3 minutes before mounting. Observation were done on Zoe microscope (BioRad).

Surface plasmon resonance

Surface plasmon resonance experiment was performed on a T200 instrument. Anti human Fc polyclonal antibody (Jackson Immunoresearch, 109-005-008) diluted at 25 µg/ml in 10 mM sodium acetate pH 5 was immobilized on CM5 sensor chips using the amine coupling chemistry according to the manufacturer's instructions (Cytiva) to get an immobilization level of 14 000 RU. ACE-2 -Fc (GenScript Z033484) was diluted at 1.2µg/ml in HBS P+ (Cytiva) to get an capture level of 100RU. For interaction measurements, ADD-RBD (ranging from 1 nM to 11nM in HBSP+) was injected over captured ACE-2 Fc in HBS P+ buffer at 30 µl/min. Anti human Fc polyclonal antibody flow cell was used for correction of the binding response. Regeneration of the surfaces was achieved by 10mM Glycine pH2. Binding curves were analyzed using BIAEvaluation software (GE Healthcare) and data was fit to a 1:1 Langmuir with drifting baseline interaction model.

Neutralization assays and pseudo-typed SARS-CoV-2 virion production

Pseudovirus production and titration

Neutralization assays were performed using lentiviral pseudotypes harbouring the SARS-CoV-2 spike and encoding luciferase. Briefly, gag/pol and luciferase plasmids were co-transfected with a SARS-CoV-2 spike plasmid with a C-term deletion of 18aa at 1/0,4/1 ratio on adherent HEK293T cells. Supernatants containing the produced pseudoviruses were harvested 72H after transfection, centrifuged, filtered through 0.45µm and concentrated 50 times on Amicon Ultra (MWCO 100KDa), aliquoted and stored at -80°C. Before use, supernatants were tittered using HeLa ACE-2 cells to determine the appropriate dilution of pseudovirus necessary to obtain about 150 000 RLU per well in a 48 well-plate.

Neutralization assay

Serial 3-fold dilutions starting from 1/10 dilution (serum), or 6µg/mL (known bNAbs) were let in contact with the pseudoviruses for 1h at 37°C in 96-w white plates (Greiner #675083), before addition of HeLa ACE2 cells. Plates were incubated 24h at 37°C, protected from evaporation, then cells were fed with 60 µL of DMEM (Gibco 11966-025) supplemented with 10% FBS (VWR 97068-086), and incubated for another 24h. Medium in each well was aspirated and replaced by 45 µL of 1X cell lysis buffer (Ozbioscience # LUC1000) for a 60 min-incubation under agitation. Thirty µL of luciferin substrate was then added and Relative Light Unit (RLU) was measured instantly by a luminometer. For competition with ADD-ST, ADD-RBD and RBD-SC the same protocol was used with initial concentration of 150µg/mL for ADD-ST, 200µg/mL and ADD-RBD and 50µg/mL for RBD-SC alone. Serums from a cohort of Grenoble region hospitalized convalescent patients were obtained with their consent, 6 to 8 months following COVID-19 diagnosis. The study was approved by the ‘Comité de Protection des Personnes SUD-EST I’ on 20 August 2020 (ref 2020-84).

Statistical analyses

For ELISA and neutralization assays, IC50 were deduced from crude data after normalization using GraphPad Prism "log(inhibitor) vs normalized response" function. Comparison of IC50 values were performed applying Kruskal-Wallis tests on the data sets, using GraphPad Prism 6 software.

FIGURES

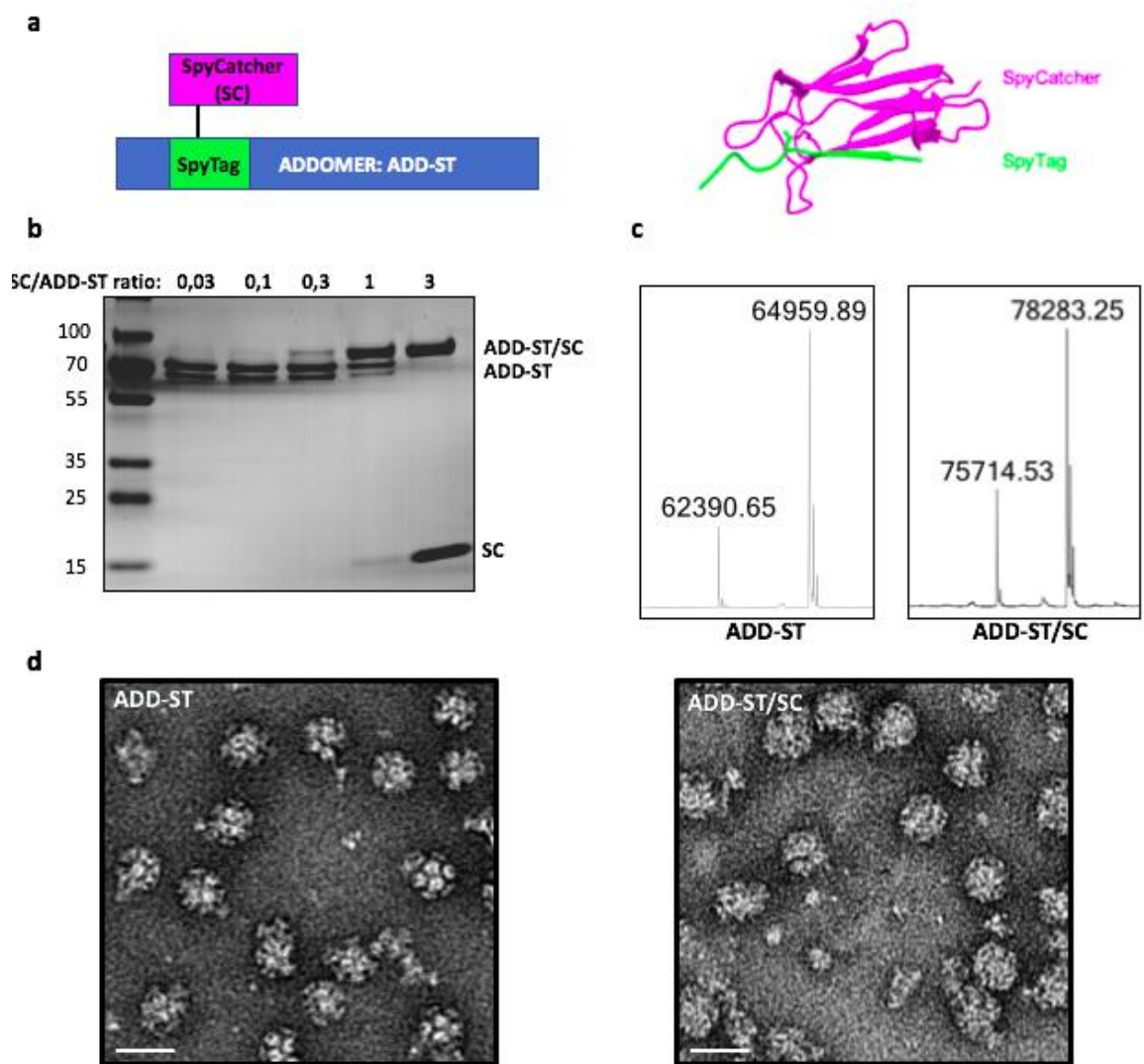


Figure 1: Application of the SpyTag/SpyCatcher cross-linking method to the ADDomer technology. (a) Diagram showing the internal insertion of SpyTag in the internal loop of an ADDomer monomer. Spytag (in green) can make an isopeptidic bond with SpyCatcher (in purple). Structure of a SpyTag covalently linked to a SpyCatcher is shown on the right (PDB code: 4MLI) (b) SDS-PAGE profile of boiled samples of ADD-ST after interaction with incremental ratio of SC showing the apparition of a higher MW covalent adduct (ADD-ST/SC). (c) Electrospray ionization graphs of ADD-ST and ADD-ST/SC showing the shift of the peaks by 13.3 kDa. The doublet is due to an alternative start of translation in ADD-ST and display the same mass shift of 13,3kDa. (d) Negative staining electron micrographs of ADD-ST and ADD-ST/SC (bar: 30nm).

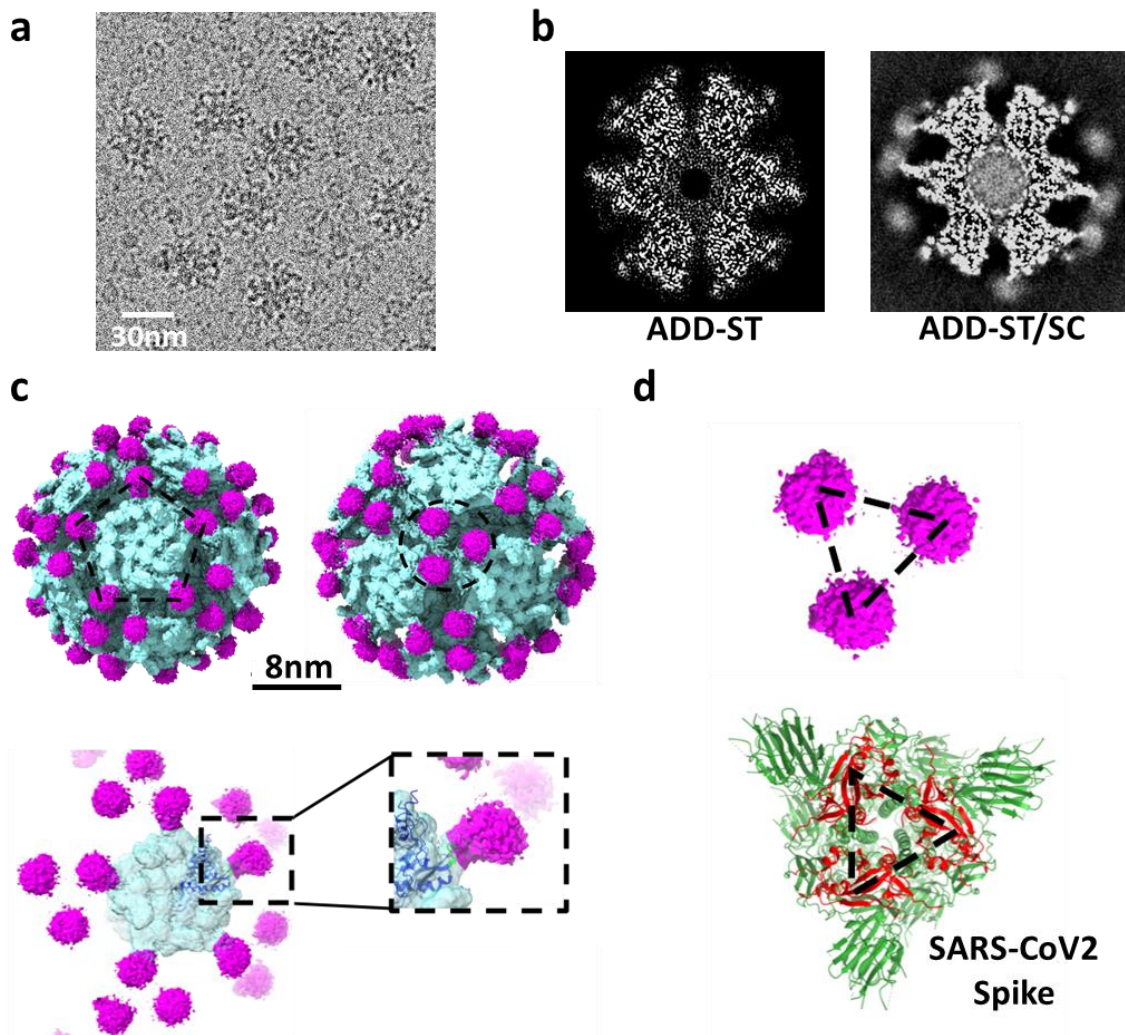


Figure 2: Cryo-EM reconstruction of ADD-ST decorated with SC. (a) Representative 2D picture of the particles frozen on ice (bar:30nm). (b) Section through the density of the 3D reconstruction without (ADD-ST) or with SC (ADD-ST/SC). (c) Isosurface representation of the ADDomer-ST/SC 3D structure showing the extra density of SC in purple onto the non-decorated ADD-ST scaffold in light blue. The particle is represented along either the 5 or 3 fold-axis (left and right, upper panel; bars: 80 and 20Å, respectively). Focus on a pentameric complex of ADD-ST/SC with a close up view onto a single SC/ST interaction (dashed line boxes in the lower panel). The atomic resolution structure (dark blue) of the HAd3 penton base (PDB 4AQO) has been fitted into the ADDomer EM density (light blue) (d) Organization of SC along the 3-fold axis of the particle (upper panel) and comparison with SARS-CoV-2 RBD architecture (in red) within the Spike protein structure (in green, PDB 6VXX) at the same scale.

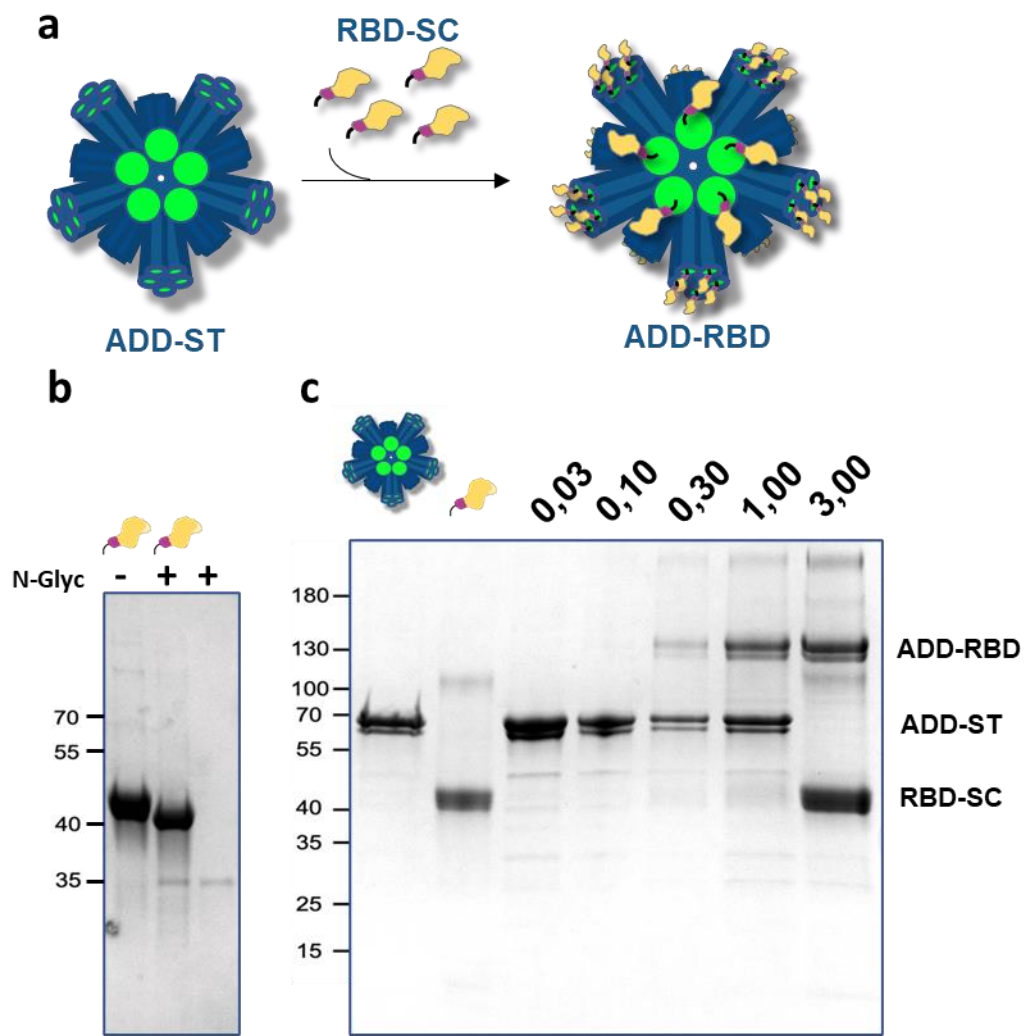


Figure 3: Fusion of SARS-CoV-2 RBD to SC enables its surface presentation on ADDomer particles. (a) Schematic representation of the spontaneous RBD-SC binding to ADD-ST to give ADD-RBD . (b) SDS-PAGE gel with RBD-SC before (-) and after (+) treatment with N-glycosidase and in absence of SC-RBD. The decrease of the molecular weight of SC-RBD after treatment indicates that it is glycosylated. (c) SDS-PAGE gel of boiled sample showing from left to right, the marker, bands of ADD-ST alone, SC-RBD alone and a fix amount of ADD-ST incubated with different ratio of RBD-SC (per particle monomer). The additional upper bands reflect the covalent adduct between ADD-ST and RBD-SC and thus the apparition of ADD-RBD. As expected, the increasing intensities of the ADD-RBD bands correlate with a decrease of non-decorated ADD-ST monomer.

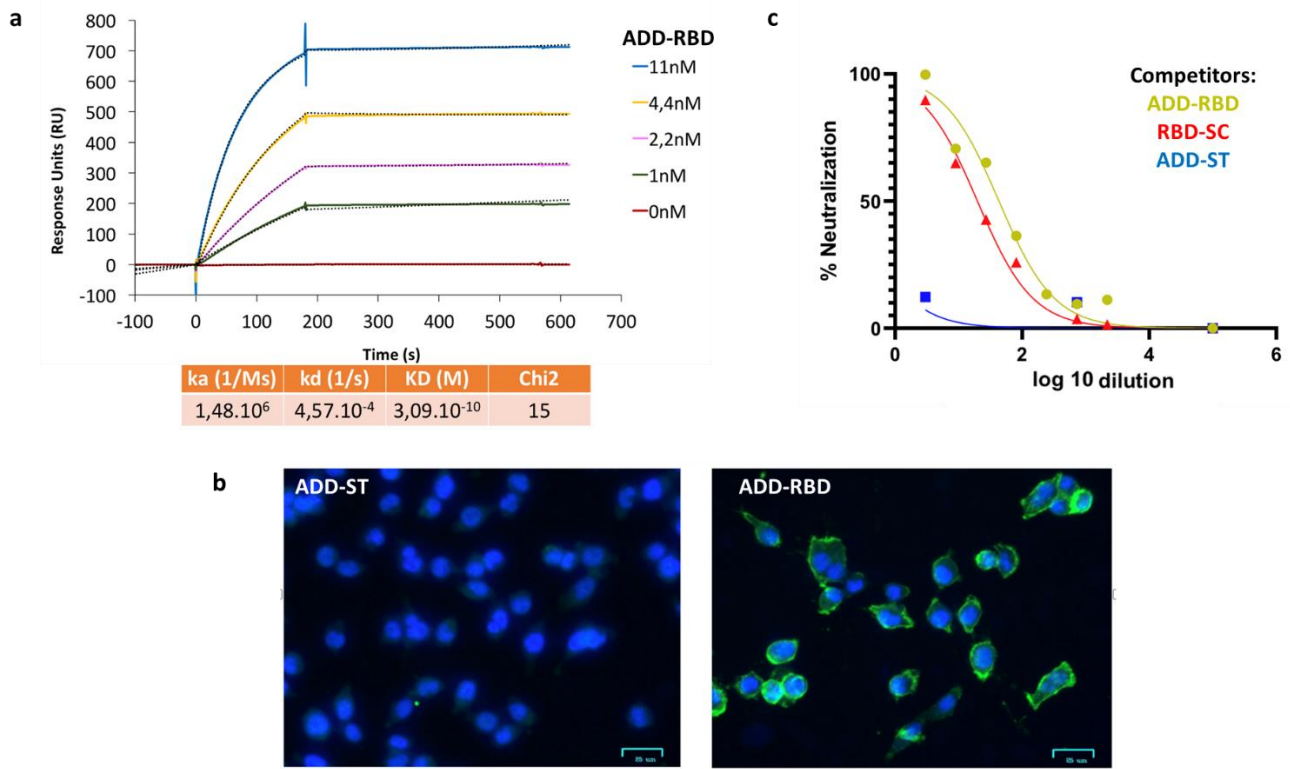


Figure 4: Functional characterization of the ADDomer particles decorated with SARS-CoV-2 RBD. (a) Surface plasmon resonance sensorgrams obtained by injection of different amounts of ADD-RBD to the immobilized ectodomain of the human ACE2 receptor fused to IgG Fc constant domain²⁹ and kinetic analysis. (b) Immunofluorescence microscopy images of HeLa-ACE2 cell at 4°C with double staining with Hoechst (blue) and anti-ADDomer Ab and an Alexa488-conjugated secondary Ab (green) in presence of non-decorated ADD-ST (left) or ADD-RBD (right) particles. (c) Competition of pseudotyped SARS-CoV-2 virus encoding luciferase with either ADD-ST (blue), RBD-SC (red) and ADD-RBD (gold) at different dilutions.

a

	Group 1	Group 2	Group 3	Group 4
RBD-SC	alone	+ADD Not displayed	+ ADD-ST Displayed	+ADD-ST Displayed
Ad pre-immunity	-	-	-	+

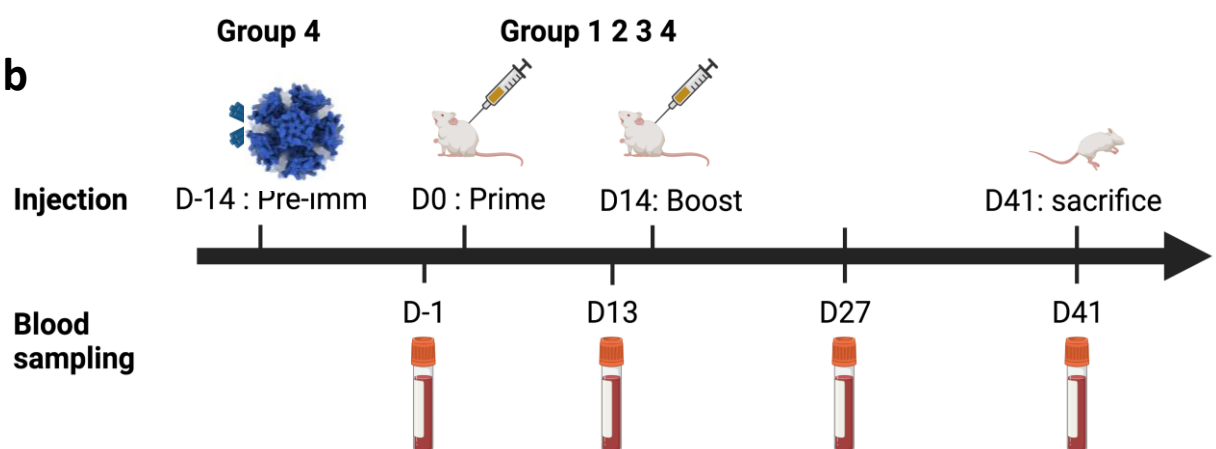
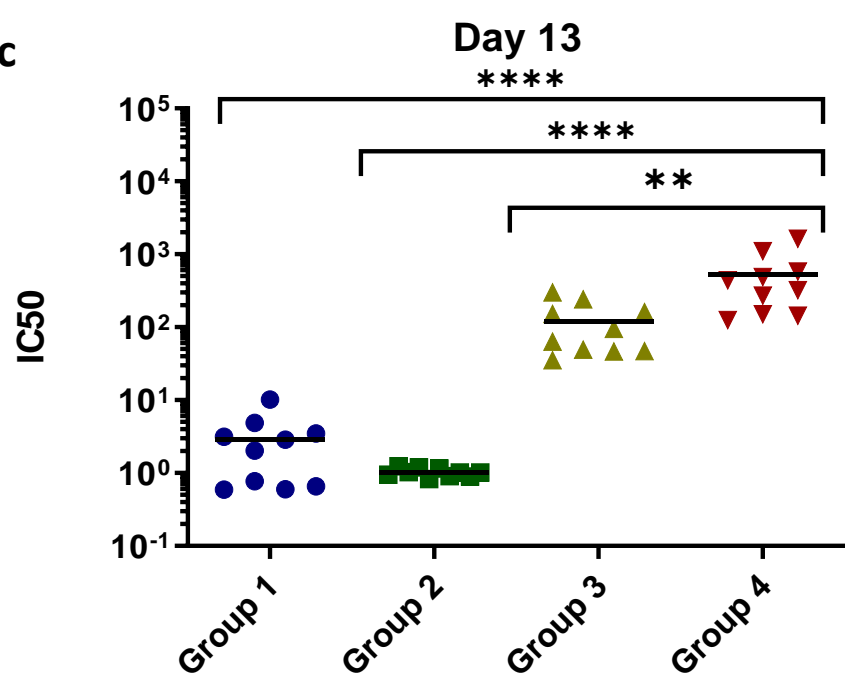
b**c**

Figure 5 : Immunization studies on mice inoculated with the same amount of RBD under different conditions.

(a) Different groups were constituted to address the respective role of RBD-SC alone (group 1), RBD-SC in presence of naked-ADDomer (group 2) and RBD-SC displayed by ADDomer (ADD-RBD) either in adenovirus naive or adenovirus pre-immunized mice (group 3 and 4 respectively). (b) Immunization schedule and blood sampling for all groups. (c) IC50 of anti RBD response 13 days after the first immunization ($n=10$). Lines are mean values (Kruskall-Wallis statistical test).

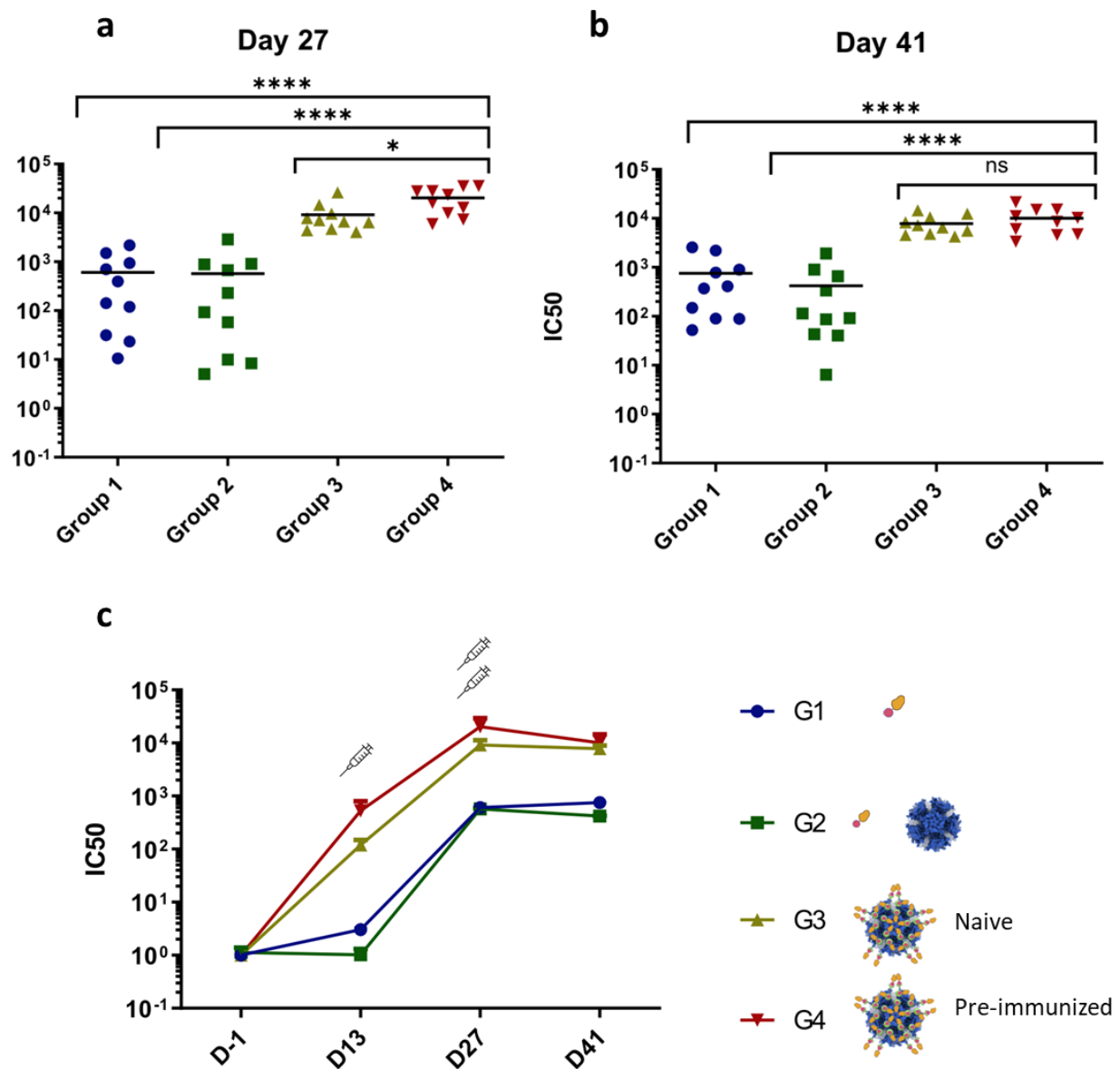


Figure 6: Anti-RBD Ab in all groups of mice 2 and 4 weeks after the booster immunization.
 (a) IC50 of anti-RBD for each individual mice from all groups, 2 weeks after the booster injection. (b) Same data, 4 weeks after the booster injection. Lines are mean values (Kruskall-Wallis statistical test). (c) Means of the anti-RBD response from all mice according to their groups and the time after the first immunization performed at Day 0.

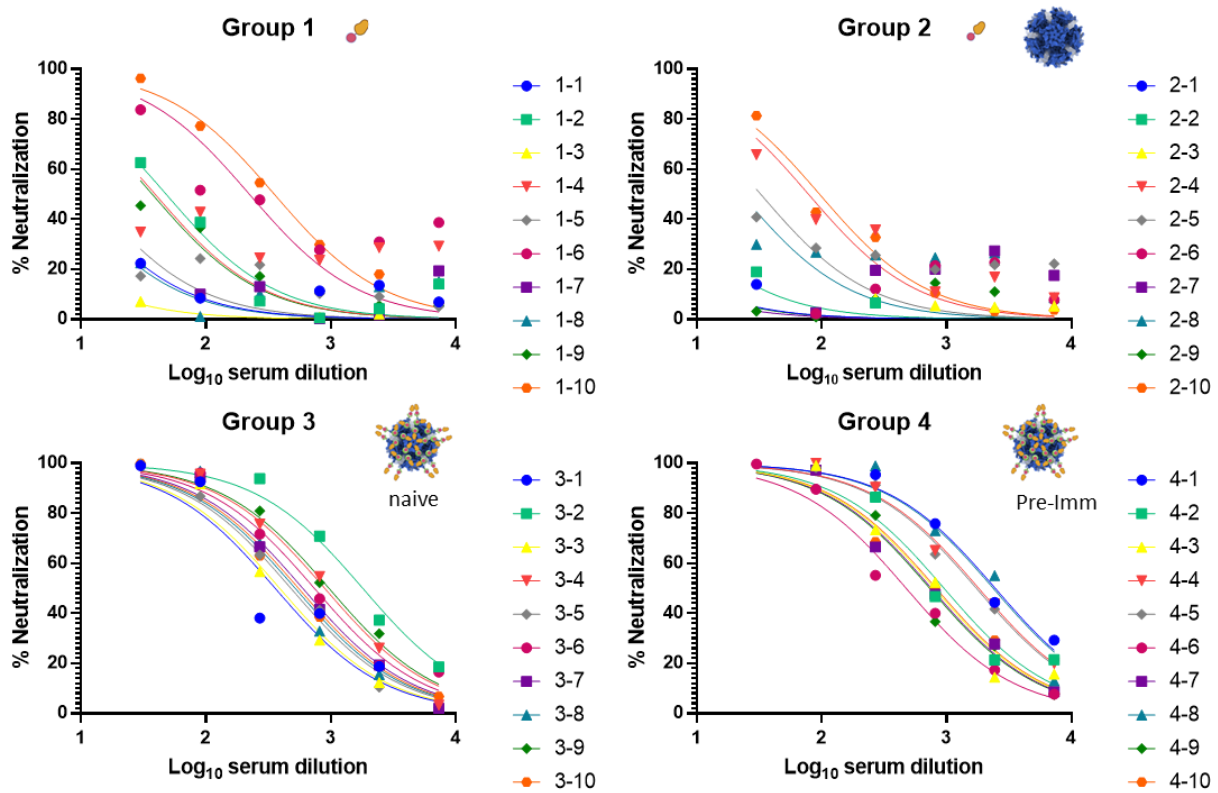
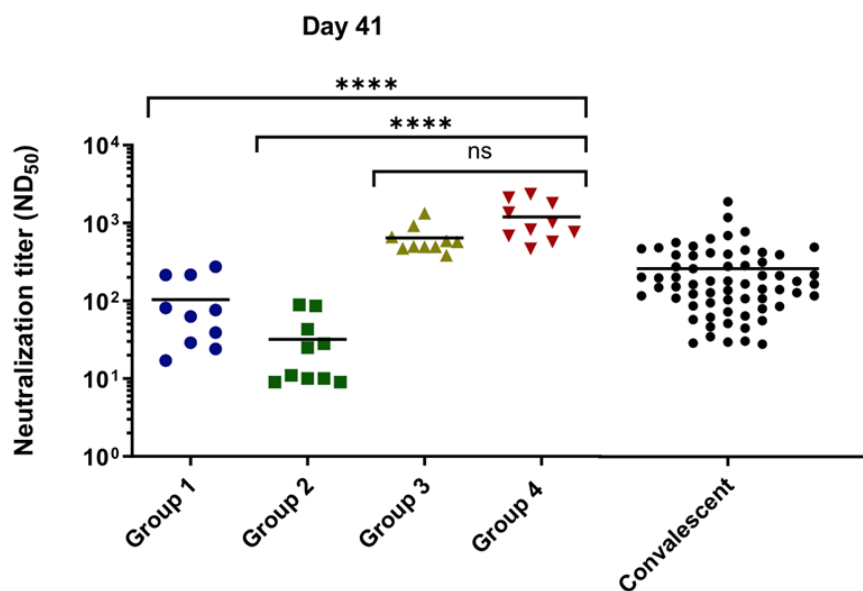
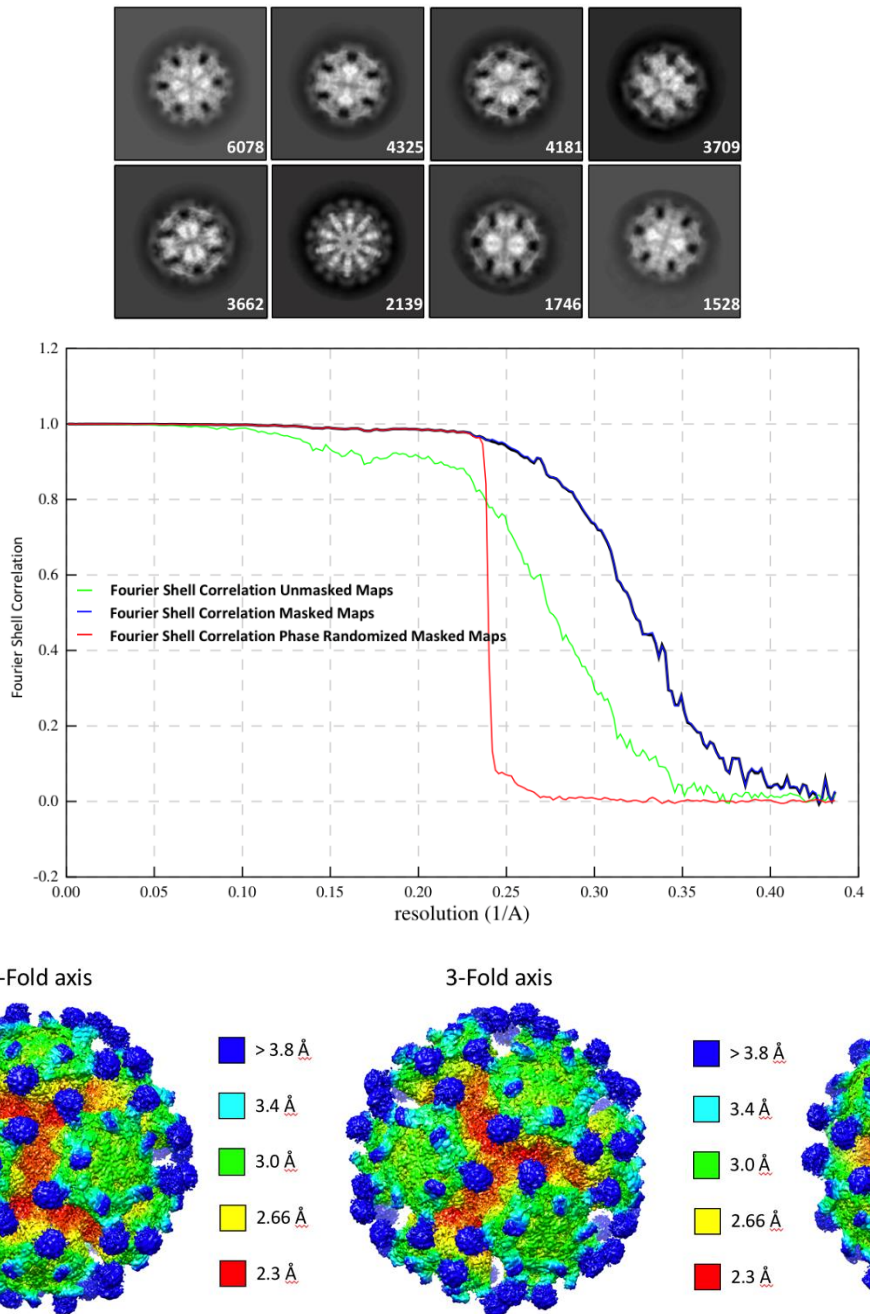
a**b**

Figure 7: Neutralization study of mice sera on SARS-CoV-2 pseudo-typed virus and comparison with COVID-19 convalescent patients.

(a) Curves showing the percentage of neutralization of individual sera of mice from all groups on viral infection by SARS-CoV-2 pseudo-typed virus. This pseudo-typed viruses encodes luciferase as a reporter of cell infection and was preincubated with three-time serial dilutions

of sera. Luciferase expression was compared to the one of non-neutralized virus. (b) Comparison of the neutralization titer at 50% of the maximal effect (ND50) from all individual mice with the mean represented by a line. Statistical analysis (Kruskall-Wallis test) demonstrates the superiority of neutralization of sera from mice immunized with RBD-decorated ADDomer particles versus both non-decorated particles and COVID-19 convalescent patients.

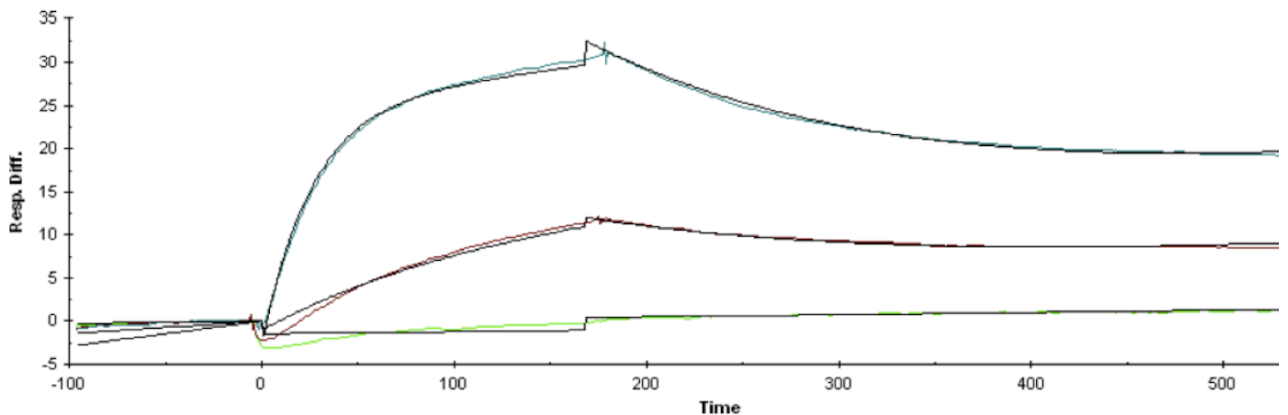
SUPPLEMENTARY FIGURES



Supplementary Fig. S1. Cryo-EM initial 2D classes and local resolution.

Initial 2D classes are shown in the upper panel with the number of particles indicated. The Fourier Shell Correlation in the middle panel gives a 2.76 Å resolution.

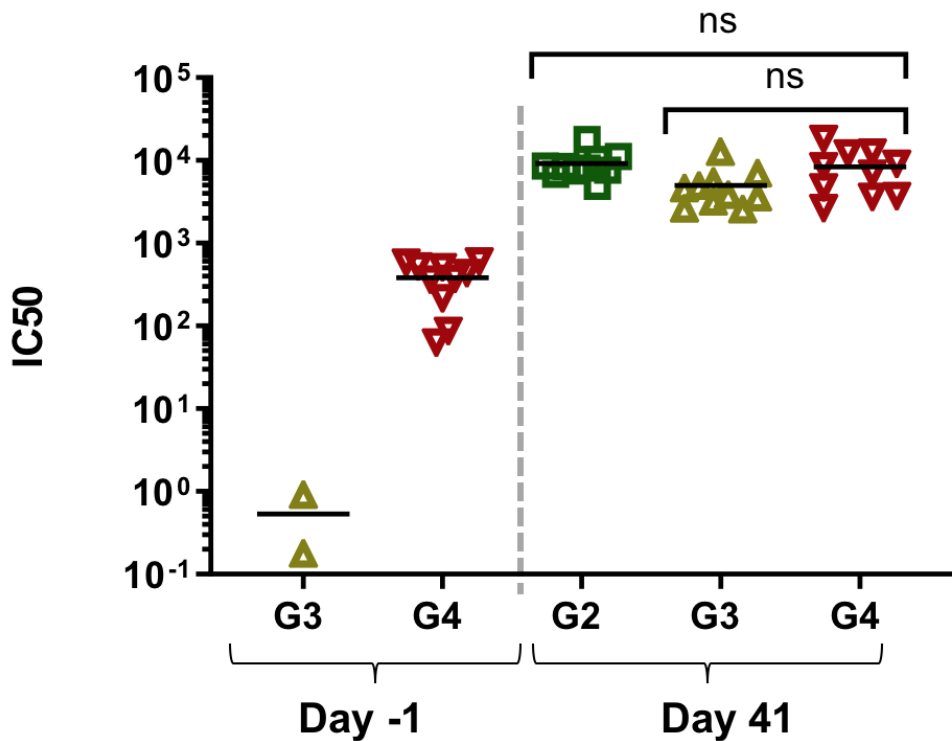
Local resolution(lower panel) of the structure is shown along the 2, 3 and 5-fold axis of the particle.



ka (1/Ms)	kd (1/s)	KD (M)	Chi2
3,37.10 ⁵	5,14.10 ⁻³	1,53.10 ⁻⁸	0,128

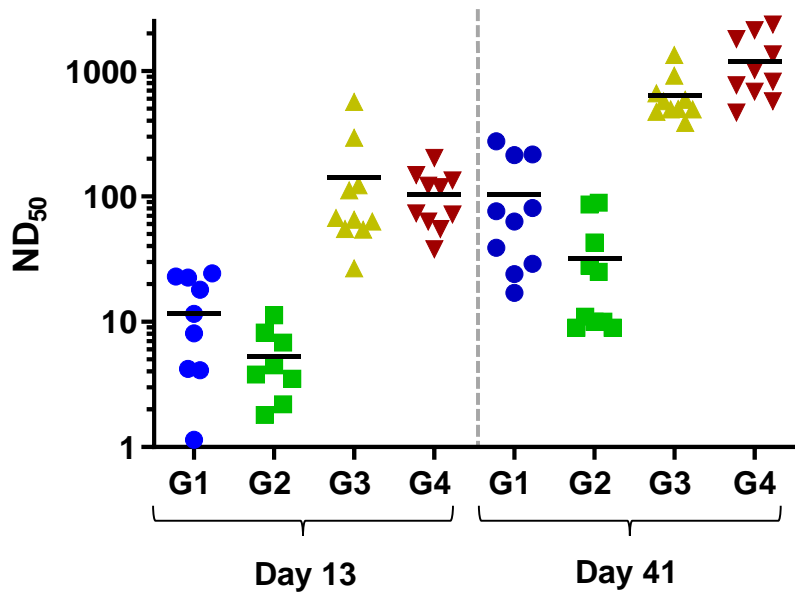
Supplementary Fig. S2. Study of RBD-SC binding to ACE2 by SPR.

RBD-SC alone (i.e. not displayed) was injected at 0, 10 and 100nM onto immobilized ACE2 receptor. The estimated kinetic constants are shown in the table.



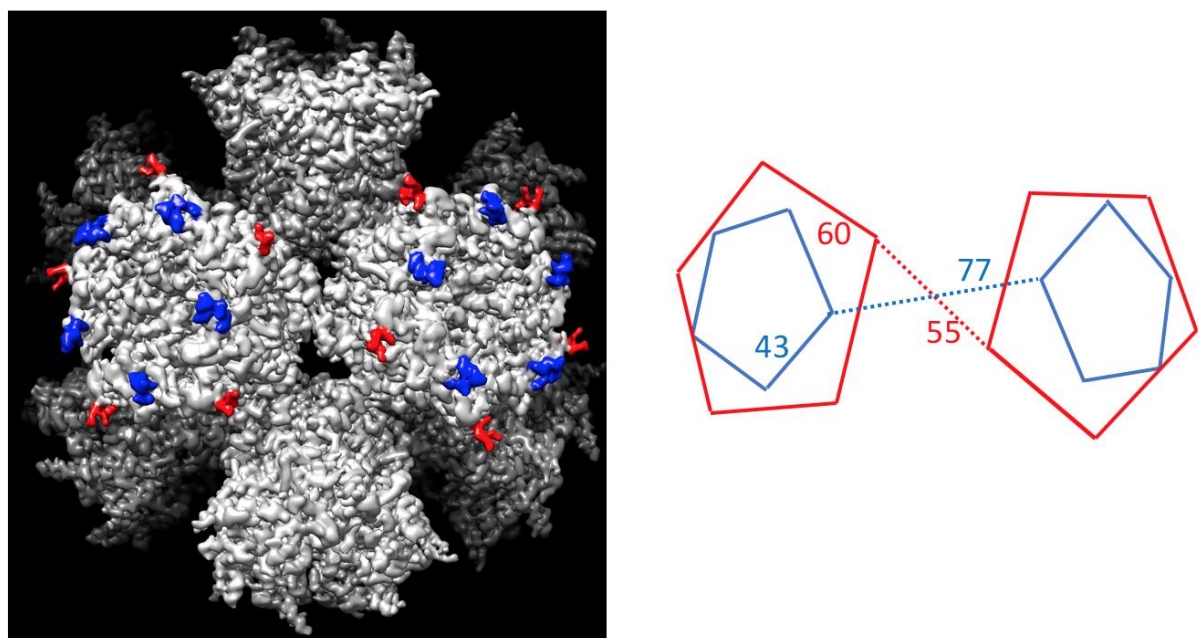
Supplementary Fig. S3. Anti-ADDomer response studied by ELISA.

Non-decorated ADDomer were coated on the well and incubated with sera from different groups of mice before the first injection (D-1) or at the end of the experiment (D41). Note that all the mice preimmunized with ADDomer (G4, D-1) were positive before injection of ADD-RBD while naïve mice (G3, D-1) were negative as expected. Mann-Whitney tests showed no difference between group 4 and groups 2 and 3 at D41.



Supplementary Fig. S4. Sera neutralization titer after one and two injections for all groups of mice.

Note that RBD displayed on ADDomer enabled to get similar or higher neutralization titer at the first injection (G3 and G4, D13) than RBD not displayed on the platform after two injections (G1 and G2 at D41).



Supplementary Fig. S5. Distance between the exposed loops in ADDomer.

The 3D structure of ADDomer in grey is shown on the left panel with the variable loops highlighted in red and the RGDL highlighted in blue on two adjacent pentamers. Distance calculation (right panel) showed the distance in Å between VL and RGDL on the same pentamer or between two adjacent pentamers.

ACKNOWLEDGMENTS

We are grateful to the ‘CNRS Prematuration program’, to the ‘ANR-Flash COVID’ and to ‘Région Auvergne Rhône-Alpes, AuRA’ for the financial support to this work. This project has received funding from the European Research Council (ERC) under the European Union’s Horizon 2020 research and innovation program (grant agreement No 682286). D.H is supported by GEFLUC Dauphiné-Savoie, Ligue contre le Cancer Comité Isère, Université Grenoble Alpes IDEX Initiatives de Recherche Stratégiques and Fondation du Souffle-Fonds de recherche en santé respiratoire (FdS-FRSR). We thank Aymeric Peuch for help with the usage of the EM computing cluster and Emmanuelle Neumann for the training of CC in negative staining and Leandro Estrozi for help with image analysis. We thank Philippe Mas, Dr Matthieu Roustit and Dr Sebastian Dergan-Dylon for help with statistical analysis. We would like to thank David Nemazee for HeLa-ACE2 cells and SARS-CoV-2 spike expression plasmid, and Pierre Charneau for plasmids encoding for lentiviral proteins and luciferase. We thank Olivier Epaulard and Julien Lupo for the COVID-19 patients cohort study. This work used the platforms of the Grenoble Instruct-ERIC centre (ISBG ; UAR 3518 CNRS-CEA-UGA-EMBL) within the Grenoble Partnership for Structural Biology (PSB), supported by FRISBI (ANR-10-INBS-05-02) and GRAL, financed within the University Grenoble Alpes graduate school (Ecole Universitaire de Recherche) CBH-EUR-GS (ANR-17-EURE-0003). The electron microscope facility is supported by the Auvergne-Rhône-Alpes Region, the Fondation Recherche Medicale (FRM), the fonds FEDER and the GIS-Infrastructures en Biologie Santé et Agronomie (IBISA). IBS acknowledges integration into the Interdisciplinary Research Institute of Grenoble (IRIG, CEA). V.D is an internship of Master de Biologie, École Normale Supérieure de Lyon, Université Claude Bernard Lyon I, Université de Lyon, 69342 Lyon Cedex 07, France.

AUTHOR CONTRIBUTIONS

P.F, M.C.D, PP conceived the experiments. Vector production and purification were performed by C.C, V.D and S.G. Structural analysis was performed by G.S, D.F and C.C. Animal experiments were performed by D.H and S.B. Molecular interaction studies was performed by E.G, C.M and E.V.S. Immunological characterization and virus neutralization was performed by A.A, I.B. and M.B With input from all authors, P.F and P.P wrote the manuscript.

Competing interests: We declare no competing interests

REFERENCES

1. Bok, K., Sitar, S., Graham, B. S. & Mascola, J. R. Accelerated COVID-19 vaccine development: milestones, lessons, and prospects. *Immunity* **54**, 1636–1651 (2021).
2. Nguyen, B. & Tolia, N. H. Protein-based antigen presentation platforms for nanoparticle vaccines. *npj Vaccines* **6**, 70 (2021).
3. Fender, P., Ruigrok, R. W., Gout, E., Buffet, S. & Chroboczek, J. Adenovirus dodecahedron, a new vector for human gene transfer. *Nat. Biotechnol.* **15**, 52–56 (1997).
4. Besson, S., Vragniau, C., Vassal-Sternmann, E., Dagher, M. C. & Fender, P. The Adenovirus Dodecahedron: Beyond the Platonic Story. **16** (2020).
5. Vragniau, C. *et al.* Synthetic self-assembling ADDomer platform for highly efficient vaccination by genetically encoded multiepitope display. *Sci Adv* **5**, eaaw2853 (2019).
6. Zakeri, B. *et al.* Peptide tag forming a rapid covalent bond to a protein, through engineering a bacterial adhesin. *Proceedings of the National Academy of Sciences* **109**, E690–E697 (2012).
7. Brune, K. D. *et al.* Plug-and-Display: decoration of Virus-Like Particles via isopeptide bonds for modular immunization. *Sci Rep* **6**, 19234 (2016).
8. Li, L., Fierer, J. O., Rapoport, T. A. & Howarth, M. Structural Analysis and Optimization of the Covalent Association between SpyCatcher and a Peptide Tag. *Journal of Molecular Biology* **426**, 309–317 (2014).
9. Keeble, A. H. & Howarth, M. Power to the protein: enhancing and combining activities using the Spy toolbox. *Chem. Sci.* **11**, 7281–7291 (2020).
10. Zhou, P. *et al.* A pneumonia outbreak associated with a new coronavirus of probable bat origin. *Nature* **579**, 270–273 (2020).
11. Khoury, D. S. Neutralizing antibody levels are highly predictive of immune protection from symptomatic SARS-CoV-2 infection. *Nature Medicine* **27**, 15 (2021).
12. McMahan, K. *et al.* Correlates of protection against SARS-CoV-2 in rhesus macaques. *Nature* **590**, 630–634 (2021).
13. Polack, F. P. *et al.* Safety and Efficacy of the BNT162b2 mRNA Covid-19 Vaccine. *n engl j med* **383**, 13 (2020).
14. Jackson, L. A. *et al.* An mRNA Vaccine against SARS-CoV-2 — Preliminary Report. *N Engl J Med* **383**, 1920–1931 (2020).
15. Heath, P. T. *et al.* Safety and Efficacy of NVX-CoV2373 Covid-19 Vaccine. *n engl j med* **383**, 12 (2021).
16. Shang, J. *et al.* Structural basis of receptor recognition by SARS-CoV-2. *Nature* **581**, 221–224 (2020).
17. Yan, R. *et al.* Structural basis for the recognition of SARS-CoV-2 by full-length human ACE2. *Science* **367**, 1444–1448 (2020).
18. Lan, J. *et al.* Structure of the SARS-CoV-2 spike receptor-binding domain bound to the ACE2 receptor. *Nature* **581**, 215–220 (2020).
19. Starr, T. N. *et al.* Deep Mutational Scanning of SARS-CoV-2 Receptor Binding Domain Reveals Constraints on Folding and ACE2 Binding. *Cell* **182**, 1295–1310.e20 (2020).
20. Piccoli, L. *et al.* Mapping Neutralizing and Immunodominant Sites on the SARS-CoV-2 Spike Receptor-Binding Domain by Structure-Guided High-Resolution Serology. *Cell* **183**, 1024–1042.e21 (2020).
21. Barnes, C. O. *et al.* Structures of Human Antibodies Bound to SARS-CoV-2 Spike Reveal Common Epitopes and Recurrent Features of Antibodies. *Cell* **182**, 828–842.e16 (2020).
22. Robbiani, D. F. *et al.* Convergent antibody responses to SARS-CoV-2 in convalescent individuals. *Nature* **584**, 437–442 (2020).
23. Brouwer, P. J. M. *et al.* Potent neutralizing antibodies from COVID-19 patients define multiple targets of vulnerability. **9** (2020).
24. Barnes, C. O. *et al.* SARS-CoV-2 neutralizing antibody structures inform therapeutic strategies. *Nature* **588**, 682–687 (2020).
25. Alsoussi, W. B. *et al.* A Potently Neutralizing Antibody Protects Mice against SARS-CoV-2 Infection. *J Immunol* **205**, 915–922 (2020).
26. Zost, S. J. *et al.* Potently neutralizing and protective human antibodies against SARS-CoV-2. *Nature* **584**, 443–449 (2020).
27. O'Brien, M. P. *et al.* Subcutaneous REGEN-COV Antibody Combination to Prevent Covid-19. *N Engl J Med* NEJMoa2109682 (2021) doi:10.1056/NEJMoa2109682.
28. Fuschiotti, P. *et al.* Structure of the dodecahedral penton particle from human adenovirus type 3. *J. Mol. Biol.* **356**, 510–520 (2006).
29. Lei, C. *et al.* Neutralization of SARS-CoV-2 spike pseudotyped virus by recombinant ACE2-Ig. *Nat Commun* **11**, 2070 (2020).

30. Epaulard, O. *et al.* Persistence at one year of neutralizing antibodies after SARS-CoV-2 infection: Influence of initial severity and steroid use. *Journal of Infection* S0163445321005077 (2021) doi:10.1016/j.jinf.2021.10.009.
31. Tan, T. K. *et al.* A COVID-19 vaccine candidate using SpyCatcher multimerization of the SARS-CoV-2 spike protein receptor-binding domain induces potent neutralising antibody responses. *Nat Commun* **12**, 542 (2021).
32. Kanekiyo, M. *et al.* Self-assembling influenza nanoparticle vaccines elicit broadly neutralizing H1N1 antibodies. *Nature* **499**, 102–106 (2013).
33. Kanekiyo, M. *et al.* Rational Design of an Epstein-Barr Virus Vaccine Targeting the Receptor-Binding Site. *Cell* **162**, 1090–1100 (2015).
34. Bachmann, M. F. & Zinkernagel, R. M. Neutralizing antiviral B cell responses. *Annu Rev Immunol* **15**, 235–270 (1997).
35. Watanabe, Y., Allen, J. D., Wrapp, D., McLellan, J. S. & Crispin, M. Site-specific glycan analysis of the SARS-CoV-2 spike. *Science* eabb9983 (2020) doi:10.1126/science.abb9983.
36. Shinde, V. *et al.* Efficacy of NVX-CoV2373 Covid-19 Vaccine against the B.1.351 Variant. *N Engl J Med* NEJMoa2103055 (2021) doi:10.1056/NEJMoa2103055.
37. Cohen, A. A. *et al.* Mosaic nanoparticles elicit cross-reactive immune responses to zoonotic coronaviruses in mice. *6* (2021).
38. Walls, A. C. *et al.* Elicitation of potent neutralizing antibody responses by designed protein nanoparticle vaccines for SARS-CoV-2. *Cell* S0092867420314501 (2020) doi:10.1016/j.cell.2020.10.043.
39. He, L. *et al.* Single-component, self-assembling, protein nanoparticles presenting the receptor binding domain and stabilized spike as SARS-CoV-2 vaccine candidates. *Sci. Adv.* **7**, eabf1591 (2021).
40. Salzer, R. *et al.* Single-dose immunisation with a multimerised SARS-CoV-2 receptor binding domain (RBD) induces an enhanced and protective response in mice. *FEBS Lett* **595**, 2323–2340 (2021).
41. Saunders, K. O. *et al.* Neutralizing antibody vaccine for pandemic and pre-emergent coronaviruses. *Nature* **594**, 553–559 (2021).
42. Vogels, R. *et al.* Replication-Deficient Human Adenovirus Type 35 Vectors for Gene Transfer and Vaccination: Efficient Human Cell Infection and Bypass of Preexisting Adenovirus Immunity. *JVI* **77**, 8263–8271 (2003).
43. Arnberg, N. Adenovirus receptors: implications for targeting of viral vectors. *Trends in Pharmacological Sciences* **33**, 442–448 (2012).
44. Haque, E., Banik, U., Monwar, T., Anthony, L. & Adhikary, A. K. Worldwide increased prevalence of human adenovirus type 3 (HAdV-3) respiratory infections is well correlated with heterogeneous hypervariable regions (HVRs) of hexon. *PLoS ONE* **13**, e0194516 (2018).
45. Lanzi, A., Ben Youssef, G., Perricaudet, M. & Benihoud, K. Anti-adenovirus humoral responses influence on the efficacy of vaccines based on epitope display on adenovirus capsid. *Vaccine* **29**, 1463–1471 (2011).
46. Anchim, A. *et al.* Humoral Responses Elicited by Adenovirus Displaying Epitopes Are Induced Independently of the Infection Process and Shaped by the Toll-Like Receptor/MyD88 Pathway. *Front Immunol* **9**, 124 (2018).
47. Heyman, B. Feedback regulation by IgG antibodies. *Immunology Letters* **88**, 157–161 (2003).
48. Veneziano, R. *et al.* Role of nanoscale antigen organization on B-cell activation probed using DNA origami. *Nat. Nanotechnol.* **15**, 716–723 (2020).
49. Fender, P. Use of dodecahedron ‘VLPs’ as an alternative to the whole adenovirus. *Methods Mol. Biol.* **1089**, 61–70 (2014).
50. Zheng, S. Q. *et al.* MotionCor2: anisotropic correction of beam-induced motion for improved cryo-electron microscopy. *Nat. Methods* **14**, 331–332 (2017).

3. Une stratégie d'immunisation par pseudoparticules virales décorées de glycoprotéine S du SARS-CoV-2 protège les macaques de l'infection

3.1 Bref résumé de l'article en français

L'équipe du Pr Weissenhorn a conçu un candidat vaccinal constitué de liposomes décorés de spicules du SARS-CoV-2 souche Wuhan. Ces spicules sont composés d'un trimère de la protéine spike (S). Une substitution de deux prolines permettant une meilleure stabilité a été introduite dans la protéine S (« spike 2P »), comme cela a été fait dans de nombreux vaccins commercialisés. De plus, les spikes utilisés dans le travail de l'équipe du Pr Weissenhorn ont été réticulés par traitement au formaldéhyde, afin d'augmenter encore davantage leur stabilité. La bonne conformation des spicules puis la décoration des liposomes a été vérifiée par microscopie électronique avant l'injection du candidat vaccinal à des primates non humains (PNH), des macaques cynomolgus. Un groupe de quatre PNH a reçu quatre injections successives de liposome-spicule : à jour un, puis à quatre, huit et 19 semaines. Chez ces macaques, les taux d'anticorps anti-RBD, anti-spicule natif, et anti-spicule réticulé, mesurés par ELISA ont été mesurés, augmentant rapidement après la première puis la deuxième immunisation, jusqu'à la semaine 6. A la douzième semaine, les titres d'Acs anti-spike (natif ou réticulé) étaient particulièrement élevés, jusqu'à trois fois les valeurs des anticorps anti-RBD, suggérant une induction d'Ac anti-spike plus forte que les Acs anti-RBD par la troisième immunisation. Cette différence était significative (test de Mann-Whitney avec $p=0,0286$) et suggérait une induction particulière d'Ac dirigés contre les épitopes n'appartenant pas au RBD. Les capacités de neutralisation du sérum des animaux vaccinés ont ensuite été mesurées par un test utilisant des pseudovirus SARS-CoV-2 et un gène reporteur luciférase. Un pic d'activité neutralisante, correspondant à un titre élevé, a été observé à la onzième semaine, trois semaines après la troisième injection vaccinale.

Afin d'évaluer la part des Acs dirigés contre le RBD dans l'activité neutralisante des sérum à ce stade, les Acs anti-RBD ont été adsorbés sur une colonne de RBD recombinant. La diminution importante de la neutralisation par les sérum déplétés des Acs anti-RBD montre que les Acs dirigés contre ce domaine étaient responsables de l'essentiel de l'activité neutralisante induite par la vaccination à la onzième semaine. Une fois démontrée la capacité du candidat vaccinal liposome-spicule à induire de fort taux d'anticorps neutralisants, ses

capacités de protection ont été évaluées *in vivo*. Pour se faire, les PNH vaccinés ont été exposés à un aérosol nasal de SARS-CoV-2, en comparaison avec un groupe d'animaux non vaccinés. La réPLICATION virale et les réponses immunitaires suite à l'exposition ont été mesurées, mettant en évidence chez les macaques non vaccinés des charges virales positives à différentes localisations (trachée, nasopharynx), des lésions visibles à l'imagerie, et des perturbations du bilan hématologique (monocytose). Aucun de ces signes d'infection n'a été observé dans le groupe des PNH vaccinés à aucun moment, suggérant qu'une immunité complète, dite stérilisante a été induite par la vaccination. Les taux d'IgG anti-spicule du groupe contrôle ont commencé à augmenter dès la première semaine suivant l'infection, témoin de la place de l'immunité adaptative suite à l'infection par le SARS-CoV-2. A l'inverse, les taux d'IgG anti RBD et anti spike (réticulé ou natif) du groupe vacciné ont légèrement diminué avec le temps après exposition, confirmant l'absence de réPLICATION virale chez ces animaux.

Au-delà de l'évaluation des réponses humorales induites par la vaccination, les réponses cellulaires T induites par la vaccination ont également été mesurées. Avant l'exposition au virus, des cellules T CD4+ spécifiques de la protéine S ont été détectées chez les animaux vaccinés, chez lesquels aucune réponse T CD8+ spécifique n'a été détectée. Deux semaines après l'exposition au virus, les macaques vaccinés n'ont pas vu leur pool de cellules T CD4+ augmenter, contrairement aux animaux contrôle infectés, confirmant de nouveau l'immunité stérilisante induite par la vaccination. Les réponses cellulaires TCD8+ des macaques vaccinés n'ont en revanche pas été augmentées.

L'émergence de variants préoccupants du SARS-CoV-2 durant l'étude a poussé les chercheurs à étudier la robustesse de la réponse induite par vaccination face à cette menace. Les sérumS prélevés cinq et huit semaines après la quatrième immunisation (schéma vaccinal complet), neutralisaient les variants Alpha, Beta et Gamma avec des titres toujours élevés, toutefois plus faibles que ceux observés avec le virus originel (sauf pour le variant Alpha).

L'équipe du Pr Weissenhorn a donc réussi à démontrer la capacité de son candidat vaccinal à induire une immunité stérilisante contre le virus SARS-CoV-2 originel dans un modèle d'infection macaque, probablement le plus proche de l'être humain. De plus, de façon intéressante, les capacités de neutralisation des sérumS des animaux vaccinés conservent de fort taux de neutralisation contre des variants préoccupants du SARS-CoV-2.

3.2 Article original (rédigé en anglais) :

Immunization with synthetic SARS-CoV-2 S glycoprotein virus-like particles protects Macaques from infection

Guidenn Sulbaran^{1#}, Pauline Maisonnasse^{2#}, Axelle Amen¹, Gregory Effantin¹, Delphine Guilligay¹, Nathalie Dereuddre-Bosquet², Judith A. Burger³, Meliawati Poniman³, Marloes Grobben³, Marlyse Buisson¹, Sebastian Dergan Dylon¹, Thibaut Naninck², Julien Lemaître², Wesley Gros², Anne-Sophie Gallouët², Romain Marlin², Camille Bouillier², Vanessa Contreras², Francis Relouzat², Daphna Fenel¹, Michel Thepaut¹, Isabelle Bally¹, Nicole Thielen¹, Franck Fieschi¹, Guy Schoehn¹, Sylvie van der Werf^{4,5}, Marit J. van Gils³, Rogier W. Sanders^{3,6}, Pascal Poignard¹, Roger Le Grand^{2*}, Winfried Weissenhorn^{1*}

¹Univ. Grenoble Alpes, CEA, CNRS, Institut de Biologie Structurale (IBS), 38000 Grenoble,

²Center for Immunology of Viral, Auto-immune, Hematological and Bacterial diseases (IMVA-HB/IDMIT), Université Paris-Saclay, Inserm, CEA, Fontenay-aux-Roses, France.

³Department of Medical Microbiology and Infection Prevention, Amsterdam University Medical Centers, Location AMC, University of Amsterdam, Amsterdam, the Netherlands;

⁴Molecular Genetics of RNA Viruses, Department of Virology, Institut Pasteur, CNRS UMR 3569, Université de Paris, Paris, France

⁵National Reference Center for Respiratory Viruses, Institut Pasteur, Paris, France

⁶Department of Microbiology and Immunology, Weill Medical College of Cornell University, New York, NY 10021, USA.

contributed equally

*Correspondence: winfried.weissenhorn@ibs.fr, roger.le-grand@cea.fr

ABSTRACT

The SARS-CoV-2 pandemic causes an ongoing global health crisis, which requires efficient and safe vaccination programs. Here, we present as a vaccine candidate synthetic SARS-CoV2 S glycoprotein-coated lipid vesicles that resemble in size and surface structure virus-like particles. Soluble S glycoprotein trimers were stabilized by formaldehyde cross-linking, which introduced two major inter protomer cross-links keeping all receptor binding domains (RBD) in the “down” conformation. Immunization of cynomolgus macaques with S coated onto lipid vesicles (S-LVs) induced high antibody titers and TH1 CD4+ biased T cell responses. Although antibody responses were initially dominated by RBD specificities, the third immunization boosted non-RBD antibody titers. Elicited antibodies showed potent neutralization against the vaccine strain and the Alpha variant after two immunizations as well as robust neutralization of Beta and Gamma strains. Vaccinated animals challenged with SARS-CoV-2 were all protected through sterilizing immunity, which correlated with the presence of nasopharyngeal anti-S IgG and IgA titers. Thus, the S-LV approach is an efficient and safe vaccine candidate based on a proven classical approach for further development and clinical testing.

INTRODUCTION

SARS-CoV-2, a betacoronavirus closely related to SARS-CoV-1 is the etiological agent of coronavirus disease (COVID-19), which quickly developed into a worldwide pandemic (Coronaviridae Study Group of the International Committee on Taxonomy of, 2020; Zhou et al., 2020) causing more than 5 million deaths as of November 2021 (<https://covid19.who.int/>) and highlighting the urgent need for effective infection control and prevention.

An important correlate of protection of antiviral vaccines is the generation of neutralizing antibodies (Earle et al., 2021; Khoury et al., 2021; Plotkin, 2020). The main SARS-CoV-2 target for inducing neutralizing antibodies is the S glycoprotein composed of the S1 subunit that harbors the receptor-binding domain (RBD) and the S2 membrane fusion subunit that anchors the S trimer in the virus membrane (Dagotto et al., 2020). RBD binding to the cellular receptor Angiotensin-converting enzyme 2 (ACE2) leads to virus attachment and subsequent S2-mediated fusion with endosomal membranes establishes infection (Letko et al., 2020; Tortorici and Veesler, 2019; Wrapp et al., 2020). S is synthesized as a trimeric precursor polyprotein that is proteolytically cleaved by furin and furin-like proteases in the Golgi generating the non-covalently linked S1-S2 heterotrimer (Hoffmann et al., 2020). The structure of S reveals a

compact heterotrimer composed of S1 NTD, RBD, RBM and two subdomains, S2, the transmembrane region and a cytoplasmic domain. The conformation of RBD is in a dynamic equilibrium between either all RBDs in a closed, receptor-inaccessible conformation or one or two RBDs in the “up”, receptor-accessible, conformation (Cai et al., 2020; Ke et al., 2020; Turonova et al., 2020; Walls et al., 2020b; Wrapp et al., 2020). Only S RBD in the ‘up’ position allows receptor binding (Lan et al., 2020; Yan et al., 2020), which triggers the S2 post fusion conformation in proteolytically cleaved S (Cai et al., 2020). S is also highly glycosylated, which affects infection (Thépaut et al., 2021) and access to neutralizing antibodies (Watanabe et al., 2020).

Antibodies targeting the S glycoprotein were identified upon SARS-CoV-2 seroconversion (Amanat et al., 2020), which mostly target RBD that is immunodominant (Piccoli et al., 2020; Premkumar et al., 2020). This led to the isolation of many neutralizing antibodies, which confirmed antibody-based vaccination strategies (Baum et al., 2020; Brouwer et al., 2020; Hansen et al., 2020; Kreer et al., 2020; Liu et al., 2020a; Pinto et al., 2020; Robbiani et al., 2020; Rogers et al., 2020; Seydoux et al., 2020a; Seydoux et al., 2020b; Wang et al., 2020a; Wec et al., 2020; Wu et al., 2020; Yuan et al., 2020; Zost et al., 2020). Many of these antibodies have been shown to provide *in vivo* protection against SARS-CoV-2 challenge in small animals and nonhuman primates (Alsoussi et al., 2020; Hassan et al., 2020; Tortorici et al., 2020; Wu et al., 2020; Zost et al., 2020) or are in clinical development and use (Weinreich et al., 2021). The magnitude of antibody responses to S during natural infection varies greatly and correlates with disease severity and duration (Chen et al., 2020; Seow et al., 2020). Basal responses are generally maintained for months (Isho et al., 2020; Iyer et al., 2020; Rodda et al., 2021) or decline within weeks after infection (Seow et al., 2020), notably in asymptomatic individuals (Long et al., 2020). Thus, any vaccine-based approach aims to induce long-lasting immunity. A number of animal models have been developed to study SARS-CoV-2 infection including the macaque model, which demonstrated induction of innate, cellular and humoral responses upon infection (Grifoni et al., 2020; Maisonnasse et al., 2020; McMahan et al., 2021; Munster et al., 2020; Rockx et al., 2020) conferring partial protection against reinfection (Deng et al., 2020; Marlin et al., 2021). Consequently, many early vaccine candidates provided protection in the macaque model including the currently licensed vaccines based on S-specific mRNA delivery (Corbett et al., 2020; Vogel et al., 2021) (BNT162b2, Pfizer/BioNTech; mRNA-1273, Moderna), adenovirus vectors (Mercado et al., 2020; van Doremale et al., 2020) (ChAdOx1 nCoV-19, Oxford/AstraZeneca; Ad26.COV2.S, Johnson & Johnson) and inactivated SARS-

CoV-2 (Gao et al., 2020; Wang et al., 2020b) (PiCoVacc/CoronaVac, Sinovac). Numerous other approaches have been evaluated as well (Klasse et al., 2021).

Employing the classical subunit approach, S subunit vaccine candidates have generated different levels of neutralizing antibody responses in preclinical testing (Liang et al., 2021; Liu et al., 2020b; Mandolesi et al., 2021; Tan et al., 2021a; Zang et al., 2020). Using self-assembly strategies of S or RBD further increased immune responses (Walls et al., 2020a; Zhang et al., 2020a) and protected against infection (Arunachalam et al., 2021; Brouwer et al., 2021; Guebre-Xabier et al., 2020).

Antigens can be also presented via liposomes, which provide a high controllable degree of multivalency, stability and prolonged circulating half-life in vivo (Alving et al., 2016; Nisini et al., 2018). Notably, liposomes coated with viral glycoproteins such as HIV-1 Env induced more efficient immune responses than immunization with single glycoprotein trimers (Bale et al., 2017; Dubrovskaya et al., 2019; Ingale et al., 2016; Martinez-Murillo et al., 2017). This is in line with a more efficient B cell activation and generation of germinal centers (GC) by multivalent presentation of Env trimers versus soluble trimers (Ingale et al., 2016).

Here we developed synthetic virus-like particles employing liposomes that are decorated with S glycoprotein trimers that have been treated by formaldehyde cross linking, which in turn stabilized S in the native conformation over a long time-period. Serum antibody recognition of cross-linked versus non-cross-linked S did not show significant binding differences. A small group of cynomolgus macaques was immunized with S-LVs, which produced high S-specific antibody titers and TH1 CD4+ T cell responses. Potent neutralization of wild-type SARS-CoV2 (WT) and of Alpha pseudovirus variants was observed after two immunizations, while Beta and Gamma pseudovirus variants were neutralized at reduced potency. Challenge of the animals with SARS-CoV-2 demonstrated that S-LV immunization protected the animals from infection revealing no detection of genomic RNA (gRNA) upon infection in nasal and tracheal swabs, nor in broncho-alveolar lavages (BAL), thus providing sterilizing immunity. This indicates that S-LVs are potential candidates for further clinical development of a safe protein-based SARS CoV-2 vaccine.

RESULTS

S-LV formation and characterization

The S glycoprotein construct ‘2P’ (Wrapp et al., 2020) was expressed in mammalian cells and purified by Ni²⁺-affinity and size exclusion chromatography (SEC) (Figure S1A), with yields

up to 10 mg/liter using Expi293F cells. This produced native trimers as determined by negative staining electron microscopy and 2-D class averaging of the single particles (Figure S1B). Since S revealed low thermostability ($T_m = 42^\circ\text{C}$) as reported previously (Wrapp et al., 2020), it was chemically cross-linked with 4% formaldehyde (FA) producing a higher molecular weight species as determined by SDS-PAGE (Figure S1C). FA cross-linking preserved the native structure (Figure S1D) over longer time periods (Figures S1E) by increasing the thermostability to a T_m of 65°C . The cryo electron microscopy structure of FA-cross-linked S (FA-S) at 3.4 \AA resolution (Figure S2 and Table S1) revealed two major sites of cross linking (Figure 1A). RBD residues R408 and K378 cross-linked neighboring RBDs producing S trimers in the closed “RBD-down” conformation (Figures 1A and B). The second site introduced inter S2 subunit bonds by cross-linking R1019 of the central S2 helix and/or S2 K776 with S2 HR1 K947 (Figure 1C). FA-S was incubated with liposomes (Phosphatidylcholine 60%, Cholesterol 36%, DGS-NTA 4%), and efficiently captured via its C-terminal His-tag. Free, unbound Fa-S was removed from the S proteoliposomes by sucrose gradient centrifugation (Figure S1F) and decoration of the liposomes with FA-S (S-LV) was confirmed by negative staining electron microscopy (Figure 1D).

S-LV immunization induced potent neutralizing antibody responses in cynomolgus macaques. S-LVs were produced for a small vaccination study of cynomolgus macaques to evaluate immunogenicity and elicitation of neutralizing antibodies. Four cynomolgus macaques were immunized with $50 \mu\text{g}$ S-LVs adjuvanted with monophospholipid A (MPLA) liposomes by the intramuscular route at weeks 0, 4, 8 and 19 (Figure 2A). Sera of the immunized macaques were analysed for binding to native S glycoprotein (S), FA cross-linked S glycoprotein (FA-S) and RBD in two weeks intervals. The results revealed similar S-specific Ab titers for all animals. S ED₅₀ titers increased from ~ 75 on week 4 to ~ 10000 on week 6 and to ~ 20000 on week 12, after the first, second and third immunization, respectively (Figure 2B). Slight reductions in titers were detected against FA-S (Figure 2C). Titers against RBD alone reached \sim ID₅₀s of ~ 100 on week 4, ~ 4500 on week 6 and slight increases on week 12 for some animals (Figure 2D). This suggests that the first and second immunization induced significant RBD titers, while the third immunization boosted non-RBD antibodies since the week 12 S-specific titers were > 4 times higher than the RBD-specific titers in contrast to previous time points at which this ratio was lower (Figure 2C). A fourth immunization did not further boost antibody generation and titers at week 22 were lower or comparable to week 12 titers (Figure 2B, C, D). We conclude that S-LV immunization induced primarily RBD-specific antibodies after the first and second

immunization, while the third immunization increased the generation of non-RBD antibodies significantly.

Serum neutralization titers using WT pseudovirus were elicited in all four animals. At week 2 after the first immunization, a ID50 titers between 100 and 1000 were observed, which dropped close to baseline at week 4, but was significantly increased at week 6, two weeks after the second immunization demonstrating ID50s between 5000 and ~20000. The ID50s then decreased at week 8 and increased to 20000 to ~40000 at week 11, three weeks after the third immunization. At week 19, neutralization potency decreased but was still high, indicating that three immunizations induced robust neutralization titers. The fourth immunization boosted neutralization titers to the same level as after the third immunization (Figure 3A).

Since antibody titers indicated the induction of high levels of RBD-specific antibodies, in order to understand the part of anti-RBD antibodies in serum neutralization we depleted the serum at week 11 by anti-RBD affinity chromatography, resulting in no detectable RBD antibodies by ELISA. RBD-specific Ab-depleted serum showed 10 to 30% neutralization compared to the complete serum, indicating some level of non-RBD specific neutralization. While RBD-specific Ab neutralization largely dominated in 2 animals, the fraction of non RBD-specific Ab neutralization activity (Figure 3B) appeared greater in the other 2, suggesting a participation of these Abs in the high neutralization titers (Figure 3A).

S-LV immunization protected cynomolgus macaques from SARS-CoV-2 infection

In order to determine the extent of S-LV vaccination induced protection, vaccinated and non-vaccinated animals (n=4) were infected with the primary SARS-CoV-2 isolate (BetaCoV/France/IDF/0372/2020) with a total dose of 1×10^5 plaque forming units (pfu). Infection was induced by combining intranasal (0.25 mL into each nostril) and intratracheal (4.5 mL) routes at week 24, 5 weeks after the last immunization. Viral load in the control animal group peaked in the trachea at 3 days post-exposure (dpe) with a median value of $6.0 \log_{10}$ copies/ml and in the nasopharynx between days 4 and 6 pe with a median copy number of $6.6 \log_{10}$ copies/ml (Figure 4A). Viral loads decreased subsequently and no virus was detected on day 10 pe in the trachea, while some animals showed viral detection up to day 14 pe in the nasopharyngeal swabs (Figure 4A). In the bronchoalveolar lavage (BAL), three CTRL animal out of four showed detectable viral loads at day 3 pe, and two of them remained detectable at day 7 pe with mean value of 5.4 and $3.6 \log_{10}$ copies/mL respectively. Rectal fluids tested positive in one animal, which also had the highest tracheal and nasopharyngeal viral loads

(Figure S3A and B). Viral subgenomic RNA (sgRNA), which is believed to estimate the number of infected and productively infected cells collected with the swabs or during the lavage, showed peak copy numbers between day 3/4 and 6 pe in the tracheal and nasopharyngeal fluids, respectively (Figure 4B). In the BALs, the two animals presenting high genomic viral loads also showed detectable sgRNA at days 3 and 7 pe, with medians of 5.1 and $3.1 \log_{10}$ copies/mL respectively (Figure 4B).

In contrast to control animals, neither gRNA nor sgRNA was detected at any point in the vaccinated group (Figures 4A, B). The mean gRNA peaks in the trachea and nasopharynx (6.0 and $6.6 \log_{10}$ copies/mL respectively) of the control group were higher ($p = 0.0286$) than those of the vaccinated group. The area under the curve was also higher in the trachea of the control group ($6.2 \log_{10}$, $p=0.286$). In the BAL, the difference was not statistically significant due to the low number of animals. The complete absence of viral RNA in the vaccinated group, both in the upper and lower respiratory tract, strongly suggested that sterilizing immunity was induced by vaccination. ID50 antibody titers against S, FA-S and RBD decreased slightly from the day of infection (week 24) to 4 weeks pe (Figure 5A, B, C), although a small increase in Ab titers is observed at week 1pe (week25). Ab titers also correlated with a slight decrease in neutralization from week 24 to 4 weeks pe, although one animal showed a small increase in neutralization on week 25, 1 week pe (Figure 5D). This demonstrated that challenge of vaccinated animals did not significantly boost their immune system. In contrast, the control group started to show clear detection of S, FA-S and RBD-specific IgG on week 2 pe (week 26) (Figure 5A, B, C), which correlated with the detection of neutralization on week 2 pe in most animals (Figure 5D). Protection of vaccinated animals further correlated with the presence of significant S and RBD-specific IgG and IgA in nasopharyngeal fluids (Figure 2E and S4). This indicated that S-LV vaccination induced mucosal immunity that very likely contributed to the sterilizing effect of vaccination.

Similar to previous observations (Maisonnasse et al., 2020; Brouwer et al., 2021), during the first 14 dpe, all control animals showed mild pulmonary lesions characterized by nonextended ground-glass opacities (GGOs) detected by chest computed tomography (CT) (Figure S5A). Vaccinated animals showed no significant impact of challenge on CT scores. The only animal showing a lesion score >10 was in the CTRL group. Whereas all control animals experienced monocytoses between days 2 and 8 pe, probably corresponding to a response to infection, monocyte counts remained stable after challenge for the vaccinated monkeys (Figure S5B), in agreement with the absence of detectable anamnestic response in the latter animals.

The levels of CD4 and CD8 specific T cells were measured in both groups of animals. Before exposure, Th1 type CD4⁺ T-cell responses were observed in all vaccinated macaques following *ex vivo* stimulation of PBMCs with S-peptide pools (Figure 6, S6 and S7). None had detectable anti-S CD8⁺ T cells (Figure S8). No significant difference was observed at day 14 pe, also in agreement with the absence of an anamnestic response in vaccinated animals. In contrast, the anti-S Th1 CD4+ response increased post exposure for most of the control animals (Figure 6 and S6).

We conclude that S-LV vaccination can produce sterilizing immunity indicating that such a vaccination scheme would be efficient to interrupt the chain of SARS-CoV-2 transmission.

S-LV vaccination generated robust neutralization of SARS-CoV-2 variants

Serum neutralization was further tested against variants B.1.1.7 (Alpha, UK), B.1.351 (Beta, SA) and P.1 (Gamma, BR). Comparing the sera of the vaccinated and the non-vaccinated group at weeks 24 and 28 showed high neutralization titers for all three variants with median ID50s ranging from 10.000 to 20.000, comparable to WT pseudovirus neutralization (Figure S9). However, since the background of pre-exposure serum neutralization of the non-vaccinated challenge group was relatively high (median ID50s ranging from 400 of 1100), we repeated the neutralization with purified IgG from serum samples of the vaccinated group from week 8 (after 2 immunizations), week 12 (3 immunizations) and weeks 24 and 28 (4 immunizations). This showed median ID50s of ~4500 for WT and Alpha on week 8 (Figure 7), comparable to WT serum neutralization (Figure 3A). Lower ID50s were observed against Beta and Gamma at week 8, respectively. Neutralization potency was increased after the third immunization (week 12) with median ID50s of ~5000 (WT), ~8000 (Alpha), ~800 (Beta) and 1000 (Gamma). Neutralization titers did not increase after the fourth immunization at week 24 and started to decrease at week 28 (Figure 7). We conclude that three immunizations provided robust protection against the variants although neutralization titers maybe have been already within the protective range after two immunizations for the three variants tested.

DISCUSSION

Many vaccines are under development, in preclinical and clinical testing (Klasse et al., 2021) and eight have been approved by regulatory agencies over the world. Here we developed a two-component system employing SARS-CoV-2 S glycoprotein coupled to liposomes. Since the stability of the wild type SARS-CoV-2 S glycoprotein is low due to its tendency to

spontaneously switch into its post fusion conformation (Cai et al., 2020), SARS-CoV-2 S was stabilized by two proline mutations that enhanced stability (Wrapp et al., 2020). However, this S ‘2P’ version still showed limited stability over time as reported (Wrapp et al., 2020), which may be due to cold sensitivity (Edwards et al., 2021). We overcame the problem of stability by using formaldehyde cross-linking that increased the thermostability to 65°C, preserving the native S conformation over extended storage time periods. Furthermore, we detected two cross-linking sites by cryo-EM which showed that cross-linking locked the native S trimer in the closed, RBD-down conformation via covalent inter-protomer interactions, which prevent conformational changes leading to the post fusion conformation. Notably, formaldehyde cross-linking is widely used in vaccine formulations (Eldred et al., 2006). S stability has been since improved by engineering six proline mutations (S ‘6P’) which increased the thermostability to 50°C (Hsieh et al., 2020) and by disulfide-bond engineering (Xiong et al., 2020). Moreover, ligand binding renders S more stable (Rosa et al., 2021; Toelzer et al., 2020).

Many previous studies have shown that immunogen multimerization strategies are highly beneficial for B cell activation including the use of synthetic liposomes (Alving et al., 2016; Nisini et al., 2018) such as HIV-1 Env-decorated liposome vaccination strategies (Dubrovskaya et al., 2019). We linked SARS-CoV-2 S to liposomes producing synthetic virus-like particles with controlled diameters. Our data show that the S-LVs show similar immunogenic properties as a number of reported self-assembling particles of SARS-CoV-2 RBD and S (Brouwer et al., 2021; Cohen et al., 2021; Guebre-Xabier et al., 2020; Tan et al., 2021b; Walls et al., 2020a; Zhang et al., 2020a). Our S-LVs induce robust and potent neutralizing responses in cynomolgus macaques, which completely protected the animals from infection by sterilizing immunity. Notably, no signs of virus replication could be detected in the upper and lower respiratory tracts consistent with the absence of clinical signs of infection such as lymphopenia and lung damage characteristics for Covid-19 disease. The important correlate of protection against SARS-CoV-2 is provided by neutralizing antibodies (Addetia et al., 2020; McMahan et al., 2021; Yu et al., 2020). The S-LV approach induces high titers already after two immunizations, with a median ID₅₀ of ~8000 two weeks after the second immunization, which is substantially higher than neutralizing Ab responses reported for vaccines tested in NHP studies, including licensed ones. Adenovirus-based vaccines (AstraZeneca ChAdOx1; Janssen AD26COV2SPP°(Mercado et al., 2020; van Doremalen et al., 2020), inactivated virus vaccines (Sinovac PiCoVacc; Sinopharm/BIBP BBIP-CorV)(Gao et al., 2020; Wang et al., 2020b), a DNA vaccine (Yu et al., 2020) and a mRNA vaccine (Pfizer/BionTech BNT162b2)(Vogel et al., 2021) showed 10-20 times lower titers compared to the S-LVs in macaques studies. Further, the Moderna mRNA-

1273 (Moderna)(Corbett et al., 2020), S trimers (Clover Biopharmaceutical) (Liang et al., 2021) and NVX-CoV2373 (Novavax)(Guebre-Xabier et al., 2020) induced similar or higher titers in macaque studies. Median ID₅₀ titers increased by a factor of ~4 after the third immunization, but did not amplify after the fourth immunization. The T cell response in the vaccinated group was biased towards TH1 CD4+ T cells consistent with licensed or other experimental vaccines (Corbett et al., 2020; Ewer et al., 2021; Ganneru et al., 2021; Keech et al., 2020; Sahin et al., 2020).

Serum neutralization was already significant after the first immunization, but increased by a factor of ~20 after the second immunization and by a factor of 3 after the third immunization indicating that two immunizations with S-LVs may suffice to confer protection. BnAb titers decline within 11 weeks after the third immunization to the levels of week 8 (prior to the third immunization) and increase slightly after the fourth immunization to the median ID₅₀ level attained after the third immunization.

Vaccination prevented lymphopenia and lung damage in animals infected with SARS-CoV-2 at a dose comparable (Corbett et al., 2020; Guebre-Xabier et al., 2020; Mercado et al., 2020; van Doremalen et al., 2020; Yu et al., 2020) or lower (Brouwer et al., 2021) than in previous studies. Protection was sterilizing since no replication could be detected in the upper and lower respiratory tract suggesting that vaccination with S-LVs will prevent virus shedding and transmission. Sterilizing immunity likely correlates with mucosal antibody responses that protects the upper respiratory tract from infection (Isho et al., 2020; Randad et al., 2020). Since we detected significant IgG and IgA in nasopharyngeal fluids at the time of viral challenge, we conclude that S-LV vaccination induces sterilizing protection by eliciting mucosal immune responses.

SARS-CoV-2 infection generates neutralizing antibodies with up to 90% targeting RBD, which is immunodominant (Piccoli et al., 2020; Robbiani et al., 2020; Suthar et al., 2020). Similarly, mRNA vaccination elicits predominately RBD-specific neutralizing antibodies (Stamatatos et al., 2021). RBD antibodies can be grouped into three classes (Barnes et al., 2020a; Barnes et al., 2020b) and seem to be easily induced by immunization as many of them are generated by few cycles of affinity maturation indicating that extensive germinal center reactions are not required (Kreye et al., 2020). Consistent with these findings we show that RBD-specific antibodies are predominant after the first and second immunization as indicated by similar S-specific and RBD-specific titers. However, after the third immunization median S-specific ED₅₀s are 3 times higher than RBD-specific ED₅₀s four weeks after the third immunization. This trend is continued after the fourth immunization which revealed a 3.5 times higher median

ID₅₀ for S than for RBD five weeks post immunization. This, thus suggests that more than two immunizations allow to expand the reactive B cell repertoire that target non-RBD S epitopes. Current variants carry the B.1 D614G mutation and have been reported to be more infectious (Cai et al., 2021; Gobeil et al., 2021; Korber et al., 2020; Ozono et al., 2021; Yuan et al., 2021; Zhang et al., 2021; Zhang et al., 2020b). Although the D614G mutation alone was reported to increase neutralization susceptibility (Weissman et al., 2021), further mutations present in Beta (B1.351 SA) and Gamma (P1, BR) reduce neutralization potencies of natural and vaccine-induced sera (Dejnirattisai et al., 2021; Edara et al., 2021; Garcia-Beltran et al., 2021; Geers et al., 2021; Hoffmann et al., 2021; Kuzmina et al., 2021; Rees-Spear et al., 2021; Zhou et al., 2021), while Alpha (B.1.1.7, UK) neutralization seems to be less affected (Supasa et al., 2021). Reduction in neutralization potency of polyclonal plasma Abs is mainly affected by mutations within the three main epitopes in the RBD. Especially the E484K mutation present in Beta and Gamma was reported to reduce neutralization by a factor of 10 (Greaney et al., 2021). Here we show that S-LV vaccination produces robust neutralization of Alpha, Beta and Gamma although the Median ID₅₀s of Beta and Gamma neutralization are reduced 20- and 5-fold after the second immunization compared to WT and Alpha. The third immunization boosted neutralization of Beta and Gamma, albeit with 6-fold (Beta) and 3-fold (Gamma) reductions in potency compared to WT, which is slightly more potent than the median ID₅₀ of vaccinated and hospitalized patient cohorts using the same assay setup (Caniels et al., 2021).

In summary, S-LV vaccination represents an efficient strategy that protects macaques from high dose challenge. Although the animals have been challenged only after the fourth immunization, which did not boost Ab titers or neutralization titers, our neutralization data suggests that the animals might have been protected after two immunizations. Furthermore, our data suggest that the third immunization increases S-protein Ab titers more significantly than RBD-specific Ab titers. This points to an increase of non-RBD antibodies which may be beneficial for neutralization of different variants. Although other regions within S, notably NTD are targets for mutation within new variants, S2 or other epitopes may be less prone to mutations due to conformational constraints. Therefore future vaccination strategies should consider boosting non-RBD antibodies to compensate for the loss of neutralization activity targeting RBD in variants. Notably, SARS-CoV-2 memory B cells are present over a long time period in convalescent (Gaebler et al., 2021; Sokal et al., 2021) and mRNA vaccinated individuals (Goel et al., 2021), which is in line with potential boosting strategies.

Limitations of study

We provide data that immunization of macaques with synthetic S glycoprotein coated liposomes induced robust antibody and neutralization titers after two immunizations. SARS-CoV-2 challenge after four immunizations revealed complete protection by sterilizing immunity. Limitations of the study are first, that the challenge has been performed only after the fourth immunization. Secondly, although the SARS-CoV-2 challenge infection has been performed five weeks after the last immunization, we cannot predict efficacy of protection months post immunization. The third limitation of the study is the small number of animals used, which prevents robust statistical analyses of the results. Fourth, although we observe robust pseudovirus neutralization of Alpha, Beta and Gamma variants, we cannot predict the efficacy of protection upon infection, which will require further studies.

RESOURCE AVAILABILITY

Cell lines

HEK293T (ATCC CRL-11268) (Caniels et al., 2021) and HEK293F (Thermo Fisher Scientific) and are human embryonic kidney cell lines. HEK293F cells are adapted to grow in suspension. HEK293F cells were cultured at 37°C with 8% CO₂ and shaking at 125 rpm in 293FreeStyle expression medium (Life Technologies). HEK293T cells were cultured at 37°C with 5% CO₂ in flasks with DMEM supplemented with 10% fetal bovine serum (FBS), streptomycin (100 µg/mL) and penicillin (100 U/mL). HEK293T/ACE2 cells (Schmidt et al., 2020) are a human embryonic kidney cell line expressing human angiotensin-converting enzyme 2. HEK293T/ACE2 cells were cultured at 37°C with 5% CO₂ in flasks with DMEM supplemented with 10% FBS, streptomycin (100 µg/mL) and penicillin (100 U/mL). VeroE6 cells (ATCC CRL-1586) are a kidney epithelial cells from African green monkeys. VeroE6 cells were cultured at 37°C with 5% CO₂ in DMEM supplemented with or without streptomycin (100 µg/mL) and penicillin (100 U/mL) and with or without 5 or 10% FBS, and with or without TPCK-trypsin. PBMC were isolated from macaque sera and cultured in RPMI1640 Glutamax+ medium (Gibco) supplemented with 10 % FBS.

Viruses

SARS-CoV-2 virus (hCoV-19/France/ IDF0372/2020 strain) was isolated by the National Reference Center for Respiratory Viruses (Institut Pasteur, Paris, France) as previously described (Lescure et al., 2020) and produced by two passages on Vero E6 cells in DMEM (Dulbecco's Modified Eagles Medium) without FBS, supplemented with 1% P/S (penicillin at 10,000 U ml⁻¹ and streptomycin at 10,000 µg ml⁻¹) and 1 µg ml⁻¹ TPCK-trypsin at 37 °C in a humidified CO₂ incubator and titrated on Vero E6 cells. Whole genome sequencing was performed as described (Lescure et al., 2020) with no modifications observed compared with the initial specimen and sequences were deposited after assembly on the GISAID EpiCoV platform under accession number ID EPI_ISL_410720.

Ethics and biosafety statement

Cynomolgus macaques (*Macaca fascicularis*) originating from Mauritian AAALAC certified breeding centers were used in this study. All animals were housed in IDMIT infrastructure facilities (CEA, Fontenay-aux-roses), under BSL-2 and BSL-3 containment when necessary

(Animal facility authorization #D92-032-02, Préfecture des Hauts de Seine, France) and in compliance with European Directive 2010/63/EU, the French regulations and the Standards for Human Care and Use of Laboratory Animals, of the Office for Laboratory Animal Welfare (OLAW, assurance number #A5826-01, US). The protocols were approved by the institutional ethical committee “Comité d’Ethique en Expérimentation Animale du Commissariat à l’Energie Atomique et aux Energies Alternatives” (CEtEA #44) under statement number A20-011. The study was authorized by the “Research, Innovation and Education Ministry” under registration number APAFIS#24434-2020030216532863.

Animals and study design

Cynomolgus macaques were randomly assigned in two experimental groups. The vaccinated group ($n = 4$) received 50 ug of SARS-CoV-2 S-LV adjuvanted with 500 mg of MPLA liposomes (Polymun Scientific, Klosterneuburg, Austria) diluted in PBS at weeks 0, 4, 8 and 19, while control animals ($n = 4$) received no vaccination. Vaccinated animals were sampled in blood at weeks 0, 2, 4, 6, 8, 11, 12, 14, 19, 21 and 22. At week 24, all animals were exposed to a total dose of 10^5 pfu of SARS-CoV-2 virus (hCoV-19/France/IDF0372/2020 strain; GISAID EpiCoV platform under accession number EPI_ISL_410720) via the combination of intranasal and intra-tracheal routes (0,25 mL in each nostril and 4,5 mL in the trachea, i.e., a total of 5 mL; day 0), using atropine (0.04 mg/kg) for pre-medication and ketamine (5 mg/kg) with medetomidine (0.042 mg/kg) for anesthesia. Nasopharyngeal, tracheal and rectal swabs, were collected at days 2, 3, 4, 6, 7, 10, 14 and 27 days past exposure (dpe) while blood was taken at days 2, 4, 7, 10, 14 and 27 dpe. Bronchoalveolar lavages (BAL) were performed using 50 mL sterile saline on 3 and 7 dpe. Chest CT was performed at 3, 7, 10 and 14 dpe in anesthetized animals using tiletamine (4 mg kg^{-1}) and zolazepam (4 mg kg^{-1}). Blood cell counts, haemoglobin, and haematocrit, were determined from EDTA blood using a DHX800 analyzer (Beckman Coulter).

METHODS DETAILS

Protein expression and purification

The SARS-CoV-2 S gene encoding residues 1-1208 with proline substitutions at residues 986 and 987 (“2P”), a “GSAS” substitution at the furin cleavage site (residues 682-685) a C-terminal T4 fibritin trimerization motif, an HRV3C protease cleavage site, a TwinStrepTag and Hexa-His-tag (Wrapp et al., 2020) was transiently expressed in FreeStyle293F cells (Thermo Fisher scientific) using polyethylenimine (PEI) 1 µg/µl for transfection. Supernatants were harvested five days post-transfection, centrifuged for 30 min at 5000 rpm and filtered using 0.20 µm filters (ClearLine®). SARS-CoV-2 S protein was purified from the supernatant by Ni²⁺-Sepharose chromatography (Excel purification resin, Cytiva) in buffer A (50 mM HEPES pH 7.4, 200 mM NaCl) and eluted in buffer B (50 mM HEPES pH 7.4, 200 mM NaCl, 500 mM imidazole). Eluted SARS-CoV-2 S containing fractions were concentrated using Amicon Ultra (cut-off: 30 KDa) (Millipore) and further purified by size-exclusion chromatography (SEC) on a Superose 6 column (GE Healthcare) in buffer A or in PBS.

For RBD expression, the following reagent was produced under HHSN272201400008C and obtained through BEI Resources, NIAID, NIH: Vector pCAGGS containing the SARS-Related Coronavirus 2, Wuhan-Hu-1 Spike Glycoprotein Receptor Binding Domain (RBD), NR-52309. The SARS-CoV-2 S RBD domain (residues 319 to 541) was expressed in EXPI293 cells by transient transfection according to the manufacturer’s protocol (Thermo Fisher Scientific). Supernatants were harvested five days after transfection and cleared by centrifugation. The supernatant was passed through a 0.45 µm filter and RBD was purified using Ni²⁺-chromatography (HisTrap HP column, GE Healthcare) in buffer C (20 mM Tris pH 7.5 and 150 mM NaCl buffer) followed by a washing step with buffer D (20 mM Tris pH 7.5 and 150 mM NaCl buffer, 75 mM imidazole) and elution with buffer E (20 mM Tris pH 7.5 and 150 mM NaCl buffer, 500 mM imidazole). Eluted RBD was further purified by SEC on a Superdex 75 column (GE Healthcare) in buffer C. Protein concentrations were determined using an absorption coefficient (A1%,1cm) at 280 nm of 10.4 and 13.06 for S protein and RBD, respectively, using the ProtParam available at <https://web.expasy.org/>.

SARS-CoV-2 S crosslinking

S protein at 1mg/ml in PBS was cross-linked with 4% formaldehyde (FA) (Sigma) overnight at room temperature. The reaction was stopped with 1 M Tris HCl pH 7.4 adjusting the sample

concentration to 7.5 mM Tris/HCl pH 7.4. FA was removed by PBS buffer exchange using 30 KDa cut-off concentrators (Amicon). FA crosslinking was confirmed by separating SARS-CoV-2 FA-S on a 10% SDS-PAGE under reducing conditions.

S protein coupling to liposomes

Liposomes for conjugating S protein were prepared as described previously (Scianimanico et al., 2000) with modifications. Briefly, liposomes were composed of 60% of L- α -phosphatidylcholine, 4% His tag-conjugating lipid, DGS-NTA-(Ni²⁺) and 36% cholesterol (Avanti Polar Lipids). Lipid components were dissolved in chloroform, mixed and placed for two hours in a desiccator under vacuum at room temperature to obtain a lipid film. The film was hydrated in filtered (0.22 μ m) PBS and liposomes were prepared by extrusion using membrane filters with a pore size of 0.1 μ m (Whatman Nuclepore Track-Etch membranes). The integrity and size of the liposomes was analyzed by negative staining-EM. For protein coupling, the liposomes were incubated overnight with FA-S or S protein in a 3:1 ratio (w/w). Free FA-S protein was separated from the FA-S-proteoliposomes (S-LVs) by sucrose gradient (5-40%) centrifugation in a SW55 rotor at 40,000 rpm for 2 h. The amount of protein conjugated to the liposomes was determined by Bradford assay and SDS-PAGE densitometry analysis comparing S-LV bands with standard S protein concentrations.

S protein thermostability

Thermal denaturation of SARS-CoV-2 S, native or FA-cross-linked was analyzed by differential scanning fluorimetry coupled to back scattering using a Prometheus NT.48 instrument (Nanotemper Technologies, Munich, DE). Protein samples were first extensively dialyzed against PBS pH 7.4, and the protein concentration was adjusted to 0.3 mg/ml. 10 μ l of sample were loaded into the capillary and intrinsic fluorescence was measured at a ramp rate of 1°C/min with an excitation power of 30 %. Protein unfolding was monitored by the changes in fluorescence emission at 350 and 330 nm. The thermal unfolding midpoint (Tm) of the proteins was determined using the Prometheus NT software.

Negative stain electron microscopy

Protein samples were visualized by negative-stain electron microscopy (EM) using 3-4 μ l aliquots containing 0.1-0.2 mg/ml of protein. Samples were applied for 10 s onto a mica carbon film and transferred to 400-mesh Cu grids that had been glow discharged at 20 mA for 30 s and

then negatively stained with 2% (wt/vol) Uranyl Acetate (UAc) for 30 s. Data were collected on a FEI Tecnai T12 LaB6-EM operating at 120 kV accelerating voltage at 23k magnification (pixel size of 2.8 Å) using a Gatan Orius 1000 CCD Camera. Two-dimensional (2D) class averaging was performed with the software Relion (Scheres, 2012) using on average 30–40 micrographs per sample. The 5 best obtained classes were calculated from around 6000 particles each.

Cryo-electron microscopy

Data collection. 3.5 μL of sample were applied to 1.2/1.3 C-Flat (Protochips Inc) holey carbon grids and they were plunged frozen in liquid ethane with a Vitrobot Mark IV (Thermo Fisher Scientific) (6 s blot time, blot force 0). The sample was observed with a Glacios electron microscope (Thermo Fischer Scientific) at 200 kV. Images were recorded automatically on a K2 summit direct electron detector (Gatan Inc., USA) in counting mode with SerialEM (Mastronarde, 2005). Movies were recorded for a total exposure of 4.5 s with 40 frames per movie and a total dose of 40 e⁻/Å². The magnification was 36,000x (1.15 Å/pixel at the camera level). The defocus of the images was changed between −1.0 and −2.5 μm. Two different datasets have been acquired on the same grid. First, 1040 movies were recorded with stage movement between each hole and then 7518 more movies were recorded with image shifts on a 3x3 hole pattern.

3D reconstruction. The movies were first drift-corrected with motioncor2 (Zheng et al., 2017). The remaining image processing was done in RELION 3.1.2 (Zivanov et al., 2018). CTF estimation was done with GCTF (Zhang, 2016). An initial set of particles (box size of 200 pixels, sampling of 2.3 Å/pixel) was obtained by auto-picking with a Gaussian blob. After 2D classification, the best looking 2D class averages were used for a second round of auto picking. Following another 2D classification step, the particles belonging to the best looking 2D class averages were used to create an *ab-initio* starting 3D model which was then used to calculate a first 3D reconstruction with C3 symmetry. The 2D projections from that 3D model were then used to do one last auto picking which resulted in a total of 2,582,857 particles. Following another 2D classification and a 3D classification (C1 symmetry, 5 classes) steps, a 3D map at 4.6 Å resolution was obtained from 240,777 particles. The particles were re-extracted (box size of 400 pixels, sampling of 1.15 Å/pixel). After another 3D refinement (C3 symmetry) and 3D classification (C1 symmetry, no alignment, 3 classes) steps, a final set of 126719 particles was

identified which resulted in a 3D reconstruction at 3.6 Å resolution. Refinement of CTF parameters, particle polishing and a second round of CTF parameter's refinement further improved the resolution to 3.4 Å. The resolution was determined by Fourier Shell Correlation (FSC) at 0.143 between two independent 3D maps. The local resolution was calculated with blocres (Cardone et al., 2013) and found to be between 3 and 5 Å. The final 3D map was sharpened with DeepEMhancer (Sanchez-Garcia et al., 2021).

Model refinement. The atomic model of the S protein in the closed conformation (PDB 6VXX) (Walls et al., 2020b) was rigid-body fitted inside the cryo-EM density map in CHIMERA (Pettersen et al., 2004). The atomic coordinates were then refined with PHENIX (Adams et al., 2010). The refined atomic models were visually checked and adjusted (if necessary) in COOT (Emsley et al., 2010). The final model was validated with MOLPROBITY (Williams et al., 2018).

The figures were prepared with CHIMERA and CHIMERAX (Goddard et al., 2018; Pettersen et al., 2004). The data collection and atomic model statistics are summarized in Table S1. The atomic coordinates and the cryo-EM map have been deposited in the Protein Data Bank and in the Electron Microscopy Data Bank under the accession codes 7QIZ and EMD-13776, respectively.

Virus quantification in NHP samples

Upper respiratory (nasopharyngeal and tracheal) and rectal specimens were collected with swabs (Viral Transport Medium, CDC, DSR-052-01). Tracheal swabs were performed by insertion of the swab above the tip of the epiglottis into the upper trachea at approximately 1.5 cm of the epiglottis. All specimens were stored between 2°C and 8°C until analysis by RT-qPCR with a plasmid standard concentration range containing an RdRp gene fragment including the RdRp-IP4 RT-PCR target sequence. SARS-CoV-2 E gene subgenomic mRNA (sgRNA) levels were assessed by RT-qPCR using primers and probes previously described (Corman et al., 2020; Wolfel et al., 2020): leader-specific primer sgLeadSARSCoV2-F CGATCTCTTGTAGATCTGTTCTC, E-Sarboco-R primer ATATTGCA GCAGTACGCACACA and E-Sarboco probe HEX-ACACTAGCCATCCTTACTGCGCTTCG-BHQ1. The protocol describing this procedure for the detection of SARS-CoV-2 is available on the WHO website (<https://www.who.int/docs/default-source/coronavirus/WHOinhouseassays.pdf>)

Chest CT and image analysis

Lung images were acquired using a computed tomography (CT) system (Vereos-Ingenuity, Philips) as previously described (Brouwer et al., 2021; Maisonnasse et al., 2020), and analyzed using INTELLISPACE PORTAL 8 software (Philips Healthcare). All images had the same window level of -300 and window width of 1,600. Lesions were defined as ground glass opacity, crazy-paving pattern, consolidation or pleural thickening as previously described (Pan et al., 2020; Shi et al., 2020). Lesions and scoring were assessed in each lung lobe blindly and independently by two persons and the final results were established by consensus. Overall CT scores include the lesion type (scored from 0 to 3) and lesion volume (scored from 0 to 4) summed for each lobe as previously described (Brouwer et al., 2021; Maisonnasse et al., 2020).

ELISA

Serum antibody titers specific for soluble native S glycoprotein, FA-cross-linked S (FA-S) and for RBD were determined using an enzyme-linked immunosorbent assay (ELISA). Briefly, 96-well microtiter plates were coated with 1 µg of S, FA-S or RBD proteins at 4°C overnight in PBS and blocked with 3% BSA for 1 h at room temperature after 3 washes with 150 µl PBS Tween-20 0.05 %. Serum dilutions were added to each well for 2h at 37°C and plates were washed 5 times with PBS Tween. A horseradish peroxidase (HRP) conjugated goat anti-monkey H+L antibody (Invitrogen #PA1-84631) was then added and incubated for 1h before excess Ab was washed out and HRP substrate added. Absorbance was determined at 450 nm. Antibody titers were expressed as ED50 (effective Dilution 50-values) and were determined as the serum dilution at which IgG binding was reduced by 50%. ED50 were calculated from crude data (O.D) after normalization using GraphPad Prism (version 6) "log(inhibitor) vs normalized response" function.

Protein coupling to Luminex beads

Proteins were covalently coupled to Magplex beads (Luminex Corporation) via a two-step carbodiimide reaction using a ratio of 75 µg SARS-CoV-2 S to 12,5 million beads. Magplex beads (Luminex Corporation) were washed with 100 mM mono-basic sodium phosphate pH 6.2 and activated for 30 min on a rotor at RT by addition of Sulfo-N-Hydroxysulfosuccinimide (Thermo Fisher Scientific) and 1-Ethyl-3-(3-dimethylaminopropyl) carbodiimide (Thermo Fisher Scientific). The activated beads were washed three times with

50 mM MES pH 5.0 and added to SARS-CoV-2 S protein, which was diluted in 50 mM MES pH 5.0. The coupling reaction was incubated for 3 h on a rotator at RT. The beads were subsequently washed with PBS and blocked with PBS containing 2% BSA, 3% FCS and 0.02% Tween-20 for 30 min on a rotator at RT. Finally, the beads were washed and stored in PBS containing 0.05% Sodium Azide at 4°C and used within 3 months.

Luminex assay

50 µL of a working bead mixture containing 20 beads per µL was incubated overnight at 4°C with 50 µL of diluted nasopharyngeal fluid. Nasopharyngeal fluids were diluted 1:20 for detection of S-specific IgG and IgA (Brouwer et al., 2021). Plates were sealed and incubated on a plate shaker overnight at 4°C. Plates were washed with TBS containing 0.05% Tween-20 (TBST) using a hand-held magnetic separator. Beads were resuspended in 50 µL of Goat-anti-monkey IgG-Biotin or Goat-anti monkey IgA-Biotin (Sigma Aldrich) and incubated on a plate shaker at RT for 2 h. Afterwards, the beads were washed with TBST, resuspended in 50 µL of Streptavidin-PE (ThermoFisher Scientific) and incubated on a plate shaker at RT for 1 h. Finally, the beads were washed with TBST and resuspended in 70 µL Magpix drive fluid (Luminex Corporation). The beads were agitated for a few minutes on a plate shaker at RT and then readout was performed on the MAGPIX (Luminex Corporation). Reproducibility of the results was confirmed by performing replicate runs.

Pseudovirus neutralization assay

Pseudovirus was produced by co-transfecting the pCR3 SARS-CoV-2-SΔ19 expression plasmid (Wuhan Hu-1; GenBank: MN908947.3) with the pHIV-1NL43 ΔEnv-NanoLuc reporter virus plasmid in HEK293T cells (ATCC, CRL-11268) (Caniels et al., 2021). The pCR3 SARS-CoV-2-SΔ19 expression plasmid contained the following mutations compared to the WT for the variants of concern: deletion (Δ) of H69, V70 and Y144, N501Y, A570D, D614G, P681H, T716I, S982A and D1118H in B.1.1.7 (Alpha, UK); L18F, D80A, D215G, L242H, R246I, K417N, E484K, N501Y, D614G and A701V in B.1.351 (Beta, SA); L18F, T20N, P26S, D138Y, R190S, K417T, E484K, N501Y, D614G, H655Y and T1027I in P.1 (Gamma, BR) (Caniels et al., 2021).

HEK293T/ACE2 cells kindly provided by Dr. Paul Bieniasz (Schmidt et al., 2020) were seeded at a density of 20,000 cells/well in a 96-well plate coated with 50 µg/mL poly-L-lysine 1 day prior to the start of the neutralization assay. Heat-inactivated sera (1:100 dilution) were serial

diluted in 3-fold steps in cell culture medium (DMEM (Gibco), supplemented with 10% FBS, penicillin (100 U/mL), streptomycin (100 µg/mL) and GlutaMax (Gibco)), mixed in a 1:1 ratio with pseudovirus and incubated for 1 h at 37°C. These mixtures were then added to the cells in a 1:1 ratio and incubated for 48 h at 37°C, followed by a PBS wash and lysis buffer added. The luciferase activity in cell lysates was measured using the Nano-Glo Luciferase Assay System (Promega) and GloMax system (Turner BioSystems). Relative luminescence units (RLU) were normalized to the positive control wells where cells were infected with pseudovirus in the absence of sera. The neutralization titers (ID_{50}) were determined as the serum dilution at which infectivity was inhibited by 50%, respectively using a non-linear regression curve fit (GraphPad Prism software version 8.3). Notably, this pseudovirus neutralization assay revealed an excellent correlation with authentic virus neutralization on a panel of human convalescent sera (Caniels et al., 2021).

Antigen specific T cell assays using non-human primate cells

To analyze the SARS-CoV-2 protein-specific T cell, 15-mer peptides ($n = 157$ and $n=158$) overlapping by 11 amino acids (aa) and covering the SARS-CoV-2 Spike sequence (aa 1 to 1273) synthesized by JPT Peptide Technologies (Berlin, Germany) and used at a final concentration of 2 µg/mL.

T-cell responses were characterized by measurement of the frequency of PBMC expressing IL-2 (PerCP5.5, MQ1-17H12, BD), IL-17a (Alexa700, N49-653, BD), IFN- γ (V450, B27, BD), TNF- α (BV605, Mab11, BioLegend), IL-13 (BV711, JES10-5A2, BD), CD137 (APC, 4B4, BD) and CD154 (FITC, TRAP1, BD) upon stimulation with the two peptide pools. CD3 (APC-Cy7, SP34-2, BD), CD4 (BV510, L200, BD) and CD8 (PE-Vio770, BW135/80, Miltenyi Biotec) antibodies was used as lineage markers. One million of PBMC were cultured in complete medium (RPMI1640 Glutamax+, Gibco; supplemented with 10 % FBS), supplemented with co-stimulatory antibodies (FastImmune CD28/CD49d, Becton Dickinson). The cells were stimulated with S sequence overlapping peptide pools at a final concentration of 2 µg/mL Brefeldin A was added to each well at a final concentration of 10µg/mL and the plate was incubated at 37°C, 5% CO₂ during 18 h. Next, cells were washed, stained with a viability dye (LIVE/DEAD fixable Blue dead cell stain kit, ThermoFisher), and then fixed and permeabilized with the BD Cytofix/Cytoperm reagent. Permeabilized cell samples were stored at -80 °C before the staining procedure. Antibody staining was performed in a single step following permeabilization. After 30 min of incubation at 4°C, in the dark, cells were washed

in BD Perm/Wash buffer then acquired on the LSRII cytometer (Beckton Dickinson). Analyses were performed with the FlowJo v.10 software. Data are presented as the sum of each peptide pool and the non-stimulated (NS) condition was multiplied by two.

Statistical analysis

Statistical significance between groups was performed using Graphpad Prism (v9.2.0). Differences between unmatched groups were compared using an unpaired Mann–Whitney U test (significance $p<0.05$), and differences between matched groups were compared using Wilcoxon signed-rank test ($p<0.1$). Statistical analysis of NHP gRNA and sgRNA were carried out using Mann-Whitney unpaired t-test in GraphPad Prism software (v8.3.0).

FIGURES

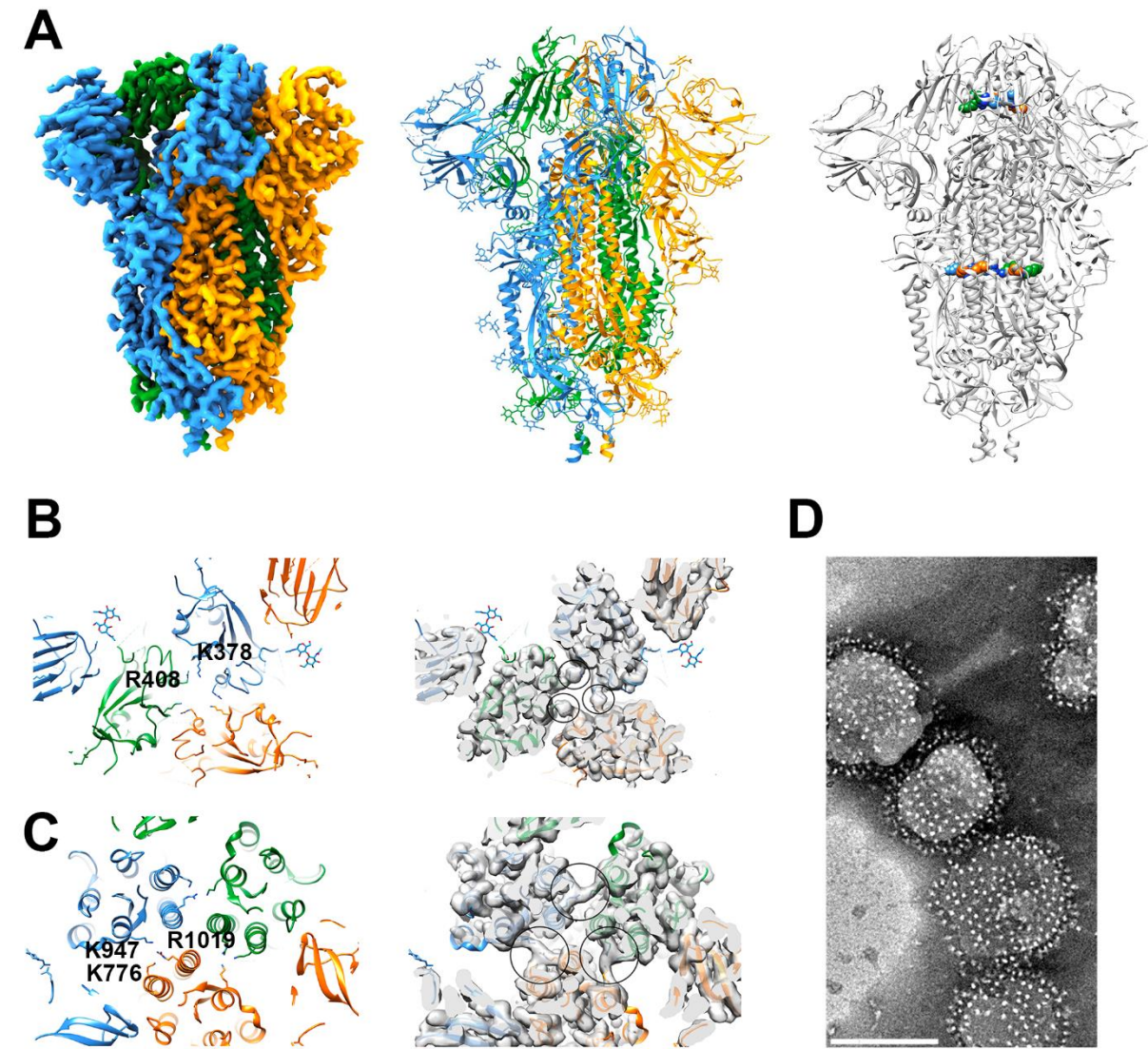


Figure 1: Structural characterization of cross-linked SARS-CoV2 S (FA-S) and FA-S coated lipid vesicles (LV).

(A) Right panel, cryo-EM density of FA-S with all three RBD down; each protomer is colored differently. The structure was calculated from 126,719 particles imposing C3 symmetry. is shown, colored according to local resolution. Middle panel, molecular model of FA-S refined to a resolution of 3.4 Å shown as ribbon. Modeled N-linked glycans are shown as all atom models. Right panel, Two major cross-linking sites were identified that covalently link RBDs and the S2 subunits from different protomers.

(B) Close-up of the cross-linking sites between RBDs. Formaldehyde cross-linked amino groups of K378 and R408 of neighboring protomers as indicated by the continuous density connecting side chains (right panel).

(C) Close-up of the cross-linking sites between S2 (left panel). Continuous density between the central helix R1019 as well as S2 K776 to S2 HR1K947 suggested two alternative cross-links between protomers with equal occupancy (right panel).

(D) FA-cross-linked S glycoprotein was incubated with liposomes containing 4% DGS-NTA lipids, purified by sucrose gradient density centrifugation and analyzed by negative staining electron microscopy revealing regular decoration of the liposomes with the S glycoprotein. Counting S on 50 S-LVs (negative staining EM two-dimensional vision) indicated 231 ± 92 trimers. We thus estimate that approximately or at least 460 ± 184 S trimers are attached to the LVs. Scale bar, 200 nm.

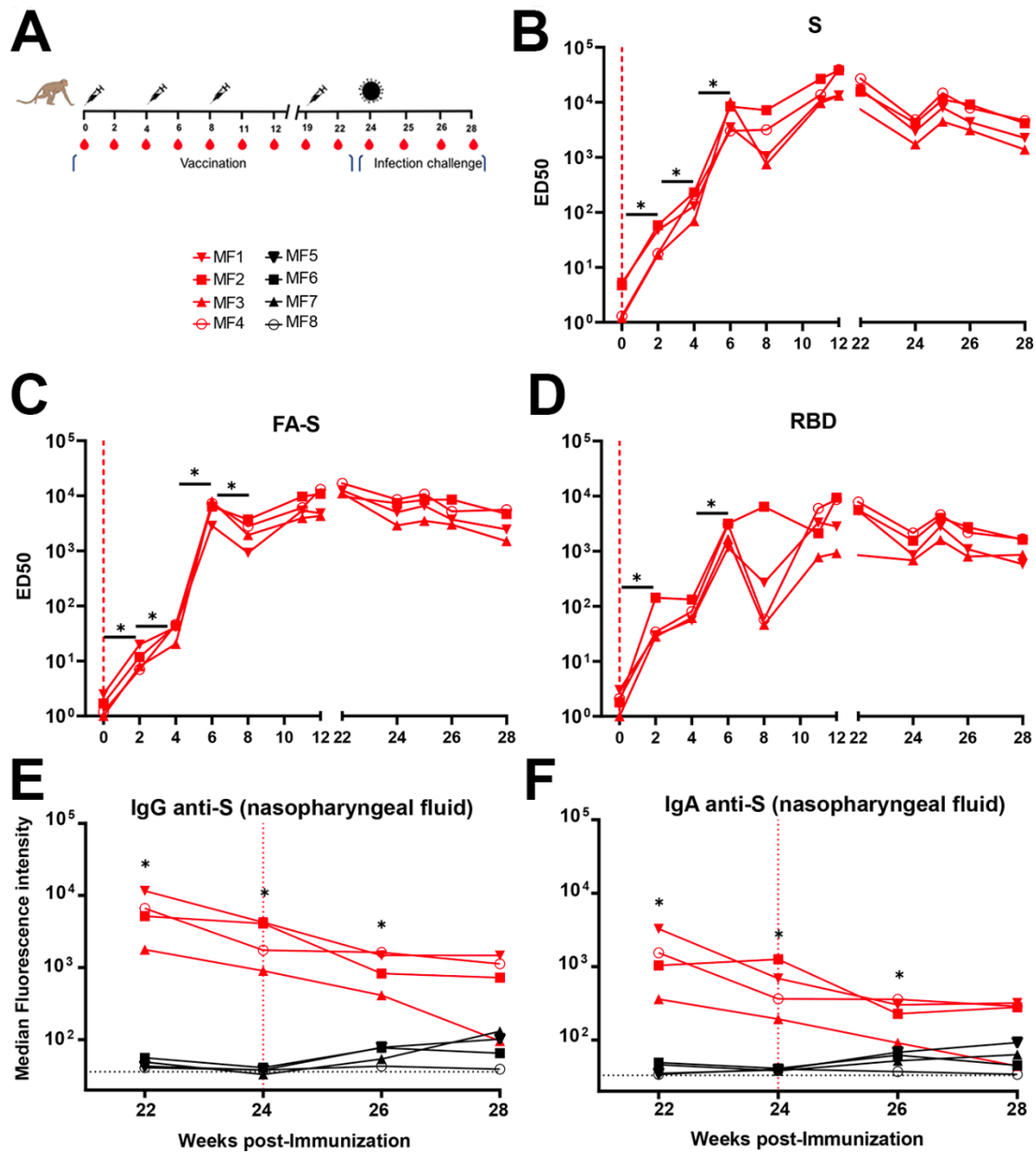


Figure 2: Antibody responses induced by S-LV vaccination of cynomolgus macaques

(A) Scheme of vaccination, challenge and sampling. Syringes indicate the time points of vaccination, red drops the time of serum collection and the virus particle the time point of challenge. Symbols of identifying individual macaques are used in all figures.

(B) ELISA of SARS-CoV-2 S-protein-specific IgG determined during the study at weeks 0, 2, 4, 6, 8, 10, 12, 22, 24, 26, 28. Ab titers of individual animals are shown.

(C) ELISA of SARS-CoV-2 FA-S-protein-specific IgG determined during the study at the indicated weeks.

(D) ELISA of SARS-CoV-2 S RBD-specific IgG determined during the study at the indicated weeks..

For panels (B), (C), and (D), differences between matched groups were compared using the Wilcoxon signed-rank test ($p<0.1$).

(E and F) Detection of S-specific IgG (E) and IgA (F) in nasopharyngeal fluids. Relative mean fluorescence intensity (MFI) of IgG and IgA binding to SARS-CoV-2 S measured with a Luminex-based serology assay in nasopharyngeal swabs. The background level is indicated by dotted lines. The vertical red line indicates the day of challenge. For panels (E), and (F), groups were compared using the Mann-Whitney U test (* $p < 0.05$)

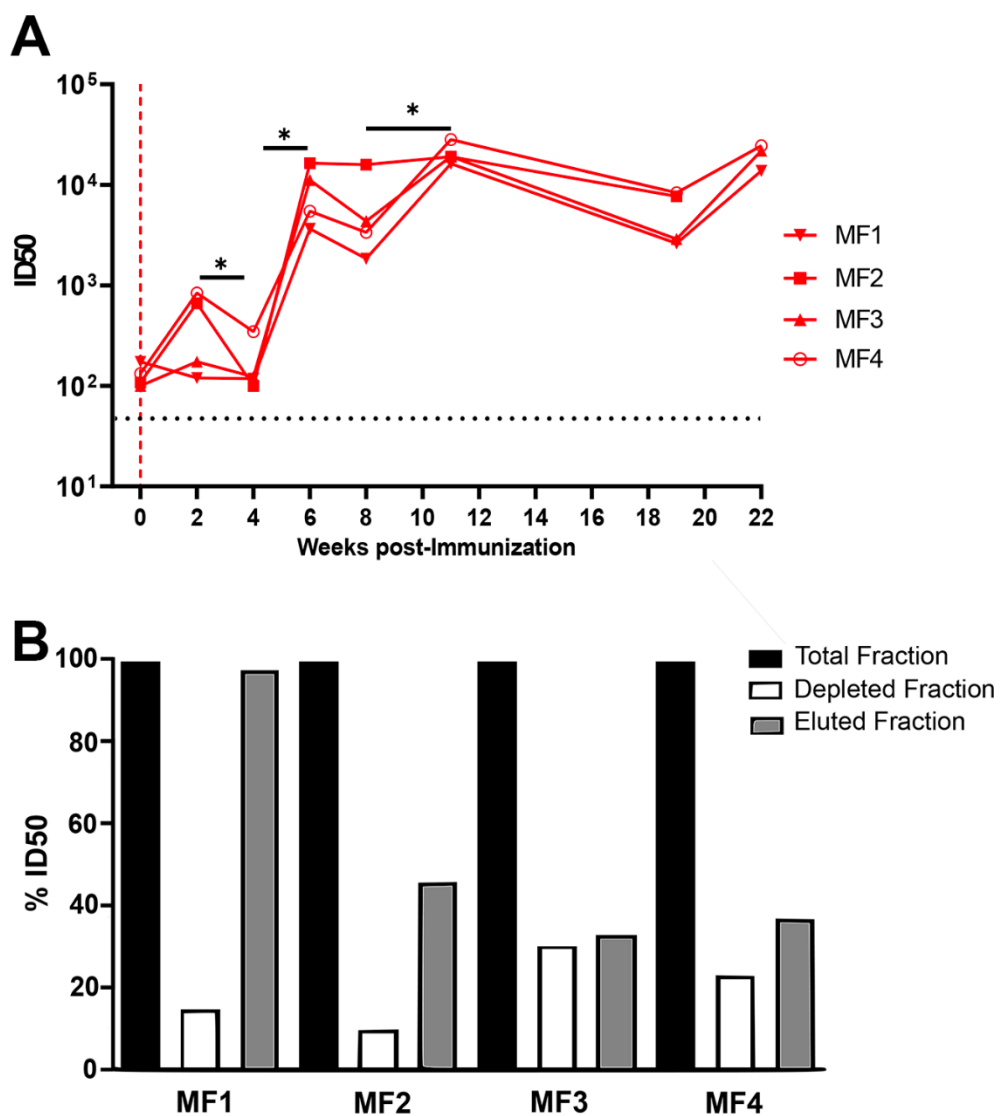


Figure 3: Serum neutralization of SARS-CoV-2 pseudovirus upon S-LV vaccination

(A) The evolution of SARS-CoV-2 neutralizing Ab titers is shown for sera collected at weeks 0, 2, 4, 6, 8, 11, 12, 19. Bars indicate median titers of the four animals. Differences between matched groups were compared using the Wilcoxon signed-rank test ($p<0.1$).

(B) Serum from week 11 was depleted of RBD-specific Abs by affinity chromatography and neutralization activity of the complete serum of each animal was set to 100 % and compared to the RBD-depleted sera and the RBD-specific sera.

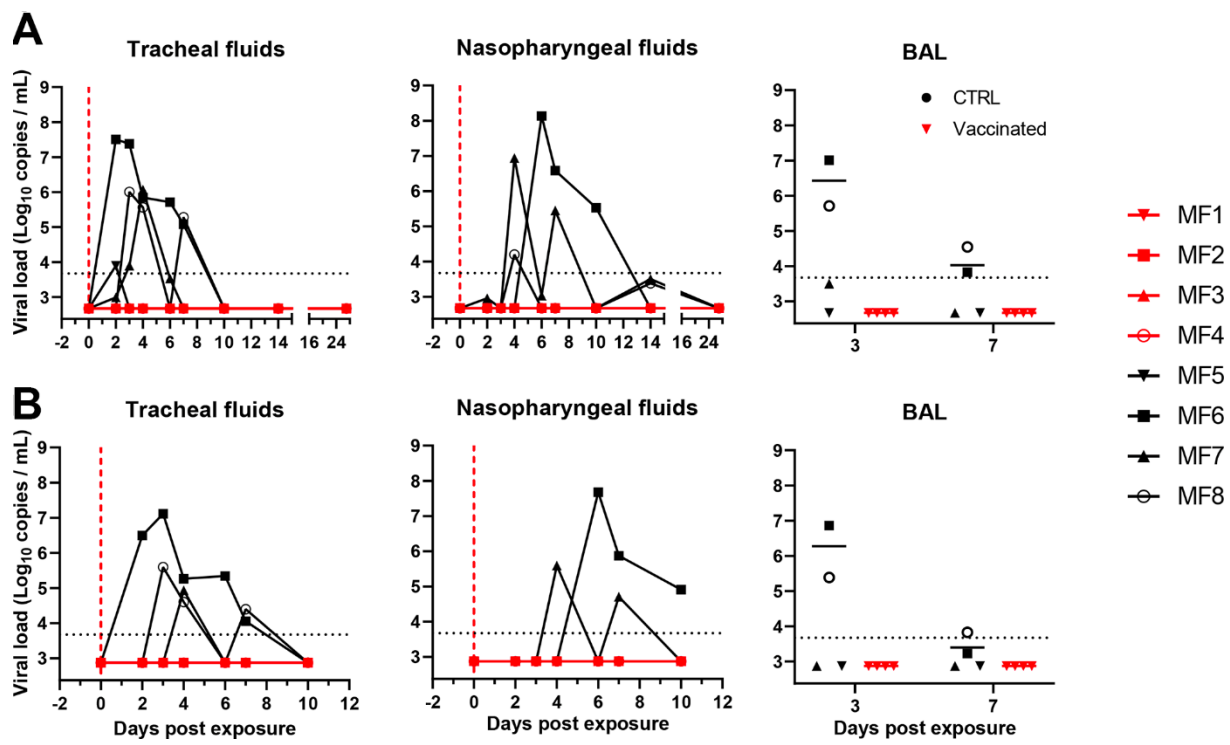


Figure 4: S-LV immunization protects cynomolgus macaques from SARS-CoV-2 infection

(A) Genomic (A) and Subgenomic (sg)RNA viral loads (B) in tracheal swabs (left) and nasopharyngeal swabs (middle) of control (black) and vaccinated (red) macaques after challenge. Viral loads in control and vaccinated macaques after challenge in BAL are shown (right). Bars indicate median viral loads. Vertical red dotted lines indicate the day of challenge. Horizontal dotted lines indicate the limit of quantification.

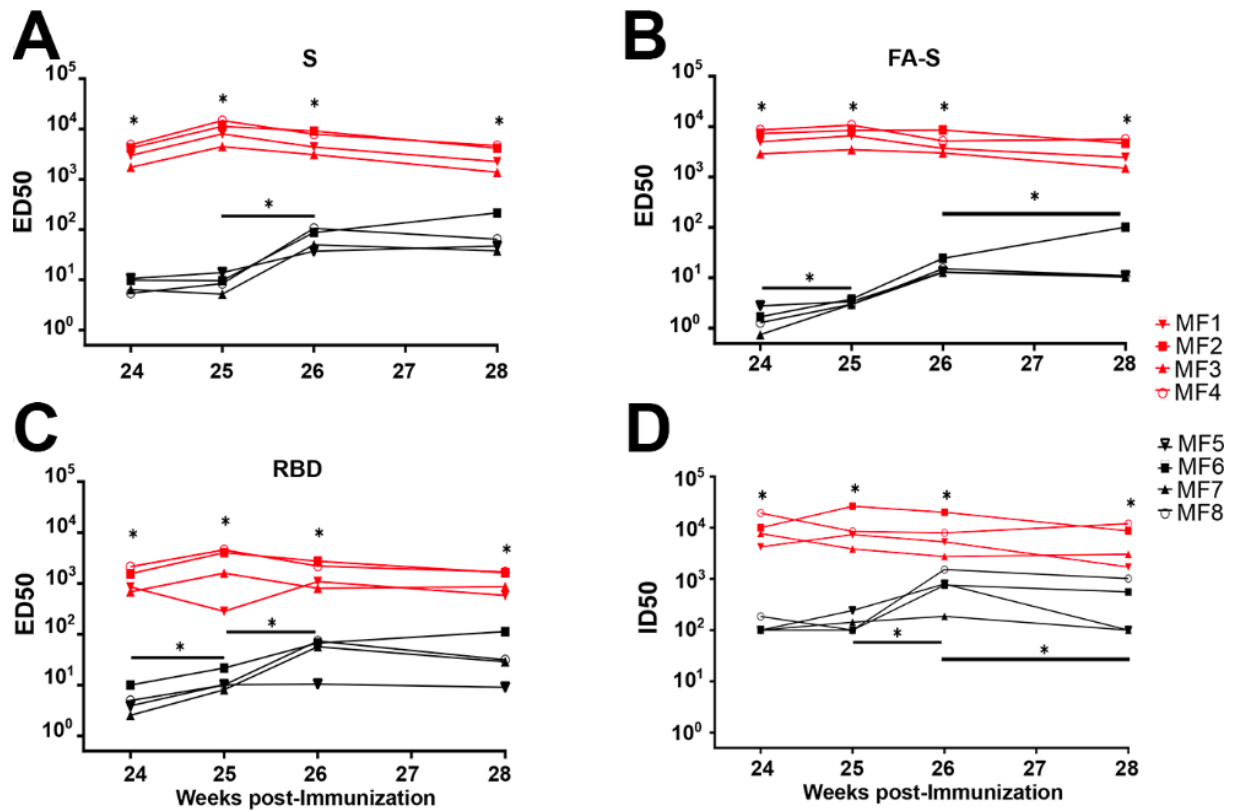


Figure 5: Serum antibody titers and neutralization of vaccinated and control group cynomolgus macaques after SARS CoV-2 challenge.

Antibody IgG titers were determined by ELISA at weeks 24 (challenge), 25, 26, 27 and 28 against (A) SARS-CoV-2 S, (B) SARS-CoV-2 FA-S and (C) SARS-CoV-2 S RBD. Vaccinated animals are shown with red symbols and control animals with black symbols.

(D) SARS CoV-2 pseudovirus neutralization titers at week 24 (challenge) and 1, 2 and 4 weeks post exposure (weeks 25, 26, 28). The Bars show the median titers.

For panels A to D, differences between matched groups were compared using the Wilcoxon signed-rank test ($p < 0.1$).

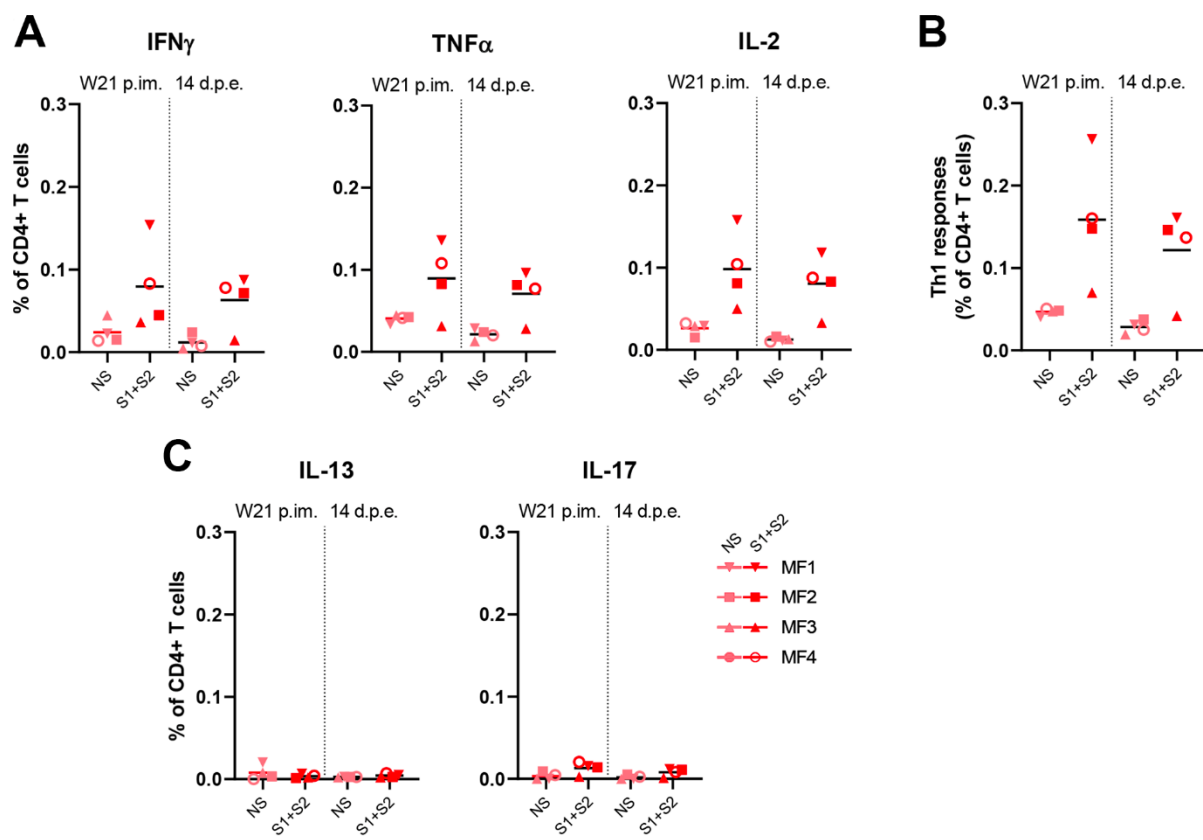


Figure 6: Antigen-specific CD4 T-cell responses in S-LV immunized cynomolgus macaques. Frequency of (A) $IFN\gamma+$, $TNF\alpha+$ and $IL-2+$, (B), Th1 ($IFN\gamma +/-$, $IL-2 +/-$, $TNF\alpha +$), (C) $IL-13+$ and $IL-17+$ antigen-specific CD4+ T cells ($CD154+$) in the total CD4+ T cell population, respectively, for each immunized macaque ($n = 4$) at week (W)21 post-immunization (p.i.m.) (i.e. two weeks after the 4th immunization, pre-exposure) and 14 days post-exposure (d.p.e.). PBMCs were stimulated overnight with medium (pink symbols) or SARS-CoV-2 S overlapping peptide pools (red symbols). Bars indicated means. Time points in each experimental group were compared using the Wilcoxon signed rank test.

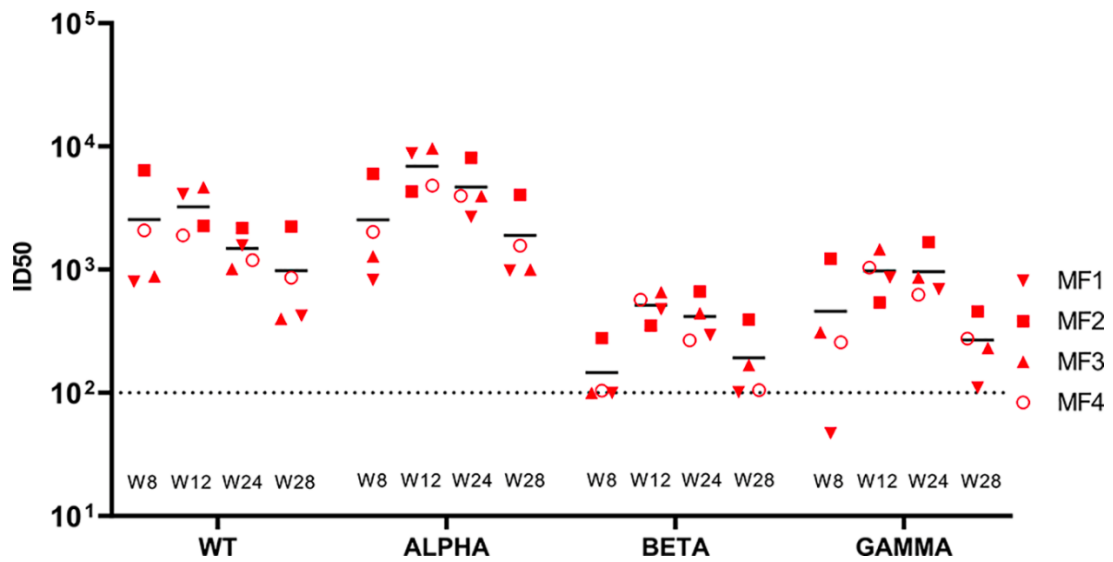
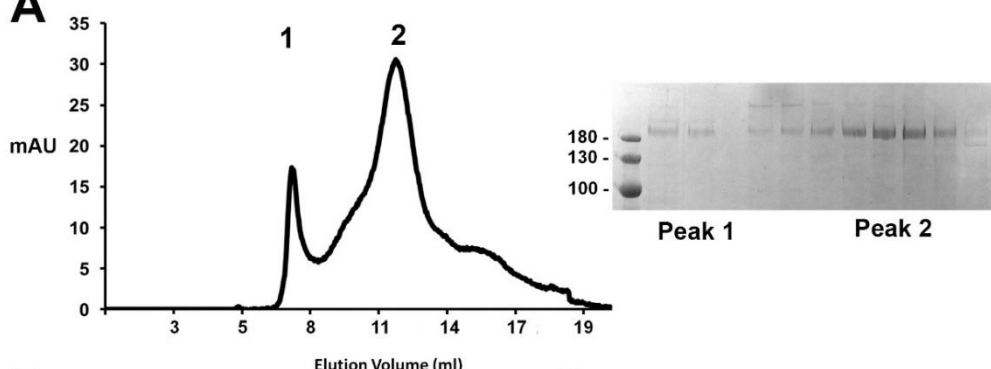


Figure 7: S- vaccination induces robust neutralization of SARS CoV-2 variants.

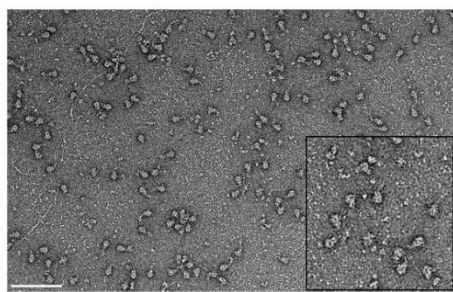
B.1.1.7 (Alpha, UK), B.1.351 (Beta, SA) and P.1 (Gamma, BR) pseudovirus neutralization titers were compared to the Wuhan vaccine strain. Titers were determined using total IgG purified from sera at weeks 8 (2 immunizations), 12 (3 immunizations), 24 and 28 (4 immunizations). Background neutralization by IgG isolated from naïve animals was <100 for all variants and is indicated by the dashed line.

SUPPLEMENTARY FIGURES

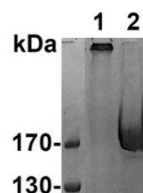
A



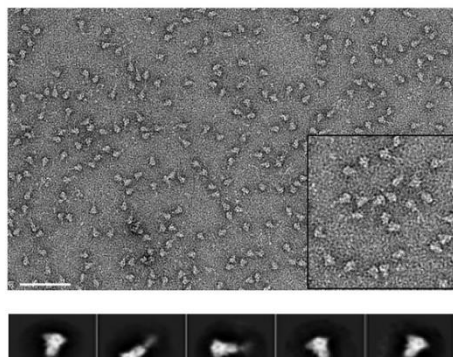
B



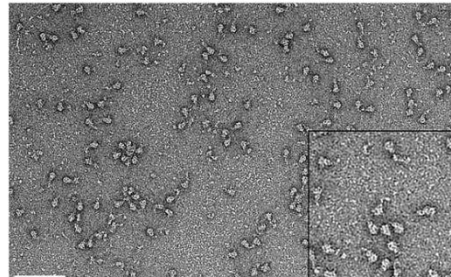
C



D



E



F

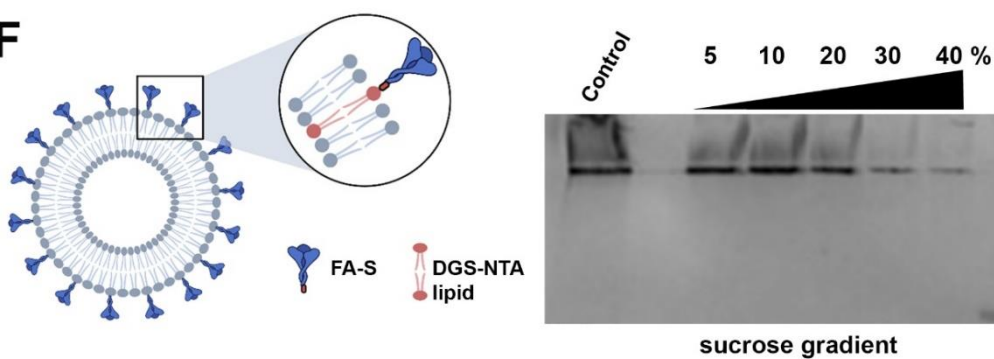


Figure S1: Expression and characterization of the SARS Cov-2 S glycoprotein.

Related to Figure 1.

- (A) SDS-PAGE and size exclusion chromatography (SEC) of purified S protein.
- (B) Negative staining electron microscopy of the S glycoprotein. 2-D class averages of the five most populated classes are shown below the panels.
- (C) SDS-PAGE of purified SARS-CoV-2 S (lane 2) and S chemically cross-linked with 4% formaldehyde (FA) (lane 1).
- (D) Negative staining electron microscopy of the S glycoprotein after FA cross-linking. 2-D class averages of the five most populated classes are shown below the panels
- (E) FA-cross-linked S glycoprotein analyzed after storage (2 weeks) at 4°C.
- Scale bars are 200 nm.
- (F) Left panel, schema of the liposome FA-S glycoprotein coupling; right panel, SDS-PAGE analysis of the S-VLP purification by sucrose gradient density centrifugation. FA-S was incubated with liposomes containing DGS NTA lipids that capture FA-S via its C-terminal His-tag. Free FA-S was removed by sucrose gradient centrifugation.

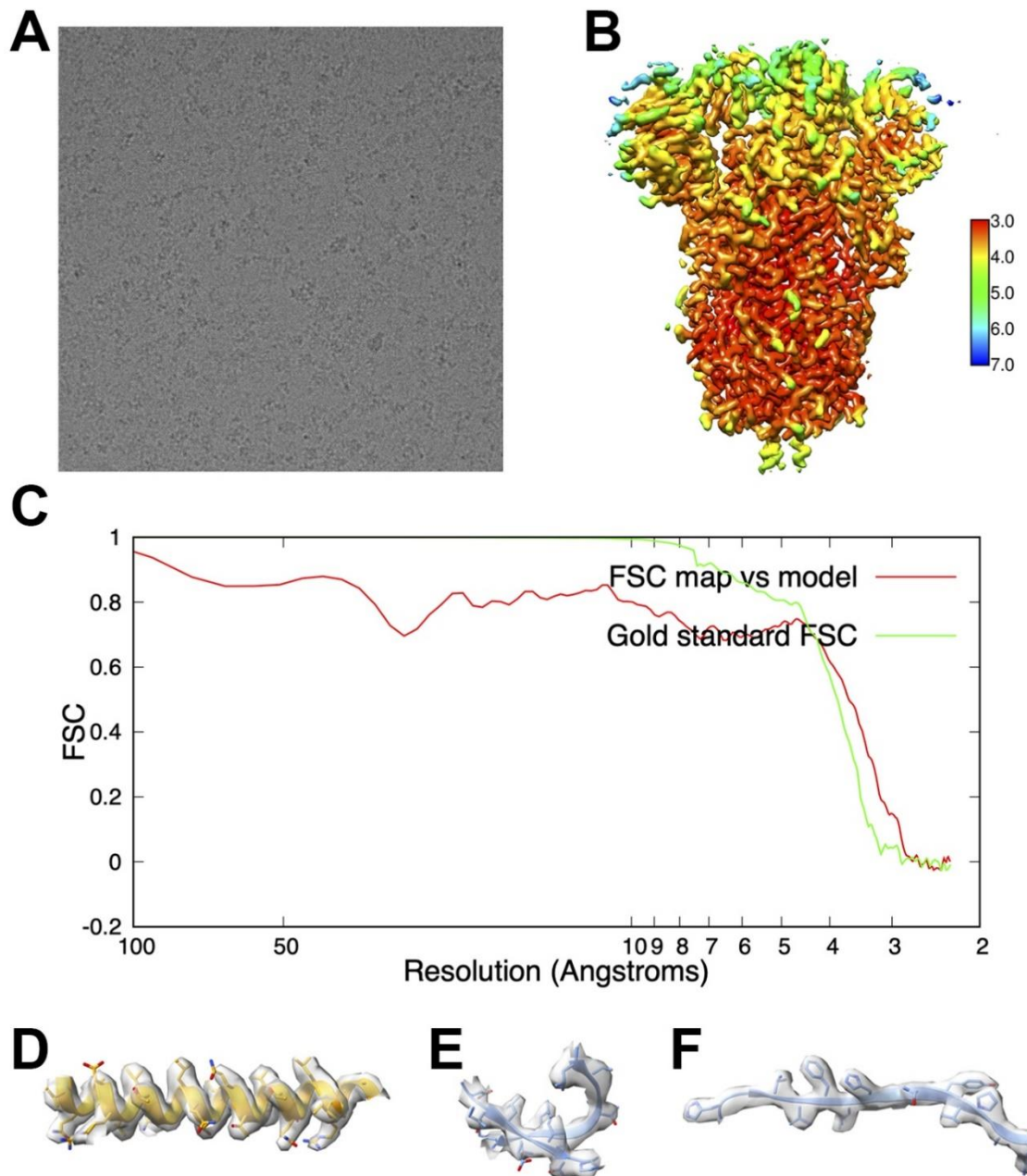


Figure S2: Cryo-EM structure validation.

(A) Cryo-EM image of the S trimer.

(B) Isosurface representation of the 3D reconstruction of the S trimer obtained by cryo-EM colored by local resolution (color code in Å).

(C) Fourier Shell Correlation (FSC) curves calculated between two independent 3D reconstructions of the S trimer (gold standard FSC, resolution of 3.4 Å at FSC=0.143) and between the cryo-EM 3D reconstruction and the refined atomic model (FSC map vs model, resolution of 3.7 Å at FSC=0.5). (D, E, F) Three different zones of the S trimer are shown to

illustrate both the high resolution of the 3D reconstruction (grey isosurface) and the quality of the refined atomic model.

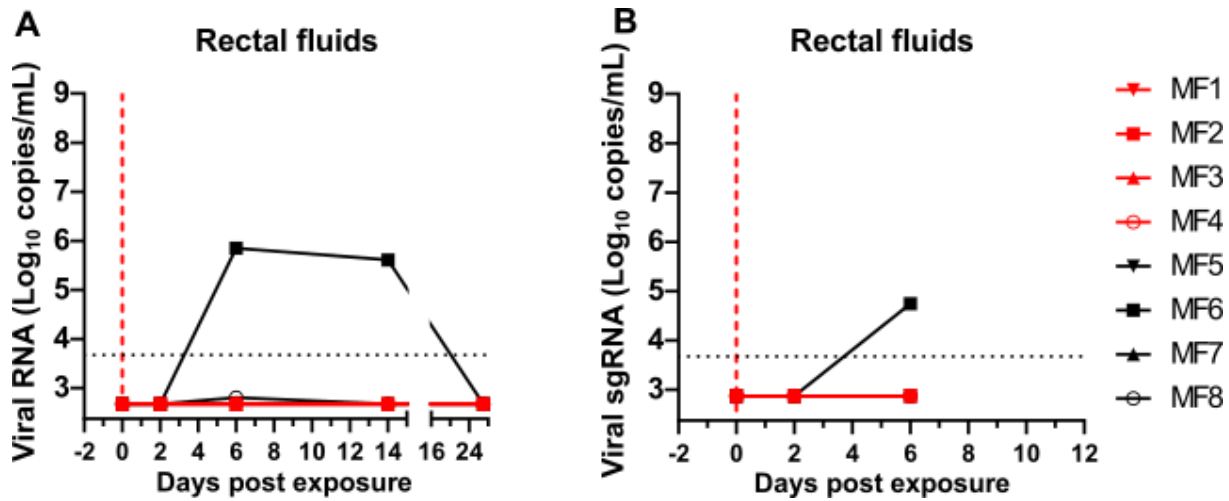


Figure S3: Viral RNA detection upon SARS CoV-2 challenge.

Genomic (A) and subgenomic (sg)RNA (B) viral loads detected in rectal fluids upon challenge of vaccinated animals (red) and control (black) animals.

Data for individual animals has been plotted. Vertical red dotted lines indicate the day of challenge. Horizontal dotted lines indicate the limit of quantification.

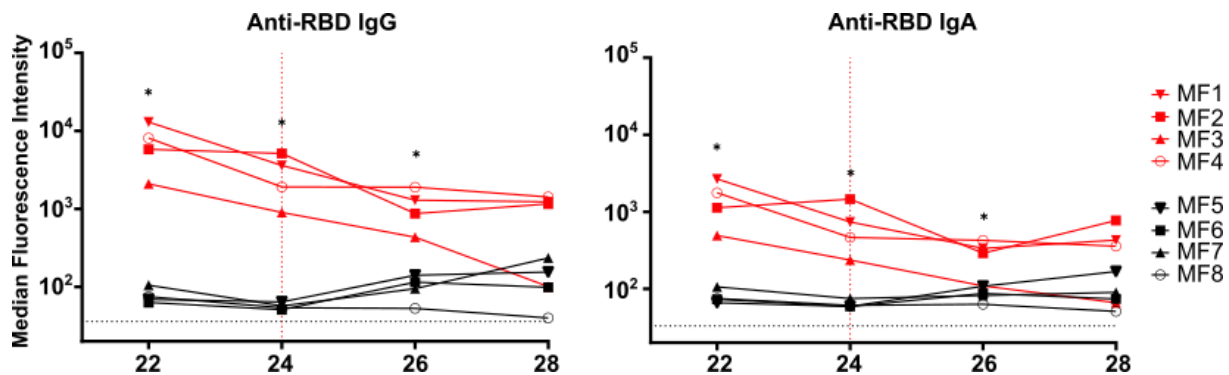


Figure S4: Detection of RBD-specific IgG and IgA in nasopharyngeal fluids.

Relative mean fluorescence intensity (MFI) of IgG and IgA binding to SARS-CoV-2 RBD measured with a Luminex-based serology assay in nasopharyngeal swabs. The background level is indicated by dotted lines. The vertical red line indicates the day of challenge. Groups were compared using the Mann-Whitney U test (*p < 0.05).

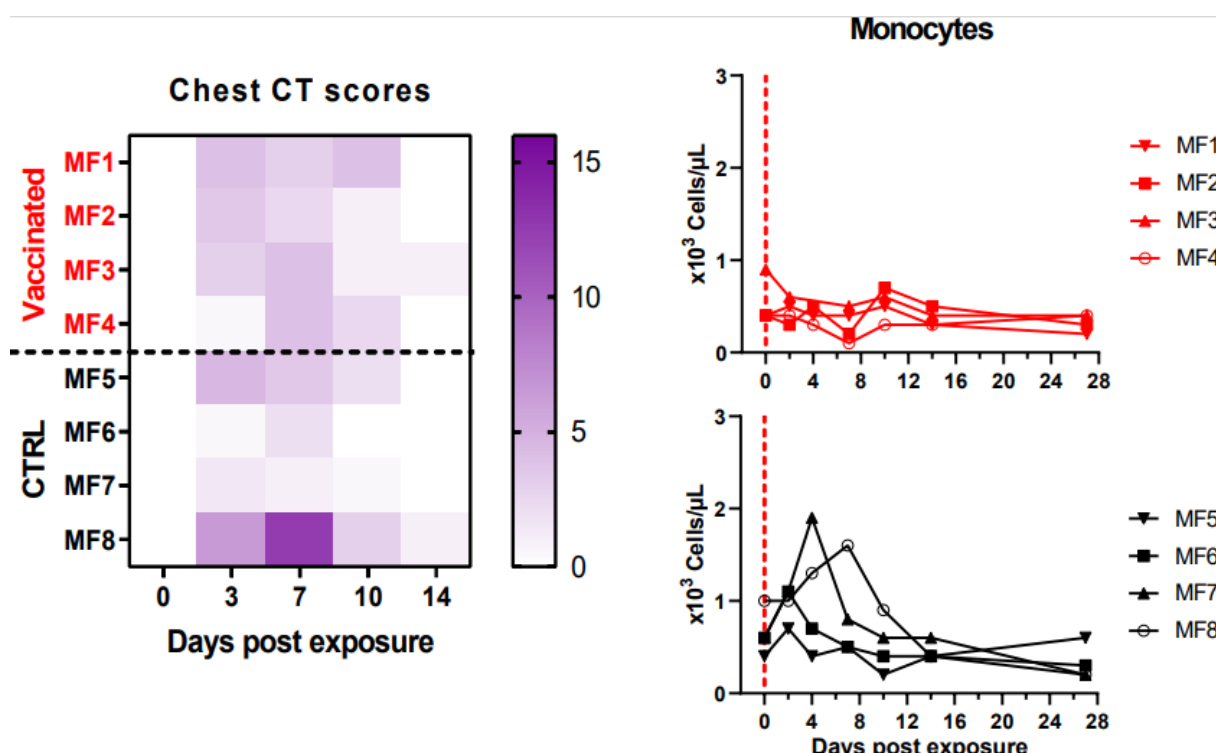


Figure S5: Clinical manifestations upon infection.

- (A) Lung CT scores of control (black) and vaccinated (red) macaques over the course of 14 days post exposure. The CT score is based on the lesion type (scored from 0 to 3) and lesion volume (scored from 0 to 4), which have been summed for each lobe.
- (B) Monocyte counts in the blood of control (black) and vaccinated (red) macaques after challenge

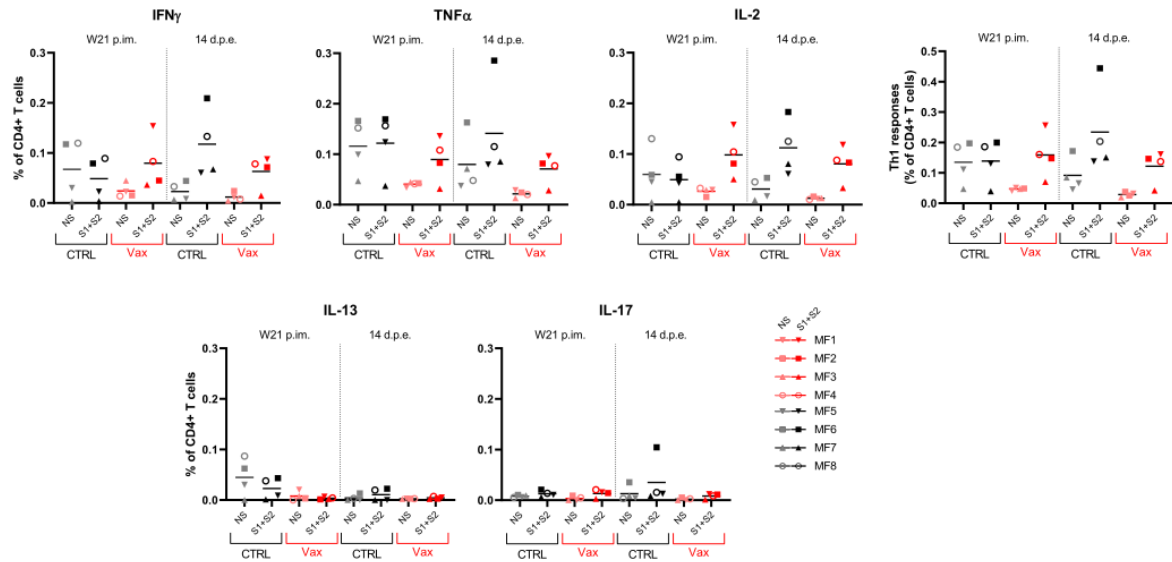


Figure S6: Antigen-specific CD4 T-cell responses in cynomolgus macaques.

Frequency of (A) IFN γ +, TNF α + and IL-2+, (B), Th1 (IFN γ +-, IL-2+-, TNF α), (C) IL-13+and IL-17+ antigen-specific CD4+ T cells (CD154+) in the total CD4+ T cell population, respectively, for each control ($n=4$, black) and immunized macaque ($n = 4$, red) at week (W)21 post-first immunization (p.i.m.) (i.e. two weeks after the 4th immunization, pre-exposure) and 14 days post-exposure (d.p.e.). PBMCs were stimulated overnight with medium (grey or pink symbols) or SARS-CoV-2 S overlapping peptide pools (black or red symbols). Bars indicate means. Time points in each experimental group were compared using the Wilcoxon signed rank test. Groups were compared using the non-parametric Mann-Whitney test.

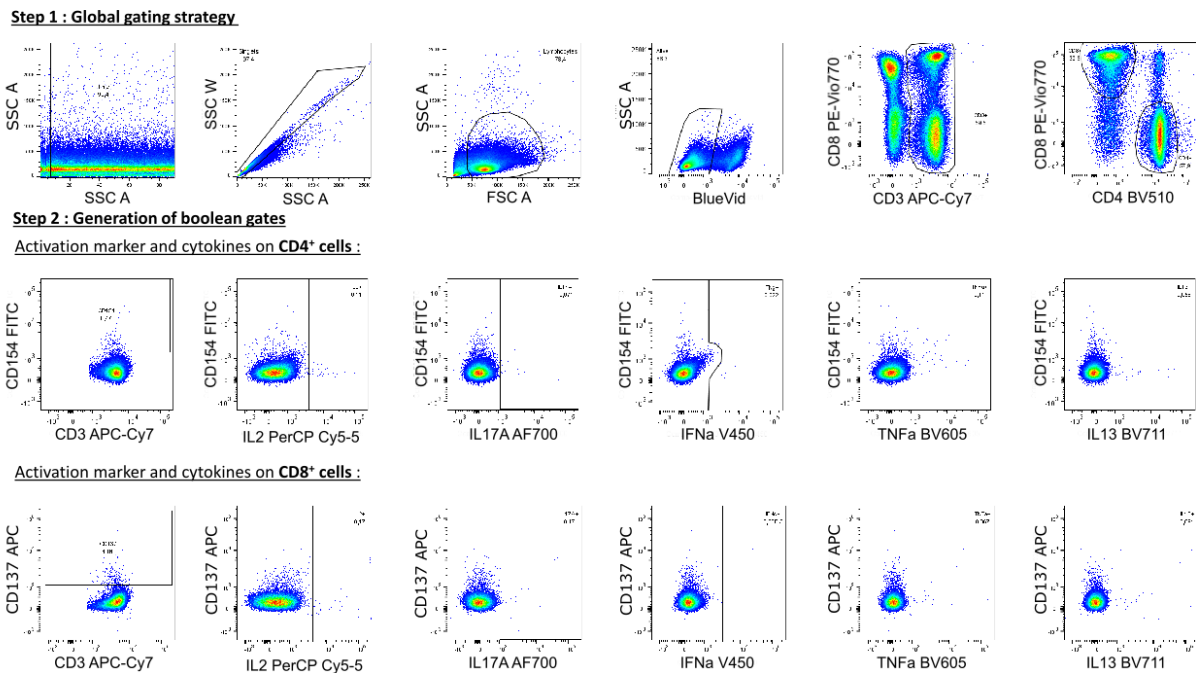


Figure S7: Gating strategy for antigen-specific CD4 and CD8 T-cell responses in cynomolgus macaques.

The analysis is focused on alive cells and singlets. T Lymphocytes are selected after a SSC-A vs FSC-A gating, according to their expression of the CD3 marker (Step 1). CD4 and CD8 positive T cells are devised corresponding their expression of CD4 and CD8.

Then for CD4 and CD8 T cell populations, expression of activation markers and cytokine production is studied (Step 2). At the end, boolean gates allow us to study the combination of activated and cytokine producing cells. All these parameters are analysed for all stimulations.

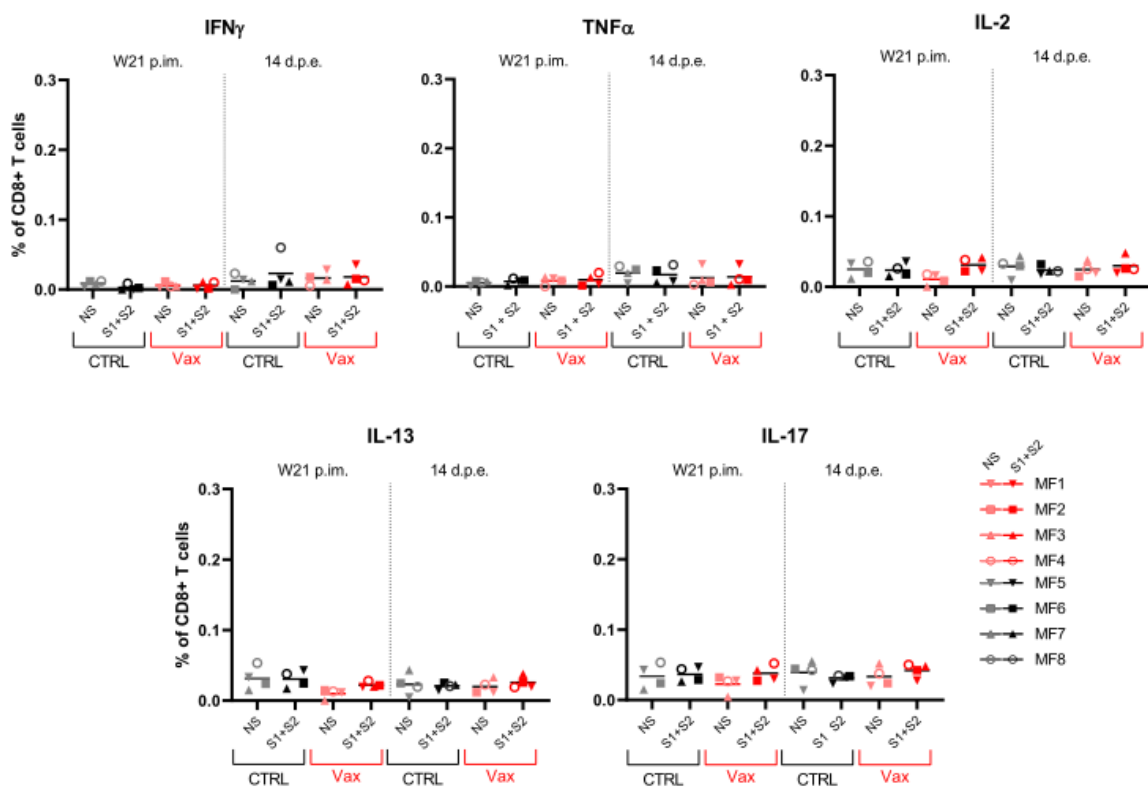


Figure S8: Antigen-specific CD8 T-cell responses in S-LV immunized cynomolgus macaques. Frequency of IFN γ + (top left), TNF α + (top middle), IL-2+ (top right), IL-13+ (bottom left) and IL-17+ (bottom right) antigen-specific CD8+ T cells (CD137+) in the total CD8+ T cell population, respectively, for each immunized macaque ($n = 4$) at week (W)21 (i.e. two weeks after the 4th immunization, pre-exposure) and 14 days post-exposure (d.p.e.). PBMCs were stimulated overnight with medium (pink symbols) or SARS-CoV-2 S overlapping peptide pools (red symbols). Bars indicate means. Time points in each experimental group were compared using the Wilcoxon signed rank test.

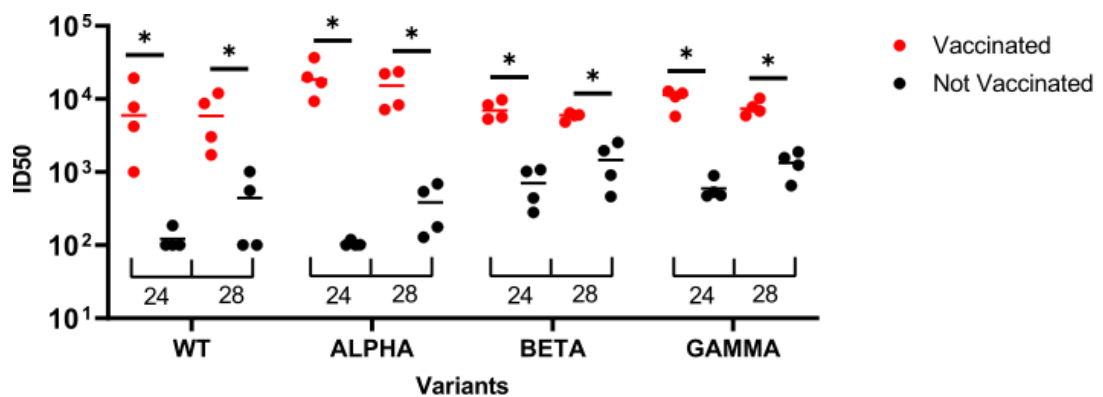


Figure S9: S-VLP vaccination induces neutralization of SARS CoV-2 variants.

B.1.1.7 (Alpha, UK), B.1.351 (Beta, SA) and P.1 (Gamma, BR) pseudovirus neutralization titers were compared to the Wuhan vaccine strain (WT). Titers were determined at weeks 24 (exposure) and 28 (4 weeks pe). Comparison of sera from vaccinated macaques and the control group indicated high background values at week 24 (challenge) for Beta and Gamma. Groups were compared using the Mann-Whitney U test (*p < 0.05). The bars indicate median titers.

ACKNOWLEDGMENTS

This work acknowledges support by the European Union's Horizon 2020 research and innovation program under grant agreement No. 681032, H2020 EHVA (WW), the ANR, RA-Covid-19 (W.W., R.I.G.) and the CNRS (W.W.). WW acknowledges access to the platforms of the Grenoble Instruct-ERIC center (IBS and ISBG; UMS 3518 CNRS-CEA-UGA-EMBL) within the Grenoble Partnership for Structural Biology (PSB), with support from FRISBI (ANR-10-INBS-05-02) and GRAL, a project of the University Grenoble Alpes graduate school (Ecoles Universitaires de Recherche) CBH-EUR-GS (ANR-17-EURE-0003). The IBS acknowledges integration into the Interdisciplinary Research Institute of Grenoble (IRIG, CEA) and financial support from CEA, CNRS and UGA. The Infectious Disease Models and Innovative Therapies (IDMIT) research infrastructure is supported by the Programme Investissements d'Avenir, managed by the National Research Agency (ANR) under reference ANR-11-INBS-0008. The Fondation Bettencourt Schueller and the Region Ile-de-France contributed to the implementation of IDMIT's facilities and imaging technologies. The non-human primate study received financial support from REACTing, the Fondation pour la Recherche Médicale (AM-CoV-Path), and the European Infrastructure TRANSVAC2 (730964). We acknowledge support from CoVIC supported by the Bill and Melinda Gates Foundation. The virus stock was obtained through the EVAg platform (<https://www.european-virus-archive.com/>), funded by H2020 (653316). The funders had no role in study design, data collection, data analysis, data interpretation, or data reporting.

We thank J. McLellan for providing the S expression vector, B. Delache, E. Burban, J. Demilly, N. Dhooge, S. Langlois, P. Le Calvez, Q. Sconosciuti, V. Magneron, M. Rimlinger, A. Berriche, J.H. Qiu, M. Potier, J. M. Robert and C. Dodan for help with animal studies, and R. Ho Tsong Fang for his supervision; L. Bossevot, M. Leonec, L. Moenne-Locoz, and J. Morin for the qRT-PCR and preparation of reagents; M. Gomez-Pacheco and J. van Wassenhove for cellular assays; N. Kahlaoui, B. Fert and C. Mayet for help with the CT scans, and C. Chapon for her supervision; M. Barendji, J. Dinh, and E. Guyon for the non-human primate sample processing; S. Keyser for the transports organization; F. Ducancel and Y. Gorin for their help with the logistics and safety management; and I. Mangeot for her help with resource management. We thank Antoine Nougairede for sharing the plasmid used for the sgRNA assay standardization. Finally, we thank Dietmar Katinger and Philipp Mundspurger (Polymun) for providing MPLA liposomes. Images in Figure 2A, Figure S1F and the graphical abstract were created with BioRender.com.

REFERENCES

- Adams, P.D., Afonine, P.V., Bunkoczi, G., Chen, V.B., Davis, I.W., Echols, N., Headd, J.J., Hung, L.W., Kapral, G.J., Grosse-Kunstleve, R.W., *et al.* (2010). PHENIX: a comprehensive Python-based system for macromolecular structure solution. *Acta Crystallogr D Biol Crystallogr* *66*, 213-221.
- Addetia, A., Crawford, K.H.D., Dingens, A., Zhu, H., Roychoudhury, P., Huang, M.L., Jerome, K.R., Bloom, J.D., and Greninger, A.L. (2020). Neutralizing Antibodies Correlate with Protection from SARS-CoV-2 in Humans during a Fishery Vessel Outbreak with a High Attack Rate. *J Clin Microbiol* *58*, e02107-02120.
- Alsooussi, W.B., Turner, J.S., Case, J.B., Zhao, H., Schmitz, A.J., Zhou, J.Q., Chen, R.E., Lei, T., Rizk, A.A., McIntire, K.M., *et al.* (2020). A Potently Neutralizing Antibody Protects Mice against SARS-CoV-2 Infection. *J Immunol* *205*, 915-922.
- Alving, C.R., Beck, Z., Matyas, G.R., and Rao, M. (2016). Liposomal adjuvants for human vaccines. *Expert Opin Drug Deliv* *13*, 807-816.
- Amanat, F., Stadlbauer, D., Strohmeier, S., Nguyen, T.H.O., Chromikova, V., McMahon, M., Jiang, K., Arunkumar, G.A., Jurczyszak, D., Polanco, J., *et al.* (2020). A serological assay to detect SARS-CoV-2 seroconversion in humans. *Nat Med* *26*, 1033-1036.
- Arunachalam, P.S., Walls, A.C., Golden, N., Atyeo, C., Fischinger, S., Li, C., Aye, P., Navarro, M.J., Lai, L., Edara, V.V., *et al.* (2021). Adjuvanting a subunit COVID-19 vaccine to induce protective immunity. *Nature* *594*, 253-258.
- Bale, S., Goebrecht, G., Stano, A., Wilson, R., Ota, T., Tran, K., Ingale, J., Zwick, M.B., and Wyatt, R.T. (2017). Covalent Linkage of HIV-1 Trimers to Synthetic Liposomes Elicits Improved B Cell and Antibody Responses. *J Virol* *91*, e00443-00417.
- Barnes, C.O., Jette, C.A., Abernathy, M.E., Dam, K.A., Esswein, S.R., Gristick, H.B., Malyutin, A.G., Sharaf, N.G., Huey-Tubman, K.E., Lee, Y.E., *et al.* (2020a). SARS-CoV-2 neutralizing antibody structures inform therapeutic strategies. *Nature* *588*, 682-687.
- Barnes, C.O., West, A.P., Jr., Huey-Tubman, K.E., Hoffmann, M.A.G., Sharaf, N.G., Hoffman, P.R., Koranda, N., Gristick, H.B., Gaebler, C., Muecksch, F., *et al.* (2020b). Structures of Human Antibodies Bound to SARS-CoV-2 Spike Reveal Common Epitopes and Recurrent Features of Antibodies. *Cell* *182*, 828-842 e816.
- Baum, A., Ajithdoss, D., Copin, R., Zhou, A., Lanza, K., Negron, N., Ni, M., Wei, Y., Mohammadi, K., Musser, B., *et al.* (2020). REGN-COV2 antibodies prevent and treat SARS-CoV-2 infection in rhesus macaques and hamsters. *Science*.
- Brouwer, P.J.M., Brinkkemper, M., Maisonnasse, P., Dereuddre-Bosquet, N., Grobben, M., Claireaux, M., de Gast, M., Marlin, R., Chesnais, V., Diry, S., *et al.* (2021). Two-component spike nanoparticle vaccine protects macaques from SARS-CoV-2 infection. *Cell* *184*, 1188-1200 e1119.
- Brouwer, P.J.M., Caniels, T.G., van der Straten, K., Snitselaar, J.L., Aldon, Y., Bangaru, S., Torres, J.L., Okba, N.M.A., Claireaux, M., Kerster, G., *et al.* (2020). Potent neutralizing antibodies from COVID-19 patients define multiple targets of vulnerability. *Science* *369*, 643-650.
- Cai, Y., Zhang, J., Xiao, T., Lavine, C.L., Rawson, S., Peng, H., Zhu, H., Anand, K., Tong, P., Gautam, A., *et al.* (2021). Structural basis for enhanced infectivity and immune evasion of SARS-CoV-2 variants. *Science* *373*, 642-648.
- Cai, Y., Zhang, J., Xiao, T., Peng, H., Sterling, S.M., Walsh, R.M., Jr., Rawson, S., Rits-Volloch, S., and Chen, B. (2020). Distinct conformational states of SARS-CoV-2 spike protein. *Science* *369*, 1586-1592.
- Caniels, T.G., Bontjer, I., van der Straten, K., Poniman, M., Burger, J.A., Appelman, B., Lavell, H.A.A., Oomen, M., Godeke, G.J., Valle, C., *et al.* (2021). Emerging SARS-CoV-2 variants of concern evade humoral immune responses from infection and vaccination. *Sci Adv* *7*, eabj5365.
- Cardone, G., Heymann, J.B., and Steven, A.C. (2013). One number does not fit all: mapping local variations in resolution in cryo-EM reconstructions. *J Struct Biol* *184*, 226-236.
- Chen, Y., Zuiiani, A., Fischinger, S., Mullur, J., Atyeo, C., Travers, M., Lelis, F.J.N., Pullen, K.M., Martin, H., Tong, P., *et al.* (2020). Quick COVID-19 Healers Sustain Anti-SARS-CoV-2 Antibody Production. *Cell* *183*, 1496-1507 e1416.

- Cohen, A.A., Gnanapragasam, P.N.P., Lee, Y.E., Hoffman, P.R., Ou, S., Kakutani, L.M., Keeffe, J.R., Wu, H.J., Howarth, M., West, A.P., *et al.* (2021). Mosaic nanoparticles elicit cross-reactive immune responses to zoonotic coronaviruses in mice. *Science* 371, 735-741.
- Corbett, K.S., Flynn, B., Foulds, K.E., Francica, J.R., Boyoglu-Barnum, S., Werner, A.P., Flach, B., O'Connell, S., Bock, K.W., Minai, M., *et al.* (2020). Evaluation of the mRNA-1273 Vaccine against SARS-CoV-2 in Nonhuman Primates. *N Engl J Med* 383, 1544-1555.
- Corman, V.M., Landt, O., Kaiser, M., Molenkamp, R., Meijer, A., Chu, D.K., Bleicker, T., Brunink, S., Schneider, J., Schmidt, M.L., *et al.* (2020). Detection of 2019 novel coronavirus (2019-nCoV) by real-time RT-PCR. *Euro Surveill* 25.
- Coronaviridae Study Group of the International Committee on Taxonomy of, V. (2020). The species Severe acute respiratory syndrome-related coronavirus: classifying 2019-nCoV and naming it SARS-CoV-2. *Nat Microbiol* 5, 536-544.
- Dagotto, G., Yu, J., and Barouch, D.H. (2020). Approaches and Challenges in SARS-CoV-2 Vaccine Development. *Cell Host Microbe* 28, 364-370.
- Dejnirattisai, W., Zhou, D., Supasa, P., Liu, C., Mentzer, A.J., Ginn, H.M., Zhao, Y., Duyvesteyn, H.M.E., Tuekprakhon, A., Nutalai, R., *et al.* (2021). Antibody evasion by the P.1 strain of SARS-CoV-2. *Cell* 184, 2939-2954 e2939.
- Deng, W., Bao, L., Liu, J., Xiao, C., Liu, J., Xue, J., Lv, Q., Qi, F., Gao, H., Yu, P., *et al.* (2020). Primary exposure to SARS-CoV-2 protects against reinfection in rhesus macaques. *Science* 369, 818-823.
- Dubrovskaya, V., Tran, K., Ozorowski, G., Guenaga, J., Wilson, R., Bale, S., Cottrell, C.A., Turner, H.L., Seabright, G., O'Dell, S., *et al.* (2019). Vaccination with Glycan-Modified HIV NFL Envelope Trimer-Liposomes Elicits Broadly Neutralizing Antibodies to Multiple Sites of Vulnerability. *Immunity* 51, 915-929 e917.
- Earle, K.A., Ambrosino, D.M., Fiore-Gartland, A., Goldblatt, D., Gilbert, P.B., Siber, G.R., Dull, P., and Plotkin, S.A. (2021). Evidence for antibody as a protective correlate for COVID-19 vaccines. *Vaccine* 39, 4423-4428.
- Edara, V.V., Norwood, C., Floyd, K., Lai, L., Davis-Gardner, M.E., Hudson, W.H., Mantus, G., Nyhoff, L.E., Adelman, M.W., Fineman, R., *et al.* (2021). Infection- and vaccine-induced antibody binding and neutralization of the B.1.351 SARS-CoV-2 variant. *Cell Host Microbe* 29, 516-521 e513.
- Edwards, R.J., Mansouri, K., Stalls, V., Manne, K., Watts, B., Parks, R., Janowska, K., Gobéil, S.M.C., Kopp, M., Li, D., *et al.* (2021). Cold sensitivity of the SARS-CoV-2 spike ectodomain. *Nat Struct Mol Biol* 28, 128-131.
- Eldred, B.E., Dean, A.J., McGuire, T.M., and Nash, A.L. (2006). Vaccine components and constituents: responding to consumer concerns. *Med J Aust* 184, 170-175.
- Emsley, P., Lohkamp, B., Scott, W.G., and Cowtan, K. (2010). Features and development of Coot. *Acta Crystallogr D Biol Crystallogr* 66, 486-501.
- Ewer, K.J., Barrett, J.R., Belij-Rammerstorfer, S., Sharpe, H., Makinson, R., Morter, R., Flaxman, A., Wright, D., Bellamy, D., Bittaye, M., *et al.* (2021). T cell and antibody responses induced by a single dose of ChAdOx1 nCoV-19 (AZD1222) vaccine in a phase 1/2 clinical trial. *Nat Med* 27, 270-278.
- Gaebler, C., Wang, Z., Lorenzi, J.C.C., Muecksch, F., Finkin, S., Tokuyama, M., Cho, A., Jankovic, M., Schaefer-Babajew, D., Oliveira, T.Y., *et al.* (2021). Evolution of antibody immunity to SARS-CoV-2. *Nature* 591, 639-644.
- Ganneru, B., Jogdand, H., Daram, V.K., Das, D., Molugu, N.R., Prasad, S.D., Kannappa, S.V., Ella, K.M., Ravikrishnan, R., Awasthi, A., *et al.* (2021). Th1 skewed immune response of whole virion inactivated SARS CoV 2 vaccine and its safety evaluation. *iScience* 24, 102298.
- Gao, Q., Bao, L., Mao, H., Wang, L., Xu, K., Yang, M., Li, Y., Zhu, L., Wang, N., Lv, Z., *et al.* (2020). Development of an inactivated vaccine candidate for SARS-CoV-2. *Science* 369, 77-81.
- Garcia-Beltran, W.F., Lam, E.C., St Denis, K., Nitido, A.D., Garcia, Z.H., Hauser, B.M., Feldman, J., Pavlovic, M.N., Gregory, D.J., Poznansky, M.C., *et al.* (2021). Multiple SARS-CoV-2 variants escape neutralization by vaccine-induced humoral immunity. *Cell* 184, 2372-2383 e2379.

- Geers, D., Shamier, M.C., Bogers, S., den Hartog, G., Gommers, L., Nieuwkoop, N.N., Schmitz, K.S., Rijssbergen, L.C., van Osch, J.A.T., Dijkhuizen, E., *et al.* (2021). SARS-CoV-2 variants of concern partially escape humoral but not T-cell responses in COVID-19 convalescent donors and vaccinees. *Sci Immunol* 6.
- Gobeil, S.M., Janowska, K., McDowell, S., Mansouri, K., Parks, R., Stalls, V., Kopp, M.F., Manne, K., Li, D., Wiehe, K., *et al.* (2021). Effect of natural mutations of SARS-CoV-2 on spike structure, conformation, and antigenicity. *Science* 373.
- Goddard, T.D., Huang, C.C., Meng, E.C., Pettersen, E.F., Couch, G.S., Morris, J.H., and Ferrin, T.E. (2018). UCSF ChimeraX: Meeting modern challenges in visualization and analysis. *Protein Sci* 27, 14-25.
- Goel, R.R., Painter, M.M., Apostolidis, S.A., Mathew, D., Meng, W., Rosenfeld, A.M., Lundgreen, K.A., Reynaldi, A., Khoury, D.S., Pattekar, A., *et al.* (2021). mRNA Vaccination Induces Durable Immune Memory to SARS-CoV-2 with Continued Evolution to Variants of Concern. *bioRxiv*.
- Greaney, A.J., Loes, A.N., Crawford, K.H.D., Starr, T.N., Malone, K.D., Chu, H.Y., and Bloom, J.D. (2021). Comprehensive mapping of mutations in the SARS-CoV-2 receptor-binding domain that affect recognition by polyclonal human plasma antibodies. *Cell Host Microbe* 29, 463-476 e466.
- Grifoni, A., Weiskopf, D., Ramirez, S.I., Mateus, J., Dan, J.M., Moderbacher, C.R., Rawlings, S.A., Sutherland, A., Premkumar, L., Jadi, R.S., *et al.* (2020). Targets of T Cell Responses to SARS-CoV-2 Coronavirus in Humans with COVID-19 Disease and Unexposed Individuals. *Cell* 181, 1489-1501 e1415.
- Guebre-Xabier, M., Patel, N., Tian, J.H., Zhou, B., Maciejewski, S., Lam, K., Portnoff, A.D., Massare, M.J., Frieman, M.B., Piedra, P.A., *et al.* (2020). NVX-CoV2373 vaccine protects cynomolgus macaque upper and lower airways against SARS-CoV-2 challenge. *Vaccine* 38, 7892-7896.
- Hansen, J., Baum, A., Pascal, K.E., Russo, V., Giordano, S., Wloga, E., Fulton, B.O., Yan, Y., Koon, K., Patel, K., *et al.* (2020). Studies in humanized mice and convalescent humans yield a SARS-CoV-2 antibody cocktail. *Science* 369, 1010-1014.
- Hassan, A.O., Case, J.B., Winkler, E.S., Thackray, L.B., Kafai, N.M., Bailey, A.L., McCune, B.T., Fox, J.M., Chen, R.E., Alsoussi, W.B., *et al.* (2020). A SARS-CoV-2 Infection Model in Mice Demonstrates Protection by Neutralizing Antibodies. *Cell* 182, 744-753 e744.
- Hoffmann, M., Arora, P., Gross, R., Seidel, A., Hornich, B.F., Hahn, A.S., Kruger, N., Graichen, L., Hofmann-Winkler, H., Kempf, A., *et al.* (2021). SARS-CoV-2 variants B.1.351 and P.1 escape from neutralizing antibodies. *Cell* 184, 2384-2393 e2312.
- Hoffmann, M., Kleine-Weber, H., and Pohlmann, S. (2020). A Multibasic Cleavage Site in the Spike Protein of SARS-CoV-2 Is Essential for Infection of Human Lung Cells. *Mol Cell* 78, 779-784 e775.
- Hsieh, C.L., Goldsmith, J.A., Schaub, J.M., DiVenere, A.M., Kuo, H.C., Javanmardi, K., Le, K.C., Wrapp, D., Lee, A.G., Liu, Y., *et al.* (2020). Structure-based design of prefusion-stabilized SARS-CoV-2 spikes. *Science* 369, 1501-1505.
- Ingale, J., Stano, A., Guenaga, J., Sharma, S.K., Nemazee, D., Zwick, M.B., and Wyatt, R.T. (2016). High-Density Array of Well-Ordered HIV-1 Spikes on Synthetic Liposomal Nanoparticles Efficiently Activate B Cells. *Cell Rep* 15, 1986-1999.
- Isho, B., Abe, K.T., Zuo, M., Jamal, A.J., Rathod, B., Wang, J.H., Li, Z., Chao, G., Rojas, O.L., Bang, Y.M., *et al.* (2020). Persistence of serum and saliva antibody responses to SARS-CoV-2 spike antigens in COVID-19 patients. *Sci Immunol* 5, eabe5511.
- Iyer, A.S., Jones, F.K., Nodoushani, A., Kelly, M., Becker, M., Slater, D., Mills, R., Teng, E., Kamruzzaman, M., Garcia-Beltran, W.F., *et al.* (2020). Persistence and decay of human antibody responses to the receptor binding domain of SARS-CoV-2 spike protein in COVID-19 patients. *Sci Immunol* 5.
- Ke, Z., Oton, J., Qu, K., Cortese, M., Zila, V., McKeane, L., Nakane, T., Zivanov, J., Neufeldt, C.J., Cerikan, B., *et al.* (2020). Structures and distributions of SARS-CoV-2 spike proteins on intact virions. *Nature* 588, 498-502.
- Keech, C., Albert, G., Cho, I., Robertson, A., Reed, P., Neal, S., Plested, J.S., Zhu, M., Cloney-Clark, S., Zhou, H., *et al.* (2020). Phase 1-2 Trial of a SARS-CoV-2 Recombinant Spike Protein Nanoparticle Vaccine. *N Engl J Med* 383, 2320-2332.
- Khoury, D.S., Cromer, D., Reynaldi, A., Schlub, T.E., Wheatley, A.K., Juno, J.A., Subbarao, K., Kent, S.J., Triccas, J.A., and Davenport, M.P. (2021). Neutralizing antibody levels are highly predictive of immune protection from symptomatic SARS-CoV-2 infection. *Nat Med* 27, 1205-1211.

- Klasse, P.J., Nixon, D.F., and Moore, J.P. (2021). Immunogenicity of clinically relevant SARS-CoV-2 vaccines in nonhuman primates and humans. *Sci Adv* 7.
- Korber, B., Fischer, W.M., Gnanakaran, S., Yoon, H., Theiler, J., Abfalsterer, W., Hengartner, N., Giorgi, E.E., Bhattacharya, T., Foley, B., *et al.* (2020). Tracking Changes in SARS-CoV-2 Spike: Evidence that D614G Increases Infectivity of the COVID-19 Virus. *Cell* 182, 812-827 e819.
- Kreer, C., Zehner, M., Weber, T., Ercanoglu, M.S., Gieselmann, L., Rohde, C., Halwe, S., Korenkov, M., Schommers, P., Vanshylla, K., *et al.* (2020). Longitudinal Isolation of Potent Near-Germline SARS-CoV-2-Neutralizing Antibodies from COVID-19 Patients. *Cell* 182, 1663-1673.
- Kreye, J., Reincke, S.M., Kornau, H.C., Sanchez-Sendin, E., Corman, V.M., Liu, H., Yuan, M., Wu, N.C., Zhu, X., Lee, C.D., *et al.* (2020). A SARS-CoV-2 neutralizing antibody protects from lung pathology in a COVID-19 hamster model. *bioRxiv*.
- Kuzmina, A., Khalaila, Y., Voloshin, O., Keren-Naus, A., Boehm-Cohen, L., Raviv, Y., Shemer-Avni, Y., Rosenberg, E., and Taube, R. (2021). SARS-CoV-2 spike variants exhibit differential infectivity and neutralization resistance to convalescent or post-vaccination sera. *Cell Host Microbe* 29, 522-528 e522.
- Lan, J., Ge, J., Yu, J., Shan, S., Zhou, H., Fan, S., Zhang, Q., Shi, X., Wang, Q., Zhang, L., *et al.* (2020). Structure of the SARS-CoV-2 spike receptor-binding domain bound to the ACE2 receptor. *Nature* 581, 215-220.
- Lescure, F.X., Bouadma, L., Nguyen, D., Parisey, M., Wicky, P.H., Behillil, S., Gaymard, A., Bouscambert-Duchamp, M., Donati, F., Le Hingrat, Q., *et al.* (2020). Clinical and virological data of the first cases of COVID-19 in Europe: a case series. *Lancet Infect Dis* 20, 697-706.
- Letko, M., Marzi, A., and Munster, V. (2020). Functional assessment of cell entry and receptor usage for SARS-CoV-2 and other lineage B betacoronaviruses. *Nat Microbiol* 5, 562-569.
- Liang, J.G., Su, D., Song, T.Z., Zeng, Y., Huang, W., Wu, J., Xu, R., Luo, P., Yang, X., Zhang, X., *et al.* (2021). S-Trimer, a COVID-19 subunit vaccine candidate, induces protective immunity in nonhuman primates. *Nat Commun* 12, 1346.
- Liu, L., Wang, P., Nair, M.S., Yu, J., Rapp, M., Wang, Q., Luo, Y., Chan, J.F., Sahi, V., Figueroa, A., *et al.* (2020a). Potent neutralizing antibodies against multiple epitopes on SARS-CoV-2 spike. *Nature* 584, 450-456.
- Liu, X., Drelich, A., Li, W., Chen, C., Sun, Z., Shi, M., Adams, C., Mellors, J.W., Tseng, C.T., and Dimitrov, D.S. (2020b). Enhanced elicitation of potent neutralizing antibodies by the SARS-CoV-2 spike receptor binding domain Fc fusion protein in mice. *Vaccine* 38, 7205-7212.
- Long, Q.X., Tang, X.J., Shi, Q.L., Li, Q., Deng, H.J., Yuan, J., Hu, J.L., Xu, W., Zhang, Y., Lv, F.J., *et al.* (2020). Clinical and immunological assessment of asymptomatic SARS-CoV-2 infections. *Nat Med* 26, 1200-1204.
- Maisonasse, P., Guedj, J., Contreras, V., Behillil, S., Solas, C., Marlin, R., Naninck, T., Pizzorno, A., Lemaitre, J., Goncalves, A., *et al.* (2020). Hydroxychloroquine use against SARS-CoV-2 infection in non-human primates. *Nature* 585, 584-587.
- Mandolesi, M., Sheward, D.J., Hanke, L., Ma, J., Pushparaj, P., Perez Vidakovics, L., Kim, C., Adori, M., Lenart, K., Lore, K., *et al.* (2021). SARS-CoV-2 protein subunit vaccination of mice and rhesus macaques elicits potent and durable neutralizing antibody responses. *Cell Rep Med* 2, 100252.
- Marlin, R., Godot, V., Cardinaud, S., Galhaut, M., Coleon, S., Zurawski, S., Dereuddre-Bosquet, N., Cavarelli, M., Gallouet, A.S., Maisonasse, P., *et al.* (2021). Targeting SARS-CoV-2 receptor-binding domain to cells expressing CD40 improves protection to infection in convalescent macaques. *Nat Commun* 12, 5215.
- Martinez-Murillo, P., Tran, K., Guenaga, J., Lindgren, G., Adori, M., Feng, Y., Phad, G.E., Vazquez Bernat, N., Bale, S., Ingale, J., *et al.* (2017). Particulate Array of Well-Ordered HIV Clade C Env Trimers Elicits Neutralizing Antibodies that Display a Unique V2 Cap Approach. *Immunity* 46, 804-817 e807.
- Mastronarde, D.N. (2005). Automated electron microscope tomography using robust prediction of specimen movements. *J Struct Biol* 152, 36-51.
- McMahan, K., Yu, J., Mercado, N.B., Loos, C., Tostanoski, L.H., Chandrashekhar, A., Liu, J., Peter, L., Atyeo, C., Zhu, A., *et al.* (2021). Correlates of protection against SARS-CoV-2 in rhesus macaques. *Nature* 590, 630-634.

- Mercado, N.B., Zahn, R., Wegmann, F., Loos, C., Chandrashekhar, A., Yu, J., Liu, J., Peter, L., McMahan, K., Tostanoski, L.H., *et al.* (2020). Single-shot Ad26 vaccine protects against SARS-CoV-2 in rhesus macaques. *Nature* 586, 583-588.
- Munster, V.J., Feldmann, F., Williamson, B.N., van Doremalen, N., Perez-Perez, L., Schulz, J., Meade-White, K., Okumura, A., Callison, J., Brumbaugh, B., *et al.* (2020). Respiratory disease in rhesus macaques inoculated with SARS-CoV-2. *Nature* 585, 268-272.
- Nisini, R., Poerio, N., Mariotti, S., De Santis, F., and Fraziano, M. (2018). The Multirole of Liposomes in Therapy and Prevention of Infectious Diseases. *Front Immunol* 9, 155.
- Ozono, S., Zhang, Y., Ode, H., Sano, K., Tan, T.S., Imai, K., Miyoshi, K., Kishigami, S., Ueno, T., Iwatani, Y., *et al.* (2021). SARS-CoV-2 D614G spike mutation increases entry efficiency with enhanced ACE2-binding affinity. *Nat Commun* 12, 848.
- Pan, F., Ye, T., Sun, P., Gui, S., Liang, B., Li, L., Zheng, D., Wang, J., Hesketh, R.L., Yang, L., *et al.* (2020). Time Course of Lung Changes at Chest CT during Recovery from Coronavirus Disease 2019 (COVID-19). *Radiology* 295, 715-721.
- Pettersen, E.F., Goddard, T.D., Huang, C.C., Couch, G.S., Greenblatt, D.M., Meng, E.C., and Ferrin, T.E. (2004). UCSF Chimera--a visualization system for exploratory research and analysis. *J Comput Chem* 25, 1605-1612.
- Piccoli, L., Park, Y.J., Tortorici, M.A., Czudnochowski, N., Walls, A.C., Beltramello, M., Silacci-Fregni, C., Pinto, D., Rosen, L.E., Bowen, J.E., *et al.* (2020). Mapping Neutralizing and Immunodominant Sites on the SARS-CoV-2 Spike Receptor-Binding Domain by Structure-Guided High-Resolution Serology. *Cell* 183, 1024-1042 e1021.
- Pinto, D., Park, Y.J., Beltramello, M., Walls, A.C., Tortorici, M.A., Bianchi, S., Jaconi, S., Culap, K., Zatta, F., De Marco, A., *et al.* (2020). Cross-neutralization of SARS-CoV-2 by a human monoclonal SARS-CoV antibody. *Nature* 583, 290-295.
- Plotkin, S.A. (2020). Updates on immunologic correlates of vaccine-induced protection. *Vaccine* 38, 2250-2257.
- Premkumar, L., Segovia-Chumbez, B., Jadi, R., Martinez, D.R., Raut, R., Markmann, A., Cornaby, C., Bartelt, L., Weiss, S., Park, Y., *et al.* (2020). The receptor binding domain of the viral spike protein is an immunodominant and highly specific target of antibodies in SARS-CoV-2 patients. *Sci Immunol* 5, eabc8413.
- Randad, P.R., Pisanic, N., Kruczynski, K., Manabe, Y.C., Thomas, D., Pekosz, A., Klein, S., Betenbaugh, M.J., Clarke, W.A., Laeyendecker, O., *et al.* (2020). COVID-19 serology at population scale: SARS-CoV-2-specific antibody responses in saliva. *medRxiv*, 2020.2005.2024.20112300.
- Rees-Spear, C., Muir, L., Griffith, S.A., Heaney, J., Aldon, Y., Snitselaar, J.L., Thomas, P., Graham, C., Seow, J., Lee, N., *et al.* (2021). The effect of spike mutations on SARS-CoV-2 neutralization. *Cell Rep* 34, 108890.
- Robbiani, D.F., Gaebler, C., Muecksch, F., Lorenzi, J.C.C., Wang, Z., Cho, A., Agudelo, M., Barnes, C.O., Gazumyan, A., Finkin, S., *et al.* (2020). Convergent antibody responses to SARS-CoV-2 in convalescent individuals. *Nature* 584, 437-442.
- Rockx, B., Kuiken, T., Herfst, S., Bestebroer, T., Lamers, M.M., Oude Munnink, B.B., de Meulder, D., van Amerongen, G., van den Brand, J., Okba, N.M.A., *et al.* (2020). Comparative pathogenesis of COVID-19, MERS, and SARS in a nonhuman primate model. *Science* 368, 1012-1015.
- Rodda, L.B., Netland, J., Shehata, L., Pruner, K.B., Morawski, P.A., Thouvenel, C.D., Takehara, K.K., Eggenberger, J., Hemann, E.A., Waterman, H.R., *et al.* (2021). Functional SARS-CoV-2-Specific Immune Memory Persists after Mild COVID-19. *Cell* 184, 169-183 e117.
- Rogers, T.F., Zhao, F., Huang, D., Beutler, N., Burns, A., He, W.T., Limbo, O., Smith, C., Song, G., Woehl, J., *et al.* (2020). Isolation of potent SARS-CoV-2 neutralizing antibodies and protection from disease in a small animal model. *Science* 369, 956-963.
- Rosa, A., Pye, V.E., Graham, C., Muir, L., Seow, J., Ng, K.W., Cook, N.J., Rees-Spear, C., Parker, E., Dos Santos, M.S., *et al.* (2021). SARS-CoV-2 can recruit a heme metabolite to evade antibody immunity. *Sci Adv* 7, eabg7607.
- Sahin, U., Muik, A., Derhovanessian, E., Vogler, I., Kranz, L.M., Vormehr, M., Baum, A., Pascal, K., Quandt, J., Maurus, D., *et al.* (2020). COVID-19 vaccine BNT162b1 elicits human antibody and TH1 T cell responses. *Nature* 586, 594-599.

- Sanchez-Garcia, R., Gomez-Blanco, J., Cuervo, A., Carazo, J.M., Sorzano, C.O.S., and Vargas, J. (2021). DeepEMhancer: a deep learning solution for cryo-EM volume post-processing. *Commun Biol* 4, 874.
- Scheres, S.H. (2012). RELION: implementation of a Bayesian approach to cryo-EM structure determination. *J Struct Biol* 180, 519-530.
- Schmidt, F., Weisblum, Y., Muecksch, F., Hoffmann, H.H., Michailidis, E., Lorenzi, J.C.C., Mendoza, P., Rutkowska, M., Bednarski, E., Gaebler, C., et al. (2020). Measuring SARS-CoV-2 neutralizing antibody activity using pseudotyped and chimeric viruses. *J Exp Med* 217, e20201181.
- Scianimanico, S., Schoehn, G., Timmins, J., Ruigrok, R.H., Klenk, H.D., and Weissenhorn, W. (2000). Membrane association induces a conformational change in the Ebola virus matrix protein. *EMBO J* 19, 6732-6741.
- Seow, J., Graham, C., Merrick, B., Acors, S., Pickering, S., Steel, K.J.A., Hemmings, O., O'Byrne, A., Kouphou, N., Galao, R.P., et al. (2020). Longitudinal observation and decline of neutralizing antibody responses in the three months following SARS-CoV-2 infection in humans. *Nat Microbiol* 5, 1598-1607.
- Seydoux, E., Homad, L.J., MacCamay, A.J., Parks, K.R., Hurlburt, N.K., Jennewein, M.F., Akins, N.R., Stuart, A.B., Wan, Y.H., Feng, J., et al. (2020a). Characterization of neutralizing antibodies from a SARS-CoV-2 infected individual. *bioRxiv*.
- Seydoux, E., Homad, L.J., MacCamay, A.J., Parks, K.R., Hurlburt, N.K., Jennewein, M.F., Akins, N.R., Stuart, A.B., Wan, Y.H., Feng, J., et al. (2020b). Analysis of a SARS-CoV-2-Infected Individual Reveals Development of Potent Neutralizing Antibodies with Limited Somatic Mutation. *Immunity* 53, 98-105 e105.
- Shi, R., Shan, C., Duan, X., Chen, Z., Liu, P., Song, J., Song, T., Bi, X., Han, C., Wu, L., et al. (2020). A human neutralizing antibody targets the receptor-binding site of SARS-CoV-2. *Nature* 584, 120-124.
- Sokal, A., Chappert, P., Barba-Spaeth, G., Roeser, A., Fourati, S., Azzaoui, I., Vandenberghe, A., Fernandez, I., Meola, A., Bouvier-Alias, M., et al. (2021). Maturation and persistence of the anti-SARS-CoV-2 memory B cell response. *Cell* 184, 1201-1213 e1214.
- Stamatatos, L., Czartoski, J., Wan, Y.H., Homad, L.J., Rubin, V., Glantz, H., Neradilek, M., Seydoux, E., Jennewein, M.F., MacCamay, A.J., et al. (2021). mRNA vaccination boosts cross-variant neutralizing antibodies elicited by SARS-CoV-2 infection. *Science*.
- Supasa, P., Zhou, D., Dejnirattisai, W., Liu, C., Mentzer, A.J., Ginn, H.M., Zhao, Y., Duyvesteyn, H.M.E., Nutalai, R., Tuekprakhon, A., et al. (2021). Reduced neutralization of SARS-CoV-2 B.1.1.7 variant by convalescent and vaccine sera. *Cell* 184, 2201-2211 e2207.
- Suthar, M.S., Zimmerman, M.G., Kauffman, R.C., Mantus, G., Linderman, S.L., Hudson, W.H., Vanderheiden, A., Nyhoff, L., Davis, C.W., Adekunle, O., et al. (2020). Rapid Generation of Neutralizing Antibody Responses in COVID-19 Patients. *Cell Rep Med* 1, 100040.
- Tan, H.X., Juno, J.A., Lee, W.S., Barber-Axthelm, I., Kelly, H.G., Wragg, K.M., Esterbauer, R., Amarasena, T., Mordant, F.L., Subbarao, K., et al. (2021a). Immunogenicity of prime-boost protein subunit vaccine strategies against SARS-CoV-2 in mice and macaques. *Nat Commun* 12, 1403.
- Tan, T.K., Rijal, P., Rahikainen, R., Keeble, A.H., Schimanski, L., Hussain, S., Harvey, R., Hayes, J.W.P., Edwards, J.C., McLean, R.K., et al. (2021b). A COVID-19 vaccine candidate using SpyCatcher multimerization of the SARS-CoV-2 spike protein receptor-binding domain induces potent neutralising antibody responses. *Nat Commun* 12, 542.
- Thépaut, M., Luczkowiak, J., Vivès, C., Labiod, N., Bally, I., Lasala, F., Grimoire, Y., Fenel, D., Sattin, S., Thielens, N., et al. (2021). DC/L-SIGN recognition of spike glycoprotein promotes SARS-CoV-2 trans-infection and can be inhibited by a glycomimetic antagonist. *PLoS Pathog* 17(5), e1009576.
- Toelzer, C., Gupta, K., Yadav, S.K.N., Borucu, U., Davidson, A.D., Kavanagh Williamson, M., Shoemark, D.K., Garzoni, F., Staufer, O., Milligan, R., et al. (2020). Free fatty acid binding pocket in the locked structure of SARS-CoV-2 spike protein. *Science* 370, 725-730.
- Tortorici, M.A., Beltramello, M., Lempp, F.A., Pinto, D., Dang, H.V., Rosen, L.E., McCallum, M., Bowen, J., Minola, A., Jaconi, S., et al. (2020). Ultrapotent human antibodies protect against SARS-CoV-2 challenge via multiple mechanisms. *Science* 370, 950-957.
- Tortorici, M.A., and Veesler, D. (2019). Structural insights into coronavirus entry. *Adv Virus Res* 105, 93-116.

- Turonova, B., Sikora, M., Schurmann, C., Hagen, W.J.H., Welsch, S., Blanc, F.E.C., von Bulow, S., Gecht, M., Bagola, K., Horner, C., *et al.* (2020). In situ structural analysis of SARS-CoV-2 spike reveals flexibility mediated by three hinges. *Science* *370*, 203-208.
- van Doremalen, N., Lambe, T., Spencer, A., Belij-Rammerstorfer, S., Purushotham, J.N., Port, J.R., Avanzato, V.A., Bushmaker, T., Flaxman, A., Ulaszewska, M., *et al.* (2020). ChAdOx1 nCoV-19 vaccine prevents SARS-CoV-2 pneumonia in rhesus macaques. *Nature* *586*, 578-582.
- Vogel, A.B., Kanevsky, I., Che, Y., Swanson, K.A., Muik, A., Vormehr, M., Kranz, L.M., Walzer, K.C., Hein, S., Guler, A., *et al.* (2021). BNT162b vaccines protect rhesus macaques from SARS-CoV-2. *Nature* *592*, 283-289.
- Walls, A.C., Fiala, B., Schafer, A., Wrenn, S., Pham, M.N., Murphy, M., Tse, L.V., Shehata, L., O'Connor, M.A., Chen, C., *et al.* (2020a). Elicitation of Potent Neutralizing Antibody Responses by Designed Protein Nanoparticle Vaccines for SARS-CoV-2. *Cell* *183*, 1367-1382 e1317.
- Walls, A.C., Park, Y.J., Tortorici, M.A., Wall, A., McGuire, A.T., and Veesler, D. (2020b). Structure, Function, and Antigenicity of the SARS-CoV-2 Spike Glycoprotein. *Cell* *181*, 281-292 e286.
- Wang, C., Li, W., Drabek, D., Okba, N.M.A., van Haperen, R., Osterhaus, A., van Kuppeveld, F.J.M., Haagmans, B.L., Grosveld, F., and Bosch, B.J. (2020a). A human monoclonal antibody blocking SARS-CoV-2 infection. *Nat Commun* *11*, 2251.
- Wang, H., Zhang, Y., Huang, B., Deng, W., Quan, Y., Wang, W., Xu, W., Zhao, Y., Li, N., Zhang, J., *et al.* (2020b). Development of an Inactivated Vaccine Candidate, BBIBP-CorV, with Potent Protection against SARS-CoV-2. *Cell* *182*, 713-721 e719.
- Watanabe, Y., Allen, J.D., Wrapp, D., McLellan, J.S., and Crispin, M. (2020). Site-specific glycan analysis of the SARS-CoV-2 spike. *Science* *369*, 330-333.
- Wee, A.Z., Wrapp, D., Herbert, A.S., Maurer, D.P., Haslwanter, D., Sakharkar, M., Jangra, R.K., Dieterle, M.E., Lilov, A., Huang, D., *et al.* (2020). Broad neutralization of SARS-related viruses by human monoclonal antibodies. *Science* *369*, 731-736.
- Weinreich, D.M., Sivapalasingam, S., Norton, T., Ali, S., Gao, H., Bhore, R., Musser, B.J., Soo, Y., Rofail, D., Im, J., *et al.* (2021). REGN-COV2, a Neutralizing Antibody Cocktail, in Outpatients with Covid-19. *N Engl J Med* *384*, 238-251.
- Weissman, D., Alameh, M.G., de Silva, T., Collini, P., Hornsby, H., Brown, R., LaBranche, C.C., Edwards, R.J., Sutherland, L., Santra, S., *et al.* (2021). D614G Spike Mutation Increases SARS CoV-2 Susceptibility to Neutralization. *Cell Host Microbe* *29*, 23-31 e24.
- Williams, C.J., Headd, J.J., Moriarty, N.W., Prisant, M.G., Videau, L.L., Deis, L.N., Verma, V., Keedy, D.A., Hintze, B.J., Chen, V.B., *et al.* (2018). MolProbity: More and better reference data for improved all-atom structure validation. *Protein Sci* *27*, 293-315.
- Wolfel, R., Corman, V.M., Guggemos, W., Seilmäier, M., Zange, S., Müller, M.A., Niemeyer, D., Jones, T.C., Vollmar, P., Rothe, C., *et al.* (2020). Virological assessment of hospitalized patients with COVID-2019. *Nature* *581*, 465-469.
- Wrapp, D., Wang, N., Corbett, K.S., Goldsmith, J.A., Hsieh, C.L., Abiona, O., Graham, B.S., and McLellan, J.S. (2020). Cryo-EM structure of the 2019-nCoV spike in the prefusion conformation. *Science* *367*, 1260-1263.
- Wu, Y., Wang, F., Shen, C., Peng, W., Li, D., Zhao, C., Li, Z., Li, S., Bi, Y., Yang, Y., *et al.* (2020). A noncompeting pair of human neutralizing antibodies block COVID-19 virus binding to its receptor ACE2. *Science* *368*, 1274-1278.
- Xiong, X., Qu, K., Ciazyńska, K.A., Hosmillo, M., Carter, A.P., Ebrahimi, S., Ke, Z., Scheres, S.H.W., Bergamaschi, L., Grice, G.L., *et al.* (2020). A thermostable, closed SARS-CoV-2 spike protein trimer. *Nat Struct Mol Biol* *27*, 934-941.
- Yan, R., Zhang, Y., Li, Y., Xia, L., Guo, Y., and Zhou, Q. (2020). Structural basis for the recognition of SARS-CoV-2 by full-length human ACE2. *Science* *367*, 1444-1448.
- Yu, J., Tostanoski, L.H., Peter, L., Mercado, N.B., McMahan, K., Mahrokhan, S.H., Nkolola, J.P., Liu, J., Li, Z., Chandrashekhar, A., *et al.* (2020). DNA vaccine protection against SARS-CoV-2 in rhesus macaques. *Science* *369*, 806-811.

- Yuan, M., Huang, D., Lee, C.D., Wu, N.C., Jackson, A.M., Zhu, X., Liu, H., Peng, L., van Gils, M.J., Sanders, R.W., *et al.* (2021). Structural and functional ramifications of antigenic drift in recent SARS-CoV-2 variants. *Science* *373*, 818-823.
- Yuan, M., Liu, H., Wu, N.C., Lee, C.D., Zhu, X., Zhao, F., Huang, D., Yu, W., Hua, Y., Tien, H., *et al.* (2020). Structural basis of a shared antibody response to SARS-CoV-2. *Science* *369*, 1119-1123.
- Zang, J., Gu, C., Zhou, B., Zhang, C., Yang, Y., Xu, S., Zhang, X., Zhou, Y., Bai, L., Wu, Y., *et al.* (2020). Immunization with the receptor-binding domain of SARS-CoV-2 elicits antibodies cross-neutralizing SARS-CoV-2 and SARS-CoV without antibody-dependent enhancement. *Cell Discov* *3*:6(1).
- Zhang, B., Chao, C.W., Tsybovsky, Y., Abiona, O.M., Hutchinson, G.B., Moliva, J.I., Olia, A.S., Pegu, A., Phung, E., Stewart-Jones, G.B.E., *et al.* (2020a). A platform incorporating trimeric antigens into self-assembling nanoparticles reveals SARS-CoV-2-spike nanoparticles to elicit substantially higher neutralizing responses than spike alone. *Sci Rep* *10*, 18149.
- Zhang, J., Cai, Y., Xiao, T., Lu, J., Peng, H., Sterling, S.M., Walsh, R.M., Jr., Rits-Volloch, S., Zhu, H., Woosley, A.N., *et al.* (2021). Structural impact on SARS-CoV-2 spike protein by D614G substitution. *Science* *372*, 525-530.
- Zhang, K. (2016). Gctf: Real-time CTF determination and correction. *J Struct Biol* *193*, 1-12.
- Zhang, L., Jackson, C.B., Mou, H., Ojha, A., Peng, H., Quinlan, B.D., Rangarajan, E.S., Pan, A., Vanderheiden, A., Suthar, M.S., *et al.* (2020b). SARS-CoV-2 spike-protein D614G mutation increases virion spike density and infectivity. *Nat Commun* *11*, 6013.
- Zheng, S.Q., Palovcak, E., Armache, J.P., Verba, K.A., Cheng, Y., and Agard, D.A. (2017). MotionCor2: anisotropic correction of beam-induced motion for improved cryo-electron microscopy. *Nat Methods* *14*, 331-332.
- Zhou, D., Dejnirattisai, W., Supasa, P., Liu, C., Mentzer, A.J., Ginn, H.M., Zhao, Y., Duyvesteyn, H.M.E., Tuekprakhon, A., Nutalai, R., *et al.* (2021). Evidence of escape of SARS-CoV-2 variant B.1.351 from natural and vaccine-induced sera. *Cell* *184*, 2348-2361 e2346.
- Zhou, P., Yang, X.L., Wang, X.G., Hu, B., Zhang, L., Zhang, W., Si, H.R., Zhu, Y., Li, B., Huang, C.L., *et al.* (2020). A pneumonia outbreak associated with a new coronavirus of probable bat origin. *Nature* *579*, 270-273.
- Zivanov, J., Nakane, T., Forsberg, B.O., Kimanius, D., Hagen, W.J., Lindahl, E., and Scheres, S.H. (2018). New tools for automated high-resolution cryo-EM structure determination in RELION-3. *Elife* *7*.
- Zost, S.J., Gilchuk, P., Case, J.B., Binshtain, E., Chen, R.E., Nkolola, J.P., Schafer, A., Reidy, J.X., Trivette, A., Nargi, R.S., *et al.* (2020). Potently neutralizing and protective human antibodies against SARS-CoV-2. *Nature* *584*, 443-449.

DISCUSSION

Cette dernière partie de la thèse a pour but de discuter des caractéristiques, performances et limites des deux candidats vaccinaux, tout en replaçant ces projets dans le cycle de développement d'un vaccin.

Au sein du paysage des stratégies vaccinales disponibles, les deux candidats sont basés sur l'injection des antigènes sous forme protéique, vectorisés par des nanoparticules. Cette famille comprend les nanoparticules inorganiques, les nanoparticules polymériques, les nanoparticules protéiques auto-assemblées, les pseudoparticules virales (Virus Like Particle en anglais), et les liposomes (1). Leur taille, comme leur nom l'indique, est de l'ordre de la dizaine à la centaine de nanomètres, leur permettant à la fois d'accéder facilement aux ganglions lymphatiques, et d'être internalisées par les cellules présentatrices d'antigène. Dans le cas des deux études, les antigènes sont présentés à la surface des nanoparticules, de façon répétée, multimérique. Cette répétition des antigènes a pour but la fixation à plusieurs BCR à la surface d'un lymphocyte B spécifique. Ce phénomène appelé cross-linking permet une meilleure activation des cellules et par conséquent l'induction d'une réponse immunitaire humorale forte (2).

Le candidat vaccinal de l'équipe du Pr Fender est une nanoparticule protéique auto-assemblée recouverte de RBD, et ce n'est pas la seule équipe à avoir utilisé cette stratégie. Nous pouvons citer le travail de He and al (3) avec une nanoparticule s'auto-assemblant, basée sur la ferritine et décorée de différentes construction de RBD, également grâce au système de fixation Spy-Tag/ Spy-Catcher. Comme pour le candidat vaccinal ADDomer-RBD, les taux d'Ac induits par immunisation avec la nanoparticule-RBD étaient plus élevés que lors de l'immunisation avec le RBD seul. Toujours dans la même idée, le travail de Zhang and al (4) a consisté à décorer le même type de nanoparticule (dérivée de la ferritine) à l'aide du système Spy-Tag/Spy-Catcher pour y fixer à la fois du RBD mais aussi un autre domaine issu de la partie S2 du spicule (domaine Heptad), démontrant une nouvelle fois la versatilité de cette plateforme. Parmi les candidats vaccinaux basés sur cette technologie ayant atteint le stade des essais cliniques, nous pouvons citer le vaccin Icosavax, actuellement en phase 3, développé par GSK qui est lui aussi une nanoparticule décorée de RBD.

Concernant le candidat de l'équipe du Pr Weissenhorn, d'autres équipes de recherche ont également travaillé avec la même stratégie, comme l'équipe de Lovell (5) qui a réussi à créer des liposomes-spicule ou des liposomes-RBD toujours immunogènes chez la souris après lyophilisation et reconstitution, soulignant le potentiel de ce type de vaccins. Cependant, parmi les vaccins actuellement en essais cliniques (Clinical Trials), aucun n'est basé sur cette stratégie

de décoration de liposome par un antigène du SARS-CoV-2. Le seul vaccin contre la COVID-19 répertorié comme utilisant des liposomes s'en sert en tant que vecteur pour transporter un ARNm codant pour le spike (EG-COVID) (6). Parmi les vaccins sur le marché, les vaccins contre la grippe Inflexal® ou Invivac® se rapprochent de cette stratégie de décoration du liposome par l'antigène d'intérêt, en utilisant des virosomes (7). Dans ce cas, l'enveloppe du virus Influenza sert de vecteur liposomal, possédant à sa surface des protéines Hémagglutinine. Cette enveloppe est obtenue par culture cellulaire de virus dont le matériel génétique est soustrait à l'aide de détergent. Par rapport aux approches virosomales, le projet du Pr Weissenhorn présente donc l'avantage non négligeable de ne pas nécessiter de culture cellulaire, car la production de liposome est basée sur des méthodes physico-chimiques.

Ainsi, pour chacun des projets a été choisi un type de nanoparticule et un antigène différent. Comme discuté dans l'article de revue, le choix du RBD comme antigène est justifié par les études associant la présence d'anticorps anti-RBD neutralisants avec la protection. Il est intéressant de noter que pour le projet ADDomer en particulier, bien que n'utilisant que le RBD, celui-ci est présenté à la surface de l'ADDomer dans une conformation trimérique très semblable à celle que l'on retrouve à la surface du spike, permettant potentiellement d'induire des Ac quaternaires.

A l'inverse, le choix du spike entier comme antigène par l'équipe du Pr Weissenhorn vise l'induction de réponses immunitaires plus larges qu'avec l'utilisation du RBD seul, permettant potentiellement une efficacité conservée plus grande face à l'apparition de variants, grâce à l'induction potentielle d'Ac ciblant des épitopes de la glycoprotéine S en dehors du RBD, dans des régions potentiellement plus conservées.

Les deux candidats n'étant pas basés sur des stratégies vaccinales impliquant l'utilisation de vecteurs vitaux répliquatifs, ou de virus atténués, ni d'ARNm, ils ne possèdent pas d'effet adjuvant par eux même, ce qui implique donc l'ajout d'un adjuvant lors de l'étape de formulation. Pour rappel, selon la définition de Giudice and al (8) un adjuvant permet l'activation précoce (à des niveaux différents selon les adjuvants) de l'immunité, se traduisant par la suite par une réponse anticorps et une réponse cellulaire plus élevées qu'en cas d'utilisation de l'antigène seul. L'effet adjuvant est temporaire (un à deux jours) et local, les composants de l'adjuvant étant rapidement éliminés du site d'injection. Le choix de l'adjuvant est une étape cruciale pour le développement d'un vaccin : en effet le même candidat vaccinal adjuvanté différemment n'induira pas nécessairement les mêmes réponses humorales et/ou

cellulaires (9). Les deux équipes ont choisi des adjuvants différents, n’impliquant pas les sels d’aluminium, adjuvant le plus fréquemment utilisé mais aussi le plus controversé.

Le vaccin ADDomer-RBD a été formulé avec l’Addavax qui est une émulsion huile dans eau à base de squalène, similaire à l’adjuvant retrouvé dans différents vaccins contre la grippe : le MF59. Ces gouttelettes stimulent le recrutement et l’activation des cellules présentatrices d’antigènes (type macrophages) au site d’injection (10) .

Le vaccin liposome-spicule est basé sur l’utilisation de MPL, monophosphoryl lipid A, dérivé detoxifié du LPS des bactéries Gram négatives *Salmonella minnesota*. Il induit principalement une réponse CD4 auxiliaire de type Th1, propriété que n’ont pas les sels d’aluminium. Le MPL est à ce titre souvent associé aux sels d’aluminium pour profiter de leurs propriétés respectives, ce qui n’a pas été le cas ici.

Une fois leurs candidats vaccinaux formulés, les deux équipes ont cherché à en évaluer l’immunogénicité dans des modèles animaux.

Le groupe du Pr Fender a utilisé des souris Balb/c, modèle animal largement utilisé dans les étapes d’évaluation pré-clinique. Si le but était principalement de démontrer que le candidat vaccinal était capable d’induire des anticorps neutralisants, il faut garder à l’esprit que le répertoire anticorps murin diffère de celui des hommes. Les souris ne sont entre autre pas capables de produire des immunoglobulines avec de longs HCDR3 (partie hypervariable de la chaîne variable lourde), et dont la variabilité est moins grande que chez l’humain (11). Par ailleurs, les souris Balb/c utilisées dans l’étude ne sont pas infectables par le SARS-CoV-2 car dépourvues de récepteurs ACE-2, et il n’a donc pas été possible de tester les capacités de l’ADDomer-RBD à protéger. Bien que plus coûteux, il existe un modèle de souris exprimant le récepteur ACE-2, mais même ce modèle connaît des limitations, car la symptomatologie est assez éloignée de celle d’une infection COVID-19 chez l’humain (12).

L’équipe du Pr Weissenhorn a eu l’opportunité de tester son candidat vaccinal directement chez le macaque, modèle beaucoup plus proche de l’homme tant pour sa capacité à s’infecter qu’à développer des symptômes. Surtout, de précédentes études réalisées dans le domaine des vaccins anti-HIV ont montré que la réponse immunitaire développée par les primates non humain, tels que les macaques, est très proche de celle développée par les humains (13) (14) (15) .

Bien que les deux candidats soient formulés différemment et testés dans des modèles animaux différents, les tests ELISA et de neutralisation ont été réalisés par l’équipe du Pr Poignard pour

les deux projets, assurant une reproductibilité des résultats, et une comparaison possible des données entre les études d'un point de vue technique.

Ainsi, l'ADDomer-RBD permet d'induire des taux d'anticorps anti-RBD avec une IC50 moyenne de 532 après quinze jours. En comparaison, le spike-liposome induit des taux d'anticorps anti-RBD avec une IC50 moyenne de 59 après quinze jours. Dans les deux cas, suite à une injection supplémentaire, les taux d'Ac augmentent encore, jusqu'à atteindre des titres moyens d'Ac anti-RBD de 10065 pour l'ADDomer-RBD, et de 82 pour le liposome-spicule. Les taux d'Ac anti-RBD induits par l'ADDomer sont donc beaucoup plus hauts que ceux induits par le liposome-spicule. Les schémas vaccinaux diffèrent par la suite, l'équipe du Pr Fender ne réalisant par d'autre rappel vaccinal, et sacrifiant les animaux à J41. Les animaux ne sont donc pas infectés, et malgré la présence de forts taux d'anticorps neutralisants, il est difficile de conclure avec certitude sur les capacités protectrices des Ac induits. A cet égard, il est intéressant de souligner la capacité du liposome-spike à induire une immunité stérilisante dans le modèle macaque, avec des taux d'Ac plus faibles.

Si les deux articles apportent déjà des résultats prometteurs, des expériences additionnelles sont en cours pour chacun des projets.

Pour le projet ADDomer-RBD, des expériences sont en cours avec un RBD correspondant au variant Delta. L'équipe du Pr Fender a produit un candidat vaccinal « mosaïque », ayant à sa surface des RBD « Wuhan » et des RBD du variant Delta. Des expériences de mesure d'immunogénicité et de pouvoir neutralisant sont en cours. Les performances de ce candidat vaccinal mosaïque seront également comparées à celles obtenues suite à l'injection d'une formulation comprenant un mélange des deux candidats vaccinaux ADDomer RBD-Wuhan, et ADDomer-RBD Delta. Des travaux similaires ont été réalisés, par exemple par l'équipe de P. Bjorkman (16) où des souris ont été immunisées avec des nanoparticules mosaïques (ou nanoparticules hétérologues), affichant à la fois le RBD du SARS-CoV2 et des RBD d'autres betacoronavirus n'infectant pour l'heure que les animaux. L'équipe a démontré que les taux d'Ac induit par immunisation avec les nanoparticules hétérologues était similaires voire plus élevés que lors de l'immunisation avec des nanoparticules homologues (n'affichant que le RBD du SARS-CoV-2).

Dans la même idée, il serait possible d'imaginer pour le projet du Pr Weissenhorn le développement d'autres formulations, cette fois avec des spicules de variants. Ainsi, un candidat vaccinal basés sur des liposomes décorés de spicules issus de mutants différents pourrait être conçue.

Dans le cas du projet liposome-spike, des études sont actuellement réalisées avec deux nouvelles constructions du candidat vaccinal. La première est un liposome décoré de spike stabilisé par 4 prolines supplémentaires par rapport à la construction 2P (aussi appelé spike 6P), lui assurant une meilleure stabilité en position pré-fusionnelle. La seconde construction est un liposome décoré par des spicules sans domaine RBD, et permettrait potentiellement de focaliser les réponses Ac vers des régions moins variables.

Pour conclure, les deux projets sont situés au tout début du pipeline de développement d'un vaccin, aux phases exploratoires, qui correspondent à la formulation du candidat vaccinal, comme présenté sur la figure 5. Les deux candidats ayant fait preuve de leur efficacité à induire des anticorps neutralisants, la prochaine étape de développement sera les tests pré-cliniques. Cette phase a pour but de déterminer le meilleur dosage et le meilleur schéma vaccinal en termes de tolérance, d'immunogénicité, et de protection. Pour le projet de l'équipe du Dr Fender ces tests devraient comprendre un passage aux primates non humains, et pour l'équipe du Dr Weissenhorn, un test sur un plus grand nombre de macaques. Impliquant un plus grand nombre d'animaux, cette étape nécessite la production en plus grands lots, premier changement d'échelle du pipeline. Ces lots doivent idéalement être conçus selon les Bonnes pratiques de Fabrication, et donc respecter des exigences d'identité, de pureté et de stabilité. (Le respect de ces règles n'est pas une obligation, mais est fortement conseillé car les lots doivent se rapprocher le plus de la forme vaccinale finale qui sera utilisée dans les essais cliniques.) Les deux projets étant basés sur des techniques d'assemblage séquentiel, la vérification de l'homogénéité des lots serait cruciale. Parmi les vaccins anti-COVID-19, la stratégie d'assemblage séquentiel du RBD sur un immunogène a été utilisée par exemple pour le Soberana, formé par conjugaison de RBD à la toxine tétanique, toxine déjà utilisée dans d'autres vaccins (17). Développé par Cuba, ce vaccin a été commercialisé à grande échelle.

Les laboratoires académiques porteurs du projet n'étant pas à même d'assurer ce type de production à grande échelle, la prochaine étape du pipeline serait de trouver un fabricant adapté. Cette étape sera conditionnée par l'intérêt des industriels pour un « énième » vaccin COVID, dans un paysage saturé de candidats plus avancés dans le pipeline. Il est plus raisonnable de penser que les deux équipes parviendront à ces étapes de développement pour d'autres pathologies infectieuses, grâce à l'adaptabilité de leurs plateformes.

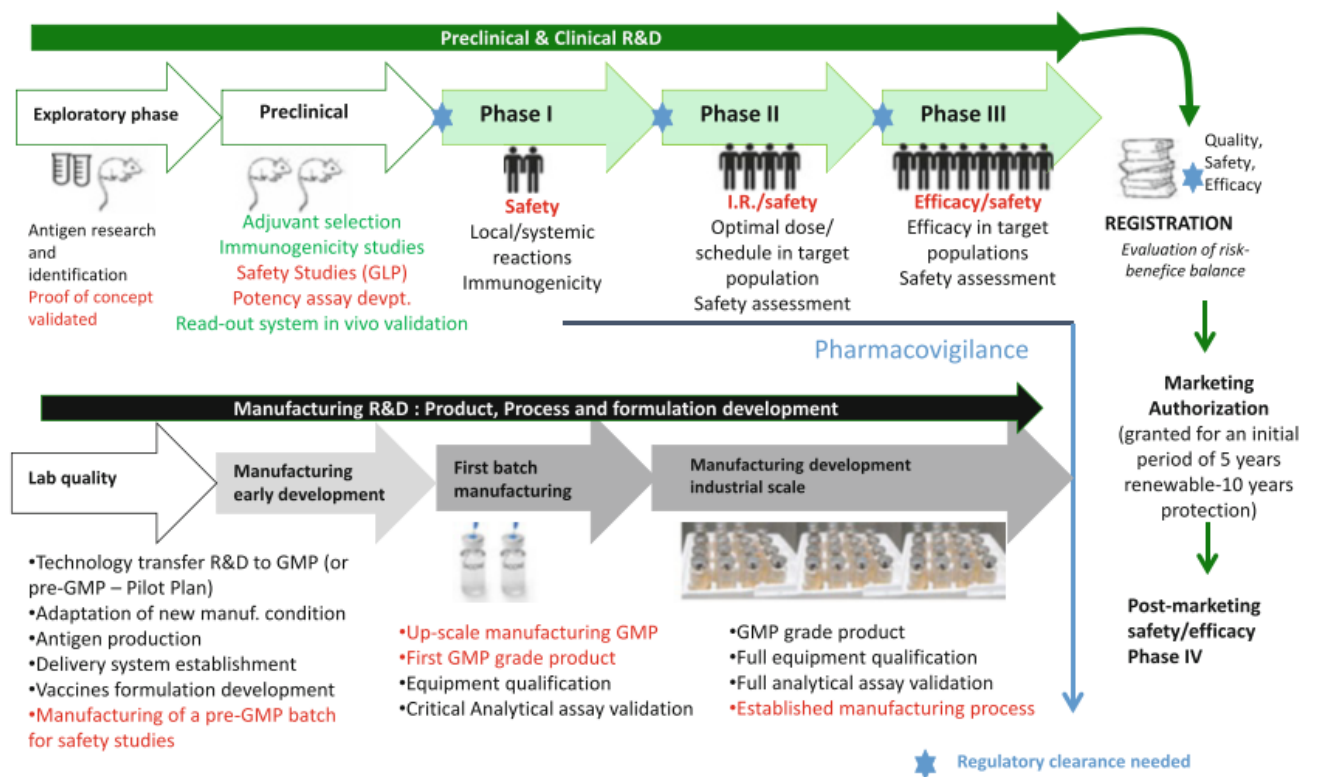


Figure 5: Etapes de développement pré-clinique et clinique d'un vaccin, Artaud and al (18).

Bibliographie de la discussion :

1. Al-Halifa S, Gauthier L, Arpin D, Bourgault S, Archambault D. Nanoparticle-based vaccines against respiratory viruses. *Front Immunol.* 2019;10(JAN):1–11.
2. Kelly HG, Kent SJ, Wheatley AK. Immunological basis for enhanced immunity of nanoparticle vaccines. *Expert Rev Vaccines* [Internet]. 2019;18(3):269–80. Available from: <https://doi.org/10.1080/14760584.2019.1578216>
3. He L, Lin X, Wang Y, Abraham C, Sou C, Ngo T, et al. Single component self assembling protein nanoparticles presenting the receptor binding domain and stabilized spike as SARS-CoV-2 vaccine candidates. 2021;(March):1–18.
4. Ma X, Zou F, Yu F, Li R, Yuan Y, Zhang Y, et al. Nanoparticle Vaccines Based on the Receptor Binding Domain (RBD) and Heptad Repeat (HR) of SARS-CoV-2 Elicit Robust Protective Immune Responses. *Immunity.* 2020;53(6):1315–1330.e9.
5. Mabrouk MT, Chiem K, Rujas E, Huang W-C, Jahagirdar D, Quinn B, et al. Lyophilized, thermostable Spike or RBD immunogenic liposomes induce protective immunity against SARS-CoV-2 in mice. *Sci Adv.* 2021;7(49):1–11.
6. Hong HC, Kwang Sung Kim, Park SA, Chun MJ, Young E, Hong, et al. An mRNA vaccine against SARS-CoV-2: Lyophilized, liposome-based vaccine 2 candidate EG-COVID induces high levels of virus neutralizing antibodies. 2021; Available from: <https://about.jstor.org/terms>
7. Autran B, Beytout J, Floret D, Jacquet A, Koeck J-L, Levy-Bruhl D, et al. Aluminium et vaccins. Haut Cons la Santé Publique [Internet]. 2013;63. Available from: <http://www.hcsp.fr/explore.cgi/avisrapportsdomaine?clefr=369>
8. Del Giudice G, Rappuoli R, Didierlaurent AM. Correlates of adjuvanticity: A review on adjuvants in licensed vaccines. *Semin Immunol* [Internet]. 2018;39(May):14–21. Available from: <https://doi.org/10.1016/j.smim.2018.05.001>
9. Arunachalam PS, Walls AC, Golden N, Atyeo C, Fischinger S, Li C, et al. Adjuvanting a subunit COVID-19 vaccine to induce protective immunity. *Nature* [Internet]. 2021;594(7862):253–8. Available from: <http://dx.doi.org/10.1038/s41586-021-03530-2>
10. Garçon N, Leroux-Roels G, Cheng WF. Vaccine adjuvants. *Perspect Vaccinol* [Internet]. 2011;1(1):89–113. Available from: <http://dx.doi.org/10.1016/j.pervac.2011.05.004>
11. Schroeder HW. Similarity and divergence in the development and expression of the mouse and human antibody repertoires. *Dev Comp Immunol.* 2006;30(1–2):119–35.
12. Bao L, Deng W, Huang B, Gao H, Liu J, Ren L, et al. The pathogenicity of SARS-CoV-2 in hACE2 transgenic mice. *Nature.* 2020;583(7818):830–3.
13. Shedlock DJ, Silvestri G, Weiner DB. Monkeying around with HIV vaccines: Using rhesus macaques to define “gatekeepers” for clinical trials. *Nat Rev Immunol.* 2009;9(10):717–28.
14. Staprans SI, Feinberg MB, Shiver JW, Casimiro DR. Role of nonhuman primates in the evaluation of candidate AIDS vaccines: An industry perspective. *Curr Opin HIV AIDS.* 2010;5(5):377–85.
15. Morgan C, Marthas M, Miller C, Duerr A, Cheng-Mayer C, Desrosiers R, et al. The use of nonhuman primate models in HIV vaccine development. *PLoS Med.* 2008;5(8):1200–4.
16. Barnes CO, Jette CA, Abernathy ME, Dam K-MA, Esswein SR, Gristick HB, et al. SARS-CoV-2 neutralizing antibody structures inform therapeutic strategies. *Nature.* 2020 Dec;588(7839):682–7.
17. Toledo-romani AME, Silva CV. Efficacy and safety of SOBERANA 02 , a COVID-19 conjugate vaccine in heterologous three-dose combination Background : SOBERANA 02 is a COVID-19 conjugate vaccine (recombinant RBD conjugated to tetanus toxoid). Phase 1 and 2 clinical trials demonstrated . 2021;
18. Artaud C, Kara L, Launay O. Vaccine development from preclinical studies to phase 1 2 clinical trials. *Methods Mol Biol.* 2019;2013:387–405.

CONCLUSION

THÈSE SOUTENUE PAR : Axelle AMEN

TITRE : STRATEGIES VACCINALES ANTI-SARS-COV-2 : EVALUATION DE L'IMMUNOGENICITE DE DEUX CANDIDATS VACCINAUX.

CONCLUSION :

Ma thèse d'exercice en pharmacie comprend comme premier travail, présenté en introduction, une revue de la littérature sur les stratégies vaccinales anti-SARS-CoV-2. Cette revue permet de contextualiser les travaux expérimentaux, présentés à la suite, à l'occasion d'une collaboration entre l'équipe de recherche du service de virologie du CHU Grenoble Alpes du Pr Pascal POIGNARD, et les équipes du Pr Weissenhorn et du Dr Fender de l'Institut de Biologie Structurale, concernant l'évaluation de l'immunogénicité de deux candidats vaccinaux.

Le candidat vaccinal de l'équipe du Dr Fender est une pseudo-particule virale non infectieuse, nommée ADDomer, formée par l'assemblage de sous unités protéiques dérivées de l'Adénovirus de type 3. Grâce à un système d'accroche par liaison covalente spontanée la surface de l'ADDomer peut être décorée par des antigènes vaccinaux, ici le domaine de fixation au récepteur ACE-2 (Receptor Binding Domain ou RBD) de la glycoprotéine spike (S) du SARS-CoV-2 (« souche Wuhan »). Le candidat vaccinal de l'équipe du Pr Weissenhorn est un liposome décoré de spicules formés de trimères de la protéine S du SARS-CoV-2, également de la souche Wuhan.

L'immunogénicité des deux candidats a été évaluée dans des modèles animaux : chez la souris pour l'ADDomer-RBD et chez le macaque pour le liposome-spicule. A cette fin nous avons mesuré par technique ELISA (Enzyme Linked ImmunoSorbent Assay) les taux d'IgG dirigés contre les antigènes vaccinaux utilisés, le RBD ou le trimère de glycoprotéine S. Nos résultats montrent que des réponses anticorps spécifiques sont induites par les deux plateformes vaccinales, à des titres élevés. La capacité des anticorps induits à bloquer la réPLICATION virale,

appelée neutralisation, a également été mesurée dans le laboratoire grâce à un système de pseudo-particules virales complémentées par la glycoprotéine spike. Les deux candidats vaccinaux sont capables d'induire de forts taux d'anticorps neutralisants (AcN) dans leurs modèles animaux respectifs. Ces AcN sont probablement responsables de la protection complète observée chez les macaques vaccinés exposés au SARS-CoV-2.

Les deux candidats vaccinaux évalués sont donc prometteurs, notamment le liposome-spicule qui a démontré sa capacité à protéger contre l'infection par le SARS-CoV-2. A ce stade, l'intérêt d'un développement en phase pré-clinique apparaît cependant questionable, devant la quantité d'autres vaccins SARS-CoV-2 sur le marché ou dans les dernières phases de développement clinique. L'utilisation de ces plateformes pourrait néanmoins être intéressante dans la perspective de protéger contre de nouveaux variants du SARS-CoV-2 ou pour élaborer un nouveau vaccin pan-coronavirus. Les travaux ont finalement permis de démontrer l'efficacité et la flexibilité de ces deux plateformes vaccinales, qui pourront être aussi adaptées dans le futur à d'autres pathologies infectieuses.

VU ET PERMIS D'IMPRIMER

Grenoble, le :

LE DOYEN



Michel SEVE

LE DIRECTEUR DE THESE :

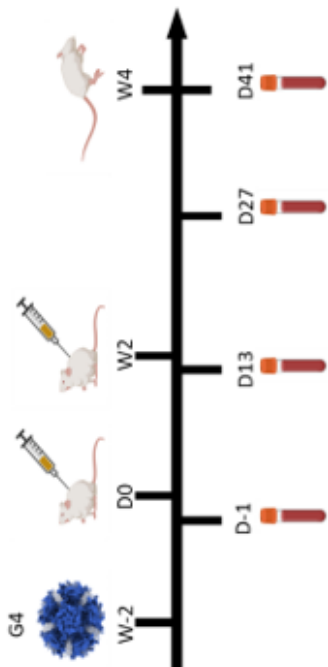
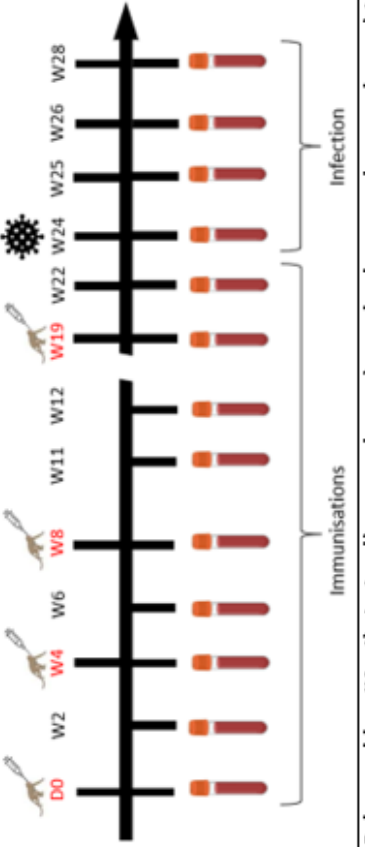

P. POIGNARD

LE TUTEUR UNIVERSITAIRE :



ANNEXE

**TABLEAU COMPARATIF SIMPLIFIÉ
DES DEUX ÉTUDES**

	Elicitation of potent SARS-CoV-2 neutralizing antibody responses through immunization using a versatile adenovirus-inspired multimerization platform. <i>Fender team.</i>	Immunization with synthetic SARS-CoV-2 S glycoprotein virus-like particles protects macaques from infection. <i>Weissenhorn team.</i>
Système vaccinal	« ADDomer » : pseudo-particule virale non infectieuse formée par l'assemblage spontané de sous unités protéiques dérivées de l'adénovirus de type 3, possédant l'étiquette Spy Tag pour la fixation de l'antigène.	Pseudo-particule virale liposomale , possédant des lipides spéciaux pour la fixation de l'antigène.
Antigène	RBD SARS-CoV-2 WT. Fixation des RBD à l'ADDomer grâce leur Spy Catcher.	Spike SARS-CoV-2 WT, stabilisé par une substitution 2P et réticulé au formaldéhyde. Fixation des spikes aux lipides du liposome grâce à leur étiquette His-Tag .
Vérification de la configuration du candidat vaccinal	Profil sur gel SDS-PAGE + spectrométrie de masse + Cryo-electron-microscopie + SPR + immuno -fluorescence sur cellules HeLa + compétition entre le candidat vaccinal et le pseudovirus pour l'entrée cellulaire.	Cryo-electron-microscopie.
Modèle animal	Souris balb/c , 10 souris par groupe.	Oncomeles macaques, 4 macaques par groupe.
Conditions testées	-Groupe 1 (G1): RBD-SC -Groupe 2 (G2): RBD-SC + ADDomer nu -Groupe 3 (G3): RBD-ADDomer -Groupe 4 (G4): RBD-ADDomer + pré-immunisation deux semaines avant début du schéma vaccinal avec ADDomer.	-Groupe vacciné (GV) -Groupe non vacciné (GNV)
Schéma vaccinal		
Induction d'anticorps spécifiques aux antigènes ?	Oui, pour tous les groupes. Apparition des Ac anti RBD dès la 1 ^{re} semaine pour les groupes vaccinés avec RBD-ADDomer (G3 et G4). Apparition des Ac anti RBD 1 semaine après boost pour les groupes vaccinés avec RBD soluble (G1 et G2). Groupes 3 et 4 ont toujours les taux les plus élevés, et le groupe avec pré-immunisation RBD (G4) a le taux le plus élevé. La pré-immunisation ADDomer favorise l'induction d'anticorps. Pas de phénomène de pré-immunité comme observé pour les vaccins à vecteur adénoviral .	Oui, apparition d'Ac dès la deuxième semaine après vaccination, avec titres maximaux à la onzième semaine . -GV : A partir de la onzième semaine, les IC50 anti spike sont plus élevés que les IC50 anti-RBD. Diminution lente des titres d'Ac malgré le challenge à la semaine 24. -GNV : apparition d'Ac deux semaines après le challenge viral, notamment IgG anti-RBD.
Réponses cellulaires T	Oui, pour tous les groupes. Les groupes vaccinés avec RBD-ADDomer ont les taux les plus élevés.	Oui, apparition d'Ac dès S6 et maximum à S11 après vaccination. -GV : Très légère baisse des titres d'Ac neutralisants malgré le challenge à S24. -GNV : Apparition des Ac quatre semaines après le challenge.
Protection après infection	Non mesurées.	Chez les macaques vaccinés, réponse TCD4+ mais pas de réponse cellulaire TCD8+.
Performances contre les variants	Pas d'infection possible.	Macaques vaccinés : Après challenge, charge virale indétectable (RNA / serRNA), pour toutes les localisations. Pas de lésions pulmonaires à l'imagerie. → Immunité stérilisante ?
	Pas testées.	Titres d'AcN contre variant Alpha similaires à ceux observés pour le WT. Titres contre variants Beta et Gamma plus bas que le WT, mais tout de même élevés. → Performances conservées contre les variants.

SERMENT DE GALIEN



Serment de Gallien



« Je jure en présence des Maîtres de la Faculté, des Conseillers de l'Ordre des Pharmaciens et de mes condisciples :

D'honorer ceux qui m'ont instruit(e) dans les préceptes de mon art et de leur témoigner ma reconnaissance en restant fidèle à leur enseignement.

D'exercer, dans l'intérêt de la santé publique, ma profession avec conscience et de respecter non seulement la législation en vigueur, mais aussi les règles de l'honneur, de la probité et du désintéressement.

De ne jamais oublier ma responsabilité et mes devoirs envers le malade et sa dignité humaine ; en aucun cas, je ne consentirai à utiliser mes connaissances et mon état pour corrompre les mœurs et favoriser des actes criminels.

Que les hommes m'accordent leur estime si je suis fidèle à mes promesses. Que je sois couvert(e) d'opprobre et méprisé(e) de mes confrères si j'y manque ».

RÉSUMÉ

Mme Axelle AMEN

Stratégies vaccinales anti-SARS-CoV-2 : évaluation de l'immunogénicité de deux candidats vaccinaux.

RESUME

Cette thèse comporte en introduction un travail de recherche bibliographique sur les diverses stratégies vaccinales anti-COVID-19 disponibles, puis un travail expérimental portant sur l'évaluation de l'immunogénicité de deux candidats vaccinaux développés par deux équipes de l'Institut de Biologie Structurale de Grenoble. Ces deux approches sont basées sur l'utilisation du spicule du SARS-CoV-2 comme antigène, afin d'induire des anticorps neutralisants protecteurs. Elles ont en commun d'utiliser des plateformes permettant une multimérisation des antigènes protéiques, connue pour induire une meilleure réponse humorale. Le premier candidat vaccinal nommé « ADDomer », développé par l'équipe du Dr Fender utilise les capacités d'auto-assemblage de sous unités protéiques (penton) de l'adénovirus de type 3 pour créer des pseudoparticules virales (VLP). Les VLP sont décorées avec le domaine de fixation au récepteur (RBD) du spicule du SARS-CoV-2. L'immunogénicité des VLP-RBD a été évaluée par injection chez la souris. La mesure de la réponse anticorps anti-RBD par ELISA (Enzyme Linked ImmunoSorbent Assay), a mis en évidence des titres élevés, apparaissant dès deux semaines après la première injection. En complément des tests ELISA, des tests de neutralisation ont démontré la capacité du candidat vaccinal à induire des anticorps neutralisants, également à des taux élevés. L'adénovirus de type 3 étant hautement prévalent dans certaines populations, l'impact de l'existence d'une pré-immunité a été étudié par pré-immunisation d'un groupe de souris avec de l'ADDomer seul, avant injection de l'ADDomer-RBD. Les réponses anticorps dans ce groupe ont été plus précoces et plus élevées que dans les groupes sans pré-immunité, suggérant un possible avantage de la pré-immunisation, contrairement à ce qui a été décrit dans les stratégies vaccinales basées sur les vecteurs géniques adénovirus humains. Le second candidat vaccinal, développé par l'équipe du Pr Weissenhorn, est basé sur l'utilisation de particules liposomales décorées de spicules du SARS-CoV-2. L'immunisation de macaques a permis de démontrer sa bonne tolérance et son immunogénicité. Des anticorps anti-RBD et des anticorps anti-spike ont été détectés dès la deuxième semaine après la première immunisation, augmentant suivant les seconde et troisième immunisations, pour atteindre des taux élevés. De même, le sérum des animaux vaccinés a montré une forte

activité neutralisante contre le SARS-CoV-2. Afin d'évaluer la protection conférée par le vaccin, les animaux ont été soumis à un aérosol nasal de SARS-CoV-2, en comparaison à un groupe contrôle de macaques non vaccinés. Aucune charge virale, ni lésion pulmonaire n'ont été détectées chez les animaux vaccinés, témoin de l'absence complète d'infection. Au contraire, les animaux contrôles ont tous développés la maladie. En conclusion, les deux approches vaccinales étudiées ont permis l'induction efficace d'anticorps anti-spicule avec une forte activité de neutralisation du SARS-CoV-2. L'approche liposome-spicule permet une protection complète, permettant très probablement d'éviter la transmission, propriété qui devra être confirmée dans de prochaines études de plus grande ampleur. L'approche ADDomer est une plateforme vaccinale intéressante pour son adaptabilité, et pourrait être utilisée pour lutter contre de futurs pathogènes.

MOTS CLÉS : Virologie, SARS-CoV-2, Immunologie, Vaccinologie, ELISA, Anticorps

SPÉCIALITÉ : Internat de pharmacie : Innovation Pharmaceutique et Recherche.

Anti-SARS-CoV-2 vaccine strategies: immunogenicity evaluation of two vaccine candidates.

ABSTRACT

The work presented in this thesis includes a bibliographic study of the various SARS-CoV-2 vaccine strategies available, followed by the evaluation of the immunogenicity of two vaccine candidates developed by two teams at the Structural Biology Institute of Grenoble. The two approaches are based on the use of the SARS-CoV-2 spike as an antigen for the induction of protective neutralising antibodies. The vaccine candidate shares the common feature of using platforms that lead to the multimerisation of protein antigens, a feature known to induce a stronger humoral response. The first vaccine candidate named "ADDomer", developed by the team of Dr Fender uses the self-assembly capabilities of adenovirus type 3 penton protein subunits to create viral pseudoparticles (VLPs). The VLPs are then decorated with recombinant receptor binding domain (RBD) of the SARS-CoV-2 spike. Immunogenicity of the vaccine candidate was assessed by immunisation of mice. Measurement of anti-RBD antibody response by Enzyme Linked ImmunoSorbent Assay (ELISA) showed high titers, appearing as early as two weeks after the first injection. In addition to the ELISA tests, neutralisation assays demonstrated the ability of the vaccine candidate to induce neutralising antibodies, also at high levels. As adenovirus type 3 is highly prevalent in certain populations, the impact of the existence of pre-immunity was studied by pre-immunising a group of mice with ADDomer alone, prior to injection of the ADDomer-RBD. Antibody responses in this group were earlier and greater than in groups without pre-immunity, suggesting a possible advantage of pre-immunisation, in contrast to what has been described in vaccine strategies based on human adenoviral vectors. The second vaccine candidate developed by the team of Professor Weissenhorn is based on the use of liposomal particles decorated with SARS-CoV-2 stabilized trimeric spikes. Immunisation of macaques demonstrated its good tolerance and high immunogenicity. Anti-RBD and anti-spike antibodies were detected as early as two weeks after the first immunisation and reached high levels following the second and third immunisations. Similarly, serum from vaccinated animals showed strong neutralising activity against SARS-CoV-2. To evaluate the protection conferred by the vaccine, the vaccinated animals were subjected to a nasal aerosol of SARS-CoV-2, compared to a control group of unvaccinated macaques. No viral load or lung lesions were detected in the vaccinated animals, indicating a

complete absence of infection and sterilizing immunity. On the contrary, the control animals all developed the disease. In conclusion, the two vaccine approaches evaluated allowed the efficient induction of anti-spike antibodies with a strong neutralising activity against SARS-CoV-2. The liposome-spike approach provided complete protection, most likely preventing transmission, a property that should be confirmed in future larger studies. The ADDomer approach is an interesting vaccine platform because of its adaptability and could be used to combat future pathogens.

KEY WORDS: Virology, SARS-CoV-2, Immunology, Vaccinology, ELISA, antibodies.

